Electrocardiogram Signal Analysis for Heartbeat Pattern Classification

Manab Kumar Das

Electrocardiogram Signal Analysis for Heartbeat Pattern Classification

Thesis submitted in partial fulfillment of the requirements for award of the degree

DOCTOR OF PHILOSOPHY

by

Manab Kumar Das

Under the supervision of

Dr. Samit Ari

Department of Electronics and Communication Engineering

National Institute of Technology, Rourkela

Rourkela-769008, INDIA

May 2015

Declaration

I hereby declare that the work presented in the thesis entitled as **Electrocardiogram Signal Analysis for Heartbeat Pattern Classification** is a bonafide record of the systematic research work done by me under the guidance of Prof. Samit Ari, Department of Electronics and Communication Engineering, National Institute of Technology, Rourkela, India and that no part thereof has been presented for the award of any other degree.

Place: NIT, Rourkela
Date: May 2015.

Manab Kumar Das

Department of Electronics and Communication Engineering
National Institute of Technology, Rourkela
Rourkela, Odisha, India 769 008.

Certificate

This is to certify that the thesis entitled **Electrocardiogram Signal Analysis for Heartbeat Pattern Classification** by **Mr. Manab Kumar Das** submitted to the National Institute of Technology, Rourkela for the degree of **Doctor of Philosophy**, is a record of bonafide research work, carried out by him in the department of Electronics and Communication Engineering under my supervision and guidance. I believe that the thesis fulfills part of the requirements for the award of degree of **Doctor of Philosophy**. To the best of my knowledge, the matter embodied in the thesis has not been submitted to any other University/Institute for the award of any other degree.

Dr. Samit Ari
Assistant Professor
Department of Electronics and Communication Engineering,
National Institute of Technology,
Rourkela, Odisha,
INDIA 769 008.

Place: NIT, Rourkela
Date: May 2015.

Dedicated to

the sacrifice and endurance of my wife, son and my parents

Acknowledgment

Throughout my PhD work I came across many people whose support helped me to complete this research work smoothly and at this moment I would like to take the opportunity to acknowledge them. First and foremost I would like to express my deep and sincere gratitude towards my respectable supervisor, Prof. Samit Ari for his invaluable guidance, constant inspiration and motivation along with enormous moral support during my difficult phase to complete this work, without his suggestions and ideas, this thesis would not be an asset for me. I am indebted to him for the valuable time he has spared for me during this work.

I am very much thankful to Prof. K. K. Mahapatra, Professor & Head of the Department, Electronics and Communication Engineering, for his continuous encouragement. Also, I am indebted to him for providing me with all the official and laboratory facilities.

I am also thankful to Prof. S. K. Sarangi, Director of National Institute of Technology, Rourkela, for allowing me to avail the necessary facilities of the Institute for the completion of this work. I am grateful to my DSC members Prof. S. Meher, Prof. D. Patra and Prof. S. Das, for their valuable comments and suggestions.

I would like to thank Prof. S. K. Patra, Prof. S. K. Behera, Prof. A. K. Swain, Prof. S. K. Das, Prof. A. K. Sahoo and Prof. U. K. Sahoo whose encouragement helped me to work hard. They have been great sources of inspiration for me and I thank them from bottom of my heart.

I acknowledge all staff members, research scholars, friends and juniors of Dept. of Electronics and Communication Engineering, NIT, Rourkela for their generous help in

various ways to complete the thesis work. I should also thank my friend Dipak Kumar Ghosh with whom I shared many of the ideas related to research work and who gave me invaluable feedback.

I would like to acknowledge my family, parents, parents-in-law, sisters and brothers for their support, strength and motivation. A special thank goes to my father, Sukdeb Das and mother, Usha Rani Das for their love, patience and understanding provided during these years. I have realized that without the selfless help from them, I could never achieve this goal. I would like to convey my heartiest regards to my parents for their boundless love and affection.

Last, but not least, this dissertation would not have been possible without Munmun and Moulik, my beloved wife and sweet son. Their understanding, support, boundless love, affection and encouragement led me to reach this point of life.

Place: NIT, Rourkela
Date: May 2015.

Manab Kumar Das (510EC305)

Contents

List of Symbols and Abbreviations

α_i	Lagrange Multiplier
η	Learning rate parameter
$\Delta^{(i)}$	Vector in the random direction
γ_n^j	Normalized wavelet coefficient at j level
$\psi_{i,l}$	Wavelet basis function
σ	Width of Gaussian function
τ	Spectral Localization
$[.]_{\uparrow}$	Up-sampling
θ	Location of the bacteria position
$\varphi_{i,l}$	Scaling function
ξ_i	Slack Variable
Acc	Classification Accuracy
Sen	Classification Sensitivity
Spe	Classification Specificity
Ppr	Classification positive predicitivity
$k(x, x_i)$	Kernel function
x_i	Input Pattern
d_i	Output Pattern

AAMI	Association for the Advancement of Medical Instrumentation
aAP	Aberrated Premature
ANN	Artificial Neural Network
ANOVA	Analysis of Variance
AP	Atrial Premature
AV	Atrio-Ventricular
BFO	Bacteria Foraging Optimization
bpm	Beats per minute
BW	Baseline Wander
CWT	Continuous Wavelet Transform
DAGSVM	Directed Acyclic graph SVM
DCT	Discrete Cosine Transform
DWT	Discrete Wavelet Transform
ECG	Electrocardiogram
EEG	Encephalographic
ELF	Extremely Low Frequency
EM	Electrode Motion
EMD	Empirical Mode Decomposition
FN	False Negative
FP	False Positive
FT	Fourier Transform
fPN	Fusion of Paced and Normal
fVN	Fusion of Ventricular and Normal
ICA	Independent Component Analysis
LBBB	Left Bundle Branch Block
LDA	Linear Discriminant Analysis
LMS	Least Means Square
MA	Motion Artifacts

MLP-BP	Multilayer Perceptron Back Propagation
MLP-NN	Multilayer Perceptron Neural Network
MIT-BIH	Massachusetts Institute of Technology-Beth Israel Hospital
NP	Nodal Junction Premature
NSR	Normal Sinus Rhythm
OAA	One Against All
OAO	One Against One
PAC	Premature Atrial Contraction
PEMF	Pulsed Electromagnetic Field
PNN	Probabilistic Neural Network
PPG	Photoplethysmographic
PSD	Power Spectral Density
PVC	Premature Ventricular
RBBB	Right Bundle Branch Block
RMSE	Root Mean Square Error
SA	Sino-Atrial
SNR	Signal to Noise Ratio
SP	Supra-Ventricular Premature
ST	Stockwell Transform
STFT	Short Term Fourier Transform
SVM	Support Vector Machine
TN	True Negative
TP	True Positive
WNN	Wavelet Neural Network
WT	Wavelet Transform
WVT	Wigner-Ville Transform

List of Figures

List of Tables

Abstract

Electrocardiogram (ECG) plays an important role in patient monitoring and diagnosis due to its ease of use and non-invasive nature. ECG is the record of fluctuation of bioelectric activity of the heart representing the cyclical contractions and relaxations of the human heart muscle. It gives important information about the functional aspects of the heart and cardiovascular system. Detection of heart diseases at an early stage can prolong life through appropriate treatment. It is very difficult for doctors to analyze the long ECG records in very short time and also the human eye is poorly suited to detect the morphological changes of ECG signal continuously. Therefore, a powerful computer aided diagnosis (CAD) system is required for the early detection of cardiac arrhythmia. Abnormality in cardiac beat of the ECG shape is generally called arrhythmia. Arrhythmia is a usual term for any cardiac disorder that differs from normal sinus rhythm. Automatic ECG signal analysis for detection of heartbeats is difficult due to the large variation in morphological and temporal characteristics of ECG waveforms of different patients as well as in the same patients. The aim of this thesis is to process and extract the useful information from ECG signals for automatic beat detection using advanced digital signal processing and pattern recognition techniques. The simple and cost-effective approach for cardiac beat detection from ECG signal has been major motivation of this thesis work. Particularly, we focus on increasing the classification accuracy for detection of ECG beats and are attempting to keep the recognition performance reasonably high even in noisy conditions. The ECG beat classification system consists of the following steps: pre-processing, feature extraction, feature optimization

and classification. In the pre-processing step, it involves following two sub-stages: (i) Normalization: normalizes the amplitude of ECG signals to zero mean and standard deviation of unity which reduces the DC offset and (ii) R-peak detection: helps to determine each cardiac beat of the ECG signal and in turn helps to extract the appropriate features from the ECG signal. The ECG beat classification performances are evaluated to detect the five types of ECG classes of the MIT-BIH arrhythmia database, namely normal (N), ventricular ectopic beat (V), supra ventricular ectopic beat (S), fusion (F) and unknown (Q) as recommended by the Association for the Advancement of Medical Instrumentation (AAMI). First, an efficient feature extraction technique is proposed based on Stockwell transform (ST) for the automatic classification of ECG beat. ST is used here to extract the morphological features which are appended with temporal features. In sequel, least mean square (LMS) based multi-class support vector machine (SVM) classifier is proposed in this work for automatic ECG beat classification. In the proposed technique, the LMS algorithm is used to modify the Lagrange multiplier, which in turn modifies the weight vector to minimize the classification error. The updated weights are used during the testing phase to classify ECG beats. Subsequently, a feature optimization technique based on bacteria foraging optimization (BFO) algorithm is proposed to remove the redundant and irrelevant features. An automatic ECG signal enhancement technique is proposed to remove noise components from the time-frequency domain represented noisy ECG signal. S-transform is used in this work to represent the noisy ECG signal in time-frequency domain. Next, masking and filtering techniques are applied to remove unwanted noise components from the time-frequency domain. The proposed technique does not require any prior information like R-peak position or reference signal like auxiliary signal.

Keywords: Artificial neural network, bacteria foraging optimization (BFO), denoising, electrocardiogram (ECG), heartbeat classification, least mean square algorithm (LMS), MIT-BIH arrhythmia database, S-transform, support vector machine (SVM), wavelet transform.

CHAPTER 1

Introduction

Electrocardiogram (ECG) is a noninvasive technique that is used as a diagnostic tool for cardiovascular diseases [1]. ECG signal is widely used as a fundamental tool for the detection and diagnosis of heart disorders. ECG is the record of variation of bioelectric potential with respect to time as the human heart beats. It provides valuable information about the functional aspects of the heart and cardiovascular system. Since ECG is the most commonly recorded signal for the patient monitoring and examination process, it is important to be reliably and quickly detect the cardiac disorders. ECG can be recorded easily with the help of surface electrodes on the limbs or chest. It is considered a representative signal of cardiac physiology, useful in diagnosing cardiac arrhythmia [2-5]. Abnormality of the ECG shape is usually called arrhythmia. Arrhythmia is a common term for any cardiac rhythm that differs from normal sinus rhythm [4]. Early detection of heart diseases can prolong life and enhance the quality of living through appropriate treatment. It is very difficult for doctors to analyze long ECG records in a short time duration and also the human eye is poorly suited to detect the morphological changes of ECG signal continuously. From the practical point of view, for the effective diagnostics, the study of ECG pattern may have to be carried out over several hours. The volume of the data being enormous, the study is tedious and time consuming and the possibility of missing the vital information is high. Therefore, a powerful computer aided diagnosis (CAD) system is required for the early detection of cardiac abnormality [5].

A number of researchers have reported automated classification and detection of heartbeat patterns based on the features extracted from ECG signals. Most of them use either time or frequency domain representation of the ECG signals as features. Depending on the features, the classification is allowed to recognize between classes. Now-a-days, the automatic ECG signal analysis faces a difficult problem due to a large variation in morphological and temporal characteristics of the ECG waveforms of different patients and the same patients. At different times, the ECG waveforms may differ for the same patient to such an extent that they are unlike each other and at the same time alike for different types of beats. Owing to this, the beat classifiers perform well on the training data but provide poor performance on the ECG waveforms of different

patients. The overall aim of the thesis is to process and extract the useful information from the ECG signal for clinical purposes and automatic cardiac beat detection using digital signal processing and pattern recognition algorithms.

1.1 Human Heart Anatomy

Heart is a muscular organ which pumps oxygenated blood to the whole body through circulatory systems. It receives the impure and deoxygenated blood through the veins and pumps it out to the lungs for purification. Heart is situated in the thoracic cavity medial to the lungs and posterior to the sternum. There are four different chambers in the heart that are right atrium, left atrium, right ventricle, left ventricle. Several atrio-ventricular and sino-atrial nodes are also seen in the heart. Fig. 1.1 represents the blood flow diagram of the human heart. The left and right atria are in the upper chamber of

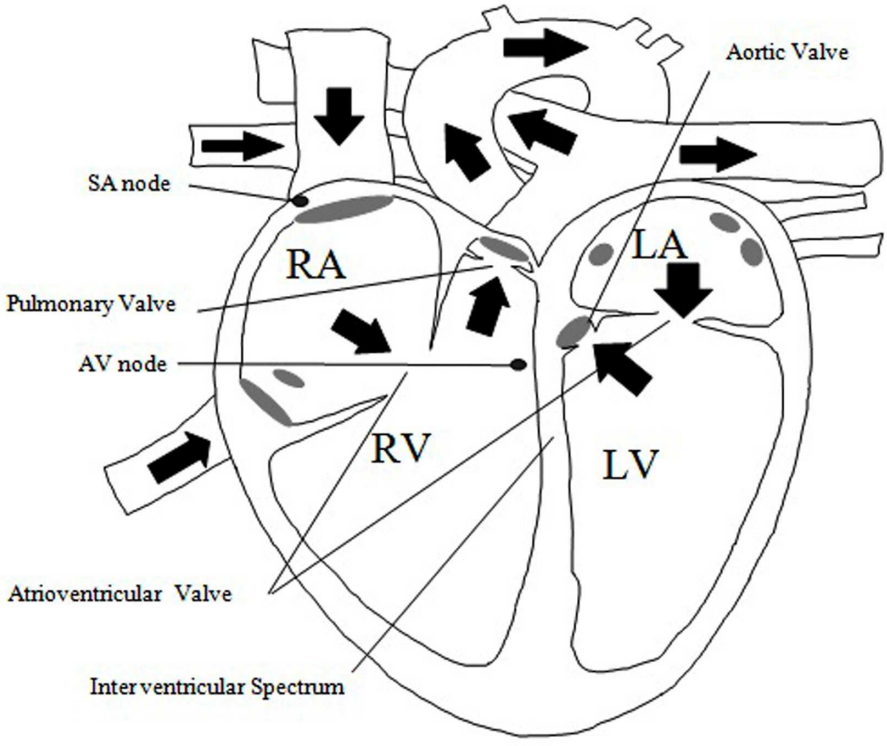

Figure 1.1: Blood flow diagram of the human heart.

the heart whereas left and right ventricles are in lower chamber of the heart. The atria are attached to the ventricles by fibrous, non-conductive tissue that keeps the ventricles electrically isolated from the atria. Deoxygenated blood is received through large veins like the superior and inferior vena cava and flows into the right atrium. The right atrium contracts and forces blood into the right ventricle. At this time, the ventricle is stretched and its pumping (contraction) efficiency is maximized. Then the blood goes from the right ventricle to lungs for purification. Left atrium receives the purified blood from lungs. During atrial contraction the purified blood in left atrium goes to the left ventricle via *mitral* valve, or *bicuspid* valve. The left ventricle contracts and pumps out the purified blood to the rest of the body via aortic valve and aorta [6], [7]. The blood circulating process through heart is divided into two stages: systole and diastole. Systole is defined as the period of the contraction of the heart ventricular muscle whereas the diastole is known as the period of the dilation of the heart ventricular cavities [8]. During diastolic period of the ventricle, the oxygenated blood is reached to the left ventricle from the left atrium by opening of the *mitral* valve and deoxygenated blood is arrived to the right ventricle from the right atrium by opening of *tricuspid* valve. In the systolic period of the heart ventricle, oxygenated blood is pumped out from left ventricle to the body by the opening of *aortic* valve through aorta and deoxygenated blood goes to the lungs from right ventricle by the opening of *semilunar* valve through pulmonary artery. The function of the heart is to contract rhythmically and pump the blood to the lungs for oxygenation and then pump this oxygenated blood for general circulation. This perfect rhythm is continuously maintained by the generated electrical signals of the heart pacemaker.

1.2 Electrocardiogram (ECG) Signal

Electrocardiography is the recording of electrical manifestation of the contractile activity of the heart. The rhythm of the heart is estimated easily as beats per minute (bpm) by counting the readily identifiable waves [9]. Any disorder in the regular rhythmic ac-

tivity of the heart or variation in the morphological pattern is termed as arrhythmia. The typical ECG signal is illustrated in Fig. 1.2. ECG signal consists of P wave, QRS complex, T wave and U wave that contains the useful information about the nature of disease afflicting the heart [6]. P-wave occurs due to the depolarization of atria when

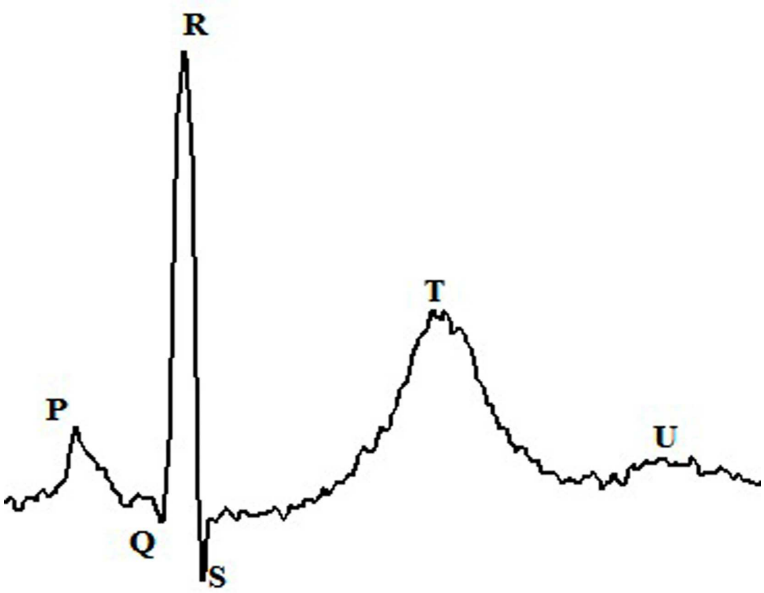

Figure 1.2: The typical ECG waveform.

the blood flows from atria to ventricles. PQ segment generates time of spreading of excitement from atria to ventricles whereas depolarization of ventricles indicates the generation of QRS complex. The blood is pumped out from the right ventricle to arterial pulmonalis and by the left ventricle to aorta. During repolarization of atria, it is overlapped by QRS complex which is invisible on the record. On the other hand, the T-wave occurs during the repolarization of ventricles. Sometimes, the U wave is seen after the T-wave which is generated during the late repolarization of Purkynje fibres in ventricles and which is also invisible [4]. The duration and intervals of different waves is shown in Fig. 1.3. The description of different waves and their duration in ECG signal is given as follows.

P-wave: It is a slow, low amplitude wave, with an amplitude of about 0.1-0.2 mV

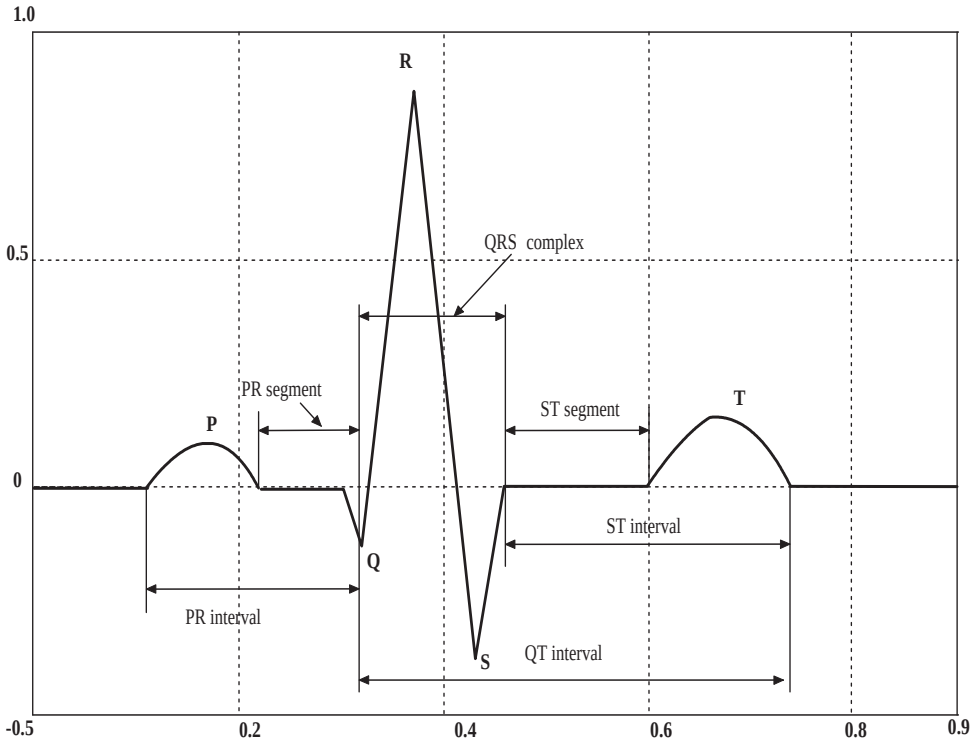

Figure 1.3: Schematic representation of normal ECG signal.

and a duration of about 60-80 ms [4].

PR-interval: The PR-interval is measured from the beginning of the P wave to the beginning of the QRS complex, with a duration 120-200 ms.

QRS complex: The QRS complex is the largest voltage deflection of approximately 1 mV. The duration of the normal QRS complex lies between 60 ms to 100 ms. It does not necessarily contain a Q wave, an R wave and an S wave. By convention, any combination of these waves can be referred to as a QRS complex. The duration, amplitude and morphology of the QRS complex is useful in diagnosing cardiac arrhythmias.

ST segment: The ST segment connects the QRS complex and the T wave with a duration of 0.08 to 0.12 ms. The junction between the QRS complex and ST segment is called J point. The ST segment generally starts at the J point and ends at the beginning of the T wave.

T wave: The amplitude of T wave is 0.1-0.3 mV and duration of 120-160 ms [4]. Medical practitioners use ECG for the following observations. (i) To detect the heart problems or blockages in the coronary arteries; (ii) To diagnose a possible heart attack or other cardiac disorders; (iii) To record the heart rate and regularity of heart beats; (iv) The orientation of the heart in the chest cavity; (v) Evidence of increased thickness and damage to the various parts of the heart muscle.

1.2.1 ECG Signal Acquisition

Electrical activity of the heart is defined as the summation of electrical activity of all heart cells. It can be recorded as changes in the voltage signal appearing on the surface of the body. The heart has its own system for generating and conducting action potentials through a complex change of ionic concentration across the cell membrane [4]. A cell consists of an ionic conductor which is separated by a semi permeable membrane. It acts as the selective ionic filter to the ions. Cells are surrounded by ionic body fluids which can conduct bioelectric signals. These body fluids mainly consist of sodium (Na^+), potassium (K^+) and chloride (Cl^-). The membrane changes its characteristic when a cell is excited by an external stimulus or ionic currents. It allows Na^+ ions to enter the cell which leads to an avalanche effect due to the change in membrane characteristic. As a result, Na^+ ions accelerate into the cell and at the same time the K^+ ions also try to leave the cell as they were in higher concentration inside the cell in the preceding resting state, but are unable to move because movement of K^+ ions is slow compared to the movement of Na^+ ions [10]. In case of resting cell, it is accumulated by positive ions which reverse the polarity. A new state of equilibrium is achieved after the rush of Na^+ ions stops. This change represents the beginning of the action potential which has the peak value of about +20 mV for most cells. When an excited cell achieving an action potential is said to be depolarized then this method is called depolarization. After some time, this depolarized cell becomes polarized again and returns to its resting potential via a process known as repolarization. This repolarization process is similar to depolarization, except that instead of Na^+ ions, the principal K^+

ions are involved in repolarization. As a result, the polarization and depolarization of cardiac tissue is generated by electrical impulses and converts into a waveform is called an ECG signal [10]. ECG signal is obtained from four chest leads and limb leads placed at six different positions of the human body [4]. The right leg is used as the reference position of the electrode. The left arm, right arm and left leg are connected with the lead I, lead II and lead III, respectively. The combination of right arm, left arm and left leg leads forms a combined reference known as Wilson's central terminal [4]. The aVL, aVR and aVF are called augmented limb leads and aV is for augmented lead, L is for the left arm, R is for the right arm and F is for the left foot. The augmented limb leads are obtained from the exploring electrode on the limb indicated by the lead name. The directions of the axes formed by the six limb leads are illustrated in Fig. 1.4 [4]. The Einthoven's triangle is the hypothetical equilateral triangle which is formed by leads I, II and III. Wilson's central terminal indicates the center of the triangle. The six leads measure the projections of the three dimensional cardiac electrical vector on to the axes illustrated in Fig. 1.4 [4]. The projections facilitate the viewing and analysis of the electrical activity of the heart. The positions for the placement of the chest leads are shown in Fig. 1.5. The six chest leads are placed on the standardized positions of the chest where Wilson's central terminal acts as reference. The V1 and V2 leads are kept at the fourth intercostal space just to the right and left of the sternum, respectively whereas the V4 is connected at the fifth intercostal space at the midclavicular line. The V3 lead is placed half way between the V2 and V4 leads. The V5 and V6 leads are connected at the axillary and the midaxillary line respectively, which are the same level as the V4 lead placed. The six leads permit viewing the cardiac electrical vector from different orientations in a cross-sectional plane: V1 and V2 reflect well activity in the right half of the heart, V3 and V4 leads describe the septal activity whereas V5 and V6 are most sensitive to the left ventricular activity [4].

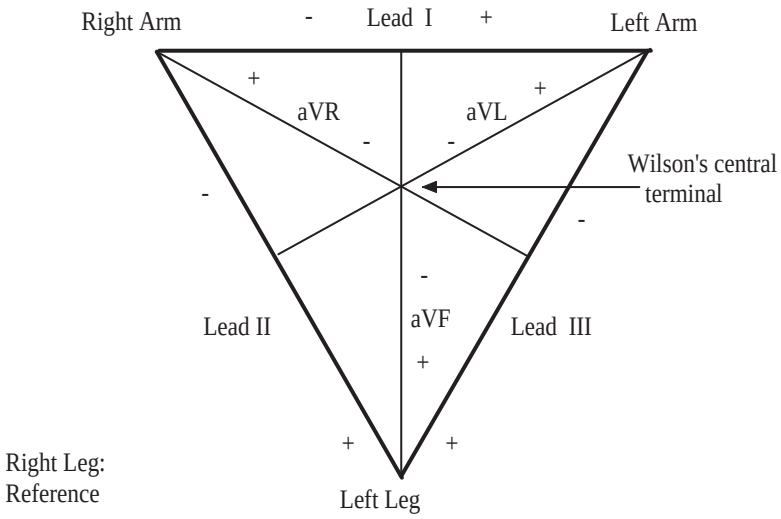

Figure 1.4: Einthoven's triangle and the axes of the six ECG leads formed by using four limb leads.

1.3 Different types of Heart arrhythmia

The normal activity of the heart where there is no deviation or variation in the morphology of ECG signal is called Normal sinus rhythm (NSR). Generally, the normal heart rate lies between 60 to 100 beats per minute. The duration of the R-R interval varies slightly with the breathing cycle. When the heart rate increases above 200 beats per minute, the rhythm is called as sinus tachycardia. If the heart rate is too slow i.e below the normal heart rate then the rhythm is known as bradycardia which can affect vital organs. When the ventricles are not completely filled before contraction due to a fast heart, the pumping efficiency drops and can adversely affect the perfusion. The different types of heart arrhythmias appear due to improper blood circulation. The few arrhythmias [4], [11] are described as follows.

1.3.1 Sinus Node Arrhythmia

Sinus node arrhythmia generates from the sino-atrial (SA) node of the heart. The electrical impulse is generated from the normal pacemaker. The characteristic feature

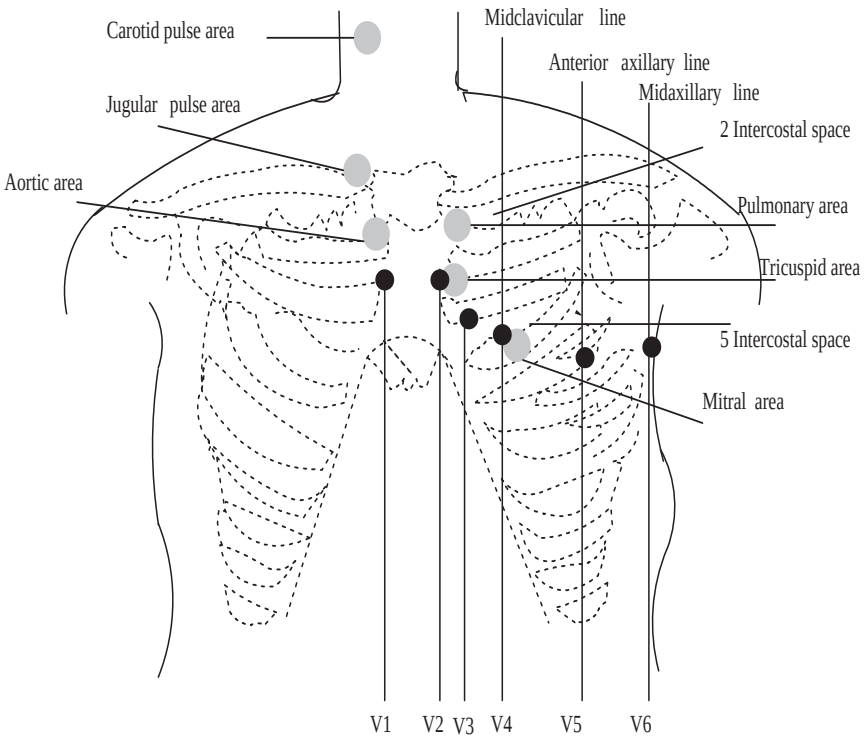

Figure 1.5: Positions for placement of the leads V1-V6 for acquisition of ECG signal.

of these types of arrhythmia is the P-wave morphology. These arrhythmias are as the following types [11]: Sinus arrhythmia, Sinus bradycardia, and Sinus arrest etc.

1.3.2 Premature Atrial Contractions

Premature atrial contractions (PAC) arrhythmia is an abnormal P-wave morphology followed by a normal QRS complex and a T wave. This type of arrhythmia arises when an ectopic pacemaker fires before the SA node. It may occur as a couplet where two PACs are generated successively. The rhythm is called to be atrial tachycardia when three or more successive PACs occur [4].

1.3.3 Junctional Arrhythmia

Junctional arrhythmias originate within the atrio-ventricular (AV) junction in the form of the impulse comprising the A-V node and its Bundle. This arrhythmia is generated due to abnormality of the P-wave and its polarity would be opposite to that of the normal sinus P-wave [11].

1.3.4 Premature Ventricular Contractions (PVC)

Generally, premature Ventricular Contractions (PVCs) arrhythmia generates from the ventricles. It usually does not depolarize the SA node or the atria. Hence, the morphology of P-waves maintains its underlying rhythm which occurs at the expected time. PVCs may occur anywhere in the heartbeat cycle. PVCs are described as isolated if they occur singularly [11].

1.3.5 Bundle Branch blocks

There are two types of bundle branch blocks such as Left bundle branch block beat (LBBB) and Right bundle branch block beat (RBBB). When the bundle branch block becomes injured it may stop conducting electrical impulses appropriately. Due to delayed activation of the left ventricle, the LBBB is generated, which means that the left ventricle contracts later than the right ventricle. A right bundle branch block (RBBB) occurs in the heart's electrical conduction system. An extra deflection shows in the QRS complex which indicates the slow and rapid depolarization of the left ventricle and the right ventricle [11].

1.3.6 Supra-ventricular Arrhythmia

Supra-ventricular and atrial arrhythmias generate in the areas above the lower chambers of heart or at the upper chamber of the heart. It is not a life threatening disease like ventricular arrhythmias and sometimes need not require any treatment. The atrial arrhythmias can happen from the consumption of tobacco, alcohol, caffeine and also

from cough and cold medicines. The rheumatic heart disease or an overactive thyroid gland (hyperthyroidism) indicates that the patient is suffering from supra-ventricular arrhythmia. The shortness of breath, heart palpitations, chest tightness, and a very fast pulse are an indication of supra-ventricular arrhythmia [11].

1.3.7 Atrial Fibrillation

Atrial fibrillation occurs where single muscle fibers in the heart twitch or contract. It is a fast, irregular rhythm. It can be life threatening like stroke which is generally seen in elderly people. The blood is pooled in the heart's upper chambers when the patient suffers with atrial fibrillation. The pooled blood leads to the formation of clumps of blood. The clumps of blood are called blood clots. Many patients with atrial fibrillation need immediate anti-platelet therapy which can prevent blood clots and avoids stroke [11].

1.3.8 Ventricular Escape

The ventricular escape beat lies between 20 to 40 bpm. These beats have the similar morphology as the LBBB or RBBB. The QRS complexes of ventricular escape beat is 120 ms. When the rate of supra-ventricular impulses arriving at the AV node or ventricle is less than the intrinsic rate of the ectopic pacemaker at that time junctional and ventricular escape rhythms occur. Severe sinus bradycardia, sinus arrest, sino-atrial exit block, high-grade second degree AV block, third degree AV block and hyperkalaemia indicate that the patient suffers from junctional and ventricular escape arrhythmias [11].

1.3.9 Junctional Escape

The duration of the QRS complex of junction escape arrhythmia is generally narrow i.e less than 120 ms. There is no relation between the QRS complexes and any preceding atrial activity (e.g. P-waves, flutter waves, fibrillatory waves). The rhythm rate of the arrhythmia is below the normal heart rhythm i.e 40-60 bpm [11].

1.4 A Brief Review of the ECG Signal Analysis

ECG signal conveys information regarding the electrical function of the heart by altering the shape of its constituent waves like P, QRS and T waves. Numerous techniques have been developed to recognize and analyze these waves using digital filtering techniques, neural network and spectro-temporal techniques [12–14]. Cardiologist takes more time to diagnose the heart disease using his naked eye. Moreover, human interpretations are poorly suited to diagnose heart diseases using ECG signal. Computerized analysis of the ECG signal could be performed much more accurately than interpretation by the unaided hand and eye [15]. Automated ECG beat classification was traditionally performed using a decision-tree-like approach, based on various features extracted from an ECG beat. It is observed that ECG feature extraction methods can be divided into two functional groups: direct method and transformation method [16]. In direct method, the features include the width and height of QRS complex, RR interval, QRS complex area, etc. On the other hand, in transformation method, the signals are transformed to obtain further information that is not readily available in the raw ECG signal. Feature vectors are formed by using this transformation. We observed that there exist two promising methods in the literature to extract features from the ECG: (i) Fourier transform [17–20], and (ii) wavelet transform [17], [21–23]. R. Haberl *et al.* [24] presented spectral mapping of the ECG signal with Fourier transform for the identification of patients with sustained ventricular tachycardia and coronary artery disease. T. Olmez [25] classified four types of ECG waves by using Fourier transform based features. Fourier transform analysis provides the signal spectrum or range of frequency amplitudes within the signal. However, Fourier transform only provides the spectral components, not their temporal relationships. As the morphological characteristics and the frequency content of the ECG signal varies in time, the analysis of the ECG signal according to time variation is also equally important to properly describe the ECG signal characteristics. This justifies the use of time-frequency representation in quantitative analysis of ECG signal.

Valtino X. Afonso *et al.* [26] reported an algorithm for the classification of arrhythmia that can distinguish shockable cardiac rhythms from non-shockable cardiac rhythms. This reported technique uses the time-frequency domain analysis based on short time Fourier transform (STFT) to compute the energy distribution of the ECG signal. Features are extracted from this energy and are used for the classification algorithm. STFT belongs to a group of joint time-frequency representations which comes from the two dimensional analyzing function. This is well-localized in both time and frequency domain. However, STFT cannot track the very sensitive sudden changes of the signal in time direction. To minimize this problem, it is necessary to keep the length of the time window as short as possible. This again reduces the frequency resolution in the time-frequency plane. Hence, there is a trade-off between time and frequency resolutions for this technique, and thus, the features are limited by the accuracy of the frequency distribution [26, 27]. Wavelet transform is an efficient tool for analyzing non-stationary ECG signals due to its time-frequency localization property. In wavelet, good time resolution and poor frequency resolution is found at high frequencies and good frequency resolution and poor time resolution is obtained at low frequencies [17]. Furthermore, the wavelet transform has demonstrated the ability to analyze the ECG signal more accurately than STFT in some pathological cases [17]. The wavelet transform can be used to decompose an ECG signal according to scale, thus allowing separation of the relevant ECG waveform morphology descriptors from the noise, interference, baseline drift, and amplitude variation of the original signal. Several researchers have used the wavelet transform for feature extraction while avoiding the aforementioned limitations [3, 17, 21–23]. Z. Dokur *et al.* [17] presented a comparison of discrete wavelet and Fourier transforms for ECG beat classification and have shown that the discrete wavelet transform is superior to the Fourier transform for ECG beat classification. In [3, 28, 29], the wavelet transform coefficients are used at the appropriate scales as morphological feature vectors of ECG signal and achieved significant classification performance.

1.4.1 Brief overviews of ECG beat classification system

The goal of the ECG beat classification system is to extract, characterize and recognize the information about cardiac diseases from ECG signals. The process of ECG beat classification system is divided into two main phases: enrolment or training phase and recognition or testing phase. A typical ECG beat classification system is shown in Fig.1.6. Both phases include the same preprocessing, feature extraction and optimization steps. The ECG beat classification system consists of the following steps: pre-processing, feature extraction, feature optimization and classification. In the preprocessing step, it involves following two sub-stages: (i) Normalization: normalizes the amplitude of ECG signals to zero mean and standard deviation of unity which reduces the DC offset and (ii) R-peak detection: helps to determine the each cardiac beat of the ECG signal and in turn helps to extract the appropriate features from ECG signal [30]. In the feature extraction stage, feature vectors are extracted from each beat of the ECG signal to represent the specific characteristic of the cardiac beat. Feature extraction technique also reduces the dimension of raw signal in a compressed manner as it will be applied to the input of the classifier. Generally, following features are used for cardiac beat classification: heart beat interval features [31], [32] frequency based features [33], higher order cumulant features [34], Hermite polynomials [35] etc. The extracted feature vectors are further optimized by removing the redundant and irrelevant features. The basic idea of feature optimization is to reduce the computation at the time of testing while achieving the best performance through the chosen optimal set of features. It involves definition of the most informative and discriminative features of the original data for classification. This can be performed by eliminating the redundant, uninformative, and noisy features. Feature optimization technique can carry out the following advantages for a ECG beat detection system: (i) a faster induction of the final classification mode, and (ii) an improvement in the classification accuracy [36]. The optimized feature vector is applied to the input of the classifier for detection of ECG beats. During the enrolment phase, the optimized feature vectors of different ECG beats are used to train the ECG beat models. The collection of enrolled models is also called an

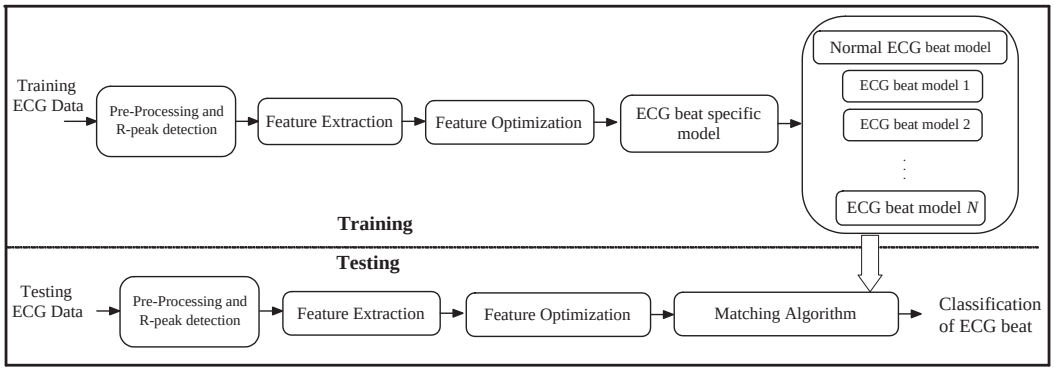

Figure 1.6: Block diagram of the ECG beat classification system.

ECG beat model database. In the recognition phase, an unknown beat of ECG signal is compared against a known ECG beat, and the best matching ECG beat determines the class of unknown beat of ECG signal. Multi-layer perceptron back propagation (MLP-BP) neural network [32, 34, 37, 38] technique is generally used for this application for its discriminative training characteristics, ability to approximate function, simple structure to implement on hardware platform.

In the last decade, a number of researchers have reported different automatic ECG classification techniques [16, 23, 39–61]. In [23], the authors developed highly accurate algorithms for detecting PVC beat, normal and other beats where wavelet-transformed ECG waves with timing information is used as feature set. The classification accuracy is 95.16% over 93,281 beats from all 40 files, and 96.82% over the 22 files outside the training set in differentiating normal, PVC, and other beats. An efficient system for recognition of the premature ventricular contraction from the normal beats and other heart diseases is reported in [39] and achieved an accuracy of 97.14% using twelve files from MIT-BIH database for ECG classification. The ECG beat classification system based on higher order statistics of subband components and an MLP-BP neural network are described in the literature [40] and achieved the classification accuracy of 96.34%. In [41], a combination method based on the mixture of complementary features and negative correlation learning methods are introduced for classifying the normal heartbeats, premature ventricular contraction (PVC) arrhythmias and other abnormal-

ities and achieved accuracy of 96.02%. The MLP-BP neural network classifier is used in [42] to classify four types of ECG beats (normal beat, congestive heart failure beat, ventricular tachyarrhythmia beat, atrial fibrillation beat) using combined feature set of Lyapunov exponents, wavelet coefficients and the power levels of power spectral density (PSD) values obtained by eigenvector methods of the ECG signal and achieved an average accuracy of 93.89%. A novel supervised neural network-based algorithm is designed to reliably distinguish in ECG records between normal and ischemic beats of the same patient using European ST-T database in [43]. In [44], the four types of ECG beats are classified using the discrete wavelet transform based feature set with combined neural network. A Grey ART-based ECG beat classifier is developed in [45] to classify the four types of ECG beats. This ECG classification method includes two phases: the off-line learning phase and the on-line examining phase and achieved an average accuracy of 98.41% using 44 ECG records of MIT-BIH arrhythmia database. In [46], a technique based on MLP-BP and combined features of discrete wavelet transform and morphology features, are proposed to classify the two types of ECG classes (normal and abnormal class) using the MIT-BIH arrhythmia data base. The fuzzy-hybrid neural network based classifier is reported in [47] to classify the four types of ECG beats (N, Non-conducted P wave, PVC and RBBB beat) using autoregressive model coefficients, higher-order cumulant and wavelet transform variances based features and the classification experiment is conducted on the small data base obtained from the MIT-BIH arrhythmia database.

In [16], a classifier is developed based on hybrid neural network to classify the ten types of ECG beats using two feature extraction methods: Fourier and wavelet transform and an accuracy of 96% is achieved. In [48], six types of beats including normal beat, PVC, fusion of ventricular and normal beat, atrial premature beat (A), RBBB beat and fusion of paced and normal beat obtained from the MIT-BIH arrhythmia database, are classified using particle swarm optimization and radial basis function neural network. A combined fuzzy clustering neural network algorithm for classification of ECG arrhythmias using type-2 fuzzy c-means clustering (T2FCM) algorithm and neural network are reported in the literature [49] to classify the ten types of ECG arrhythmias (normal

beat, sinus bradycardia, ventricular tachycardia, sinus arrhythmia, atrial premature contraction, paced beat, RBBB, LBBB, atrial fibrillation and atrial flutter) obtained from MIT-BIH database. The classification experiments are conducted using the small database taken from MIT-BIH arrhythmia data base. In [50], a comparative study of the heartbeat classification abilities of two different ECG feature extraction techniques is presented and five types of heatbeat (normal beats, RBBB, LBBB, PVC and paced beats) are classified in the reported work using K^{th} nearest neighbor rule. In [51], a new neural network model with adaptive activation function (NNAAF) is implemented to classify the ten types of ECG arrhythmias and achieved an average accuracy of 98.19%. An ECG arrhythmia classification scheme consisting of a feature reduction method combining principal component analysis (PCA) with linear discriminant analysis (LDA) is reported to classify the eight different types of arrhythmia from ECG beats using a probabilistic neural network (PNN) classifier and achieved an average classification accuracy of 99.71% in [52]. A novel independent components (ICs) arrangement strategy to cooperate with the independent component analysis (ICA) method is used for eight types of ECG beat classification and achieved the classification accuracy more than 98.7% [53]. ECG arrhythmia recognition via a neuro-support vector machine-kNN hybrid classifier with virtual QRS image-based geometrical features is used in the literature [54] and this learning machine is applied to seven arrhythmias belonging to fifteen different records and achieved an accuracy of 98.06%. The wavelet transform and particle swarm optimization techniques are used to classify the six types of ECG beats (normal (N), RBBB, LBBB, PVC, APC and paced beats (PB)) and achieved an average accuracy of 88.84% in [55]. In [56], the six types of ECG beats (N, LBBB, RBBB, APC, VPC, and PB) are classified using local fractal dimension based nearest neighbor classifier. In [57], the experimental pilot study is presented to investigate the effects of pulsed electromagnetic field (PEMF) at extremely low frequency (ELF) in response to photoplethysmographic (PPG), electrocardiographic (ECG), electroencephalographic (EEG) activity using discrete wavelet transform based feature set. A comparative study of DWT, CWT and DCT transform on ECG arrhythmia classification are presented and classified five ECG

beats using limited number of ECG beats of the MIT-BIH database [58]. The k-NN algorithm is used to classify the five types of heart beat using higher order statistics (HOS) of wavelet packet decomposition (WPD) coefficients based feature set [59]. The classification performance which is reported in [59] as average sensitivity of 90%, average selectivity of 92% and average specificity of 98%. An ECG beat classification system is introduced based on wavelet transform and probabilistic neural network (PNN) to discriminate six types of ECG beats and shown an accuracy of 99.65% [61].

The abnormal electrical activity of the heart rate or rhythm, or variation in the morphological pattern is known as arrhythmia. It could be diagnosed by the analysis of recorded ECG waveform. Therefore, a number of literatures is reported for the detection of cardiac arrhythmias using ECG signal. Most of them use either time or frequency domain representation of the ECG signals, on the basis of which many features are defined and allowed the recognition between the different classes. However, these reported techniques did not follow any internationally accepted standard and recommendation. The performance of these techniques are also inconsistent particularly when a new patient's ECG signal is added to the test dataset. Therefore, these techniques are not suitable for clinical application. Association for the Advancement of Medical Instrumentation (AAMI) recommended a standard for ECG beat classification to detect cardiac arrhythmias using ECG signal. In this AAMI standard, different types of cardiac arrhythmias of MIT-BIH database are divided into five types of ECG beat classes. Few algorithms for automatic classification and detection of ECG heartbeat pattern as per AAMI standard have been reported in the literature [3,31,62,63]. In [31], a classifier based on mixture of experts (MOE) is developed using the combination of local classifier and global classifier. In this reported technique [31], the local classifier requires a cardiologist to annotate a segment of patient specific ECG signal and achieved an accuracy of 94.0% in distinguishing the two classes of ECG beats. In [62], the morphological and temporal features are extracted to classify the five classes of ECG beats using linear discriminant classifier and achieved a lower average accuracy of 85.9%. The disadvantage of this method [62] is that this fixed classification method did not take any variation

in ECG pattern caused by personal or environmental differences. In [63], Jiang *et al.* have used the Hermite transform coefficients and time intervals between two neighboring R-peaks of ECG signals based features and block based neural network (BbNN) as a classifier and detected five types of ECG beat with an accuracy of 96.6%. In this method, there are around 10-15 parameters/thresholds which are set empirically with respect to the dataset used. Another problem of this method is that the reported BbNN classifier requires equal sizes for input and output layers. In [3], wavelet transform based morphological feature set combined with direct RR-interval based temporal feature set and MLP-BP classifier are used to detect the five types ECG beats. Wavelet transform has few limitations like better frequency resolution and poor time resolution for low frequencies and vice versa for high frequencies. Another difficulty of wavelet analysis is its non-adaptive nature. Once the basic wavelet is selected, one needs to use it to analyze all the ECG data. The reported technique [3] considers only the fourth level of decomposition where frequency range lies between 4 Hz-22 Hz using Daubechies-2 wavelet although ECG signal frequency lies between 0.5 Hz to 100 Hz. This reported technique [3] takes only RR-interval as temporal feature which is not sufficient for the classification of different ECG beats. The different ECG arrhythmias have different time duration of P-wave, QRS complex and T-wave. Two ECG arrhythmias may have similar morphology and same RR timing interval information but their other timing information may be different [23]. For example, fusion beats are difficult to distinguish from normal beats because fusion beats are the union of ventricular and normal beats and their morphology and timing information (RR-interval) also closely resembles those of normal beats [23]. Therefore, in addition to direct RR interval, other temporal features like pre RR interval, post RR interval, average RR interval and local RR interval are also equally important for ECG beat classification. In general, ECG signal classification techniques based on past approaches have not performed well due to their inconsistent performance when classifying a new patient's ECG waveform. This makes them unreliable to be widely used clinically, and causes severe degradation in their performance for larger database [62].

Since, ECG is the most commonly recorded signal for the patient monitoring and examination process, it is important to be able to reliably and quickly detect the cardiac disorders. During acquisition and transmission, ECG signals are generally affected by different noises like channel noise, muscle artifacts, electrode motion and baseline wander. ECG would be much more useful as a diagnostic tool if unwanted noise embedded in the signal is removed. Many researchers have been reported to address the ECG signal enhancement. Most of the studies focused their attention to remove very common sources of noises like white noise or one (or two other noises). The traditional approaches for ECG enhancement include filter banks [64,65], low pass filters [66], extended Kalman filter [67], empirical mode decomposition (EMD) [68], state vectors with time delay [69]. Wavelet transform is also used for noise reduction from ECG signal [70, 71]. In [72], a modified wavelet transform is also reported for denoising the ECG signal and shown a small improvement of signal to noise ratio (SNR) over traditional wavelet transform. In [73], a thresholding scheme for multichannel electrocardiogram (MECG) signal based on local kurtosis and wavelet transform is reported to denoise the ECG signal. A nonlinear Bayesian filtering framework is reported in [74] for the filtering of single channel noisy ECG recordings. Two types of noises, Gaussian noise and muscle artifact noise, are considered in this work for ECG signal enhancement [74]. An approach for ECG signal noise removal based on wavelet neural network (WNN) is investigated in [75, 76]. It is shown that WNN can successfully remove white noise; however, more complicated situations (such as baseline drift, electrode contact artifact, muscle contraction noise, etc.) are not considered. Typically, these above techniques are involved only for cases where the ECG signal is contaminated either by white Gaussian noise or one or two other types of real noise. However, ECG signals are also contaminated with other wide range of noises which is a major concern. Another problem is the selection of the threshold value. Many methods exist for choosing the value of threshold, S-median is one of them [70]. Although in [70], a S-median based algorithm is reported for selecting the threshold, but it has some drawbacks. In S-median based algorithm, the tuning factor b is selected as unity in most of the cases, but optimal value of b is desirable for denoising.

Another factor is the level dependent adaptation factor which is absent in the existing S-median thresholding algorithm.

The above reported techniques have following drawbacks: (i) In general, all these methods have not performed well due to their inconsistent performance when classifying a new patient's ECG waveform, (ii) most of these techniques are tested only on limited ECG database and the generalization performances of these methods on large databases are not tested, (iii) despite many ECG beat classification methods reported in the earlier literature, only few have followed an international standard like, ANSI/AAMI EC57:1998, (iv) most of them use either time or frequency domain representation of the ECG signals, on the basis of which many features are defined and applied for ECG beat classification.

1.5 Contribution in the thesis

This thesis deals with the analysis of ECG signal for the classification of heart beats. The major contributions of the thesis can be summarized as follows:

- Proposition of a novel feature extraction technique based on Stockwell transform (S-transform). Generally, the wavelet transform is used as feature extraction technique for ECG beat classification because of its ability to characterize time-frequency information. Sometimes, the interpretation of the wavelet can also be counter intuitive for ECG signal analysis. It is only capable of probing the local amplitude or power spectrum. If a local event occurs only in the low frequency range of the ECG signal, one will still be forced to look for its effect in the high frequency range of the signal. Such interpretation will be difficult to analyze an ECG signal from a wavelet based method. Another difficulty of wavelet analysis is its non-adaptive nature. Once the basic wavelet is selected, one needs to use it to analyze all the ECG data. Therefore, S-transform based feature extraction technique is proposed in this work because it has following advantages to overcome the above mentioned drawbacks of wavelet transform: (i) Frequency invariant am-

plitude response, (ii) progressive resolution and (iii) absolutely referenced phase information. In addition, ST represents the signal in the time-frequency domain, rather than the time-scale axis used in WT. Therefore, interpretation of the frequency information in the ST is more straightforward than that in the WT. This will be beneficial in extracting the important features from the ECG signal. In this chapter, two types of features are extracted from ECG signal: (i) Temporal features: Four different temporal features that are pre RR interval, post RR interval, average RR interval and local RR interval are extracted from the ECG signal. (ii) Morphological features: Morphological changes of the ECG beats are considered by these features. Combined features which couple the morphological features with temporal features, are more constant among patients and are proposed in this work in order to achieve high classification performance for larger datasets.

- Proposition of least mean square (LMS) based multi-class support vector machine (SVM) classifier for ECG beat detection. Many researchers use MLP-NN classifier, SVM classifier for classification of ECG beats. The MLP-NN classifier has some following limitation (i) it suffers from slow convergence to local and global minima and from random settings of weights, initial values, (ii) selection of hiddne nodes. On the other hand the SVM classifiers do not trap in local minima points and need less training input therefore they are faster than ANN. In this work, the goal of this proposed LMS based multiclass SVM is to project the data into higher dimensional input space where the different classes become linearly separable to reconstruct an optimal separating hyperplane. The proposed technique relies on the basic idea that in order to improve the performance of multi-class SVM, the pattern separability or margin between the clusters needs to be increased. To implement this idea, LMS algorithm is adopted to update the adjustable weights at training phase such that the classification error will be minimized and width of the separation region between the clusters will be increased. The updated weights are used during the testing phase to classify ECG beats. The LMS algorithm is

generally the best choice because of its simplicity, ease of computation, and that it does not require off-line gradient estimations or repetitions of data.

- Proposition of an optimization technique to select a subset of features for ECG beat classification by eliminating the redundant and irrelevant features. The basic idea of feature selection is to reduce the computation at the time of testing while achieving the best performance through the chosen optimal set of features. It involves definition of the most informative and discriminative features of the original data for classification. In this chapter, Bacteria Foraging Optimization (BFO) algorithm is applied in this work to reduce the dimension of the combined feature set which couples morphological and temporal features. The BFO technique is used in this thesis because it can deal with complex search spaces in situations where only minimum knowledge is available, and it converges quickly in order to reach the global minimum solution.

- Proposition of an automatic ECG signal enhancement technique to remove noise components from time-frequency domain represented noisy ECG signal. The ST uses time-frequency axis rather than the time-scale axis used in the WT. Therefore, the interpretation on the frequency information in the ST is more straight forward than in the WT, which will be beneficial to remove noise components. ST is used to represent the noisy ECG signal in time-frequency domain. The noise components are removed from the time-frequency domain represented noisy ECG signal by automatic binary masking and filtering. The proposed technique does not require any reference signal as auxiliary signal or prior information like R-peak position.

1.6 MIT-BIH Database Description

Since 1975, the Boston's Beth Israel Hospital (now the Beth Israel Deaconess Medical Center) and Massachusetts Institute of Technology (MIT) have supported their own research for ECG arrhythmia analysis. One of the first major products of that effort

Table 1.1: Five categories of ECG beats based on AAMI recommendation.

AAMI CLASS	**MIT-BIH Heart Beat Types**				
Normal beat (N)	Normal beat (N)	Left bundle branch block beat (L)	Right bundle branch block beat (R)	Atrial escape beat (e)	Nodal (junctional) escape beat (j)
Supra ventricular ectopic beat (S)	Atrial premature beat (A)	Aberrated atrial premature beat (a)	Nodal (junctional) premature beat (J)	Supraventricular premature beat (S)	- -
Ventricular ectopic beat (V)	Premature ventricular contraction (V)	Ventricular escape beat (E)	- -	- -	- -
Fusion beat (F)	Fusion of ventricular and normal beat (F)	- -	- -	- -	- -
Unknown beat (Q)	Paced beat (/)	Fusion of paced and normal beat (f)	Unclassified beat (Q)	- -	- -

is the MIT-BIH Arrhythmia Database, which they completed and began distributing in 1980. Apart from ECG abnormality detection, the database is also helpful in the basic study of cardiac dynamics. Moreover, MIT-BIH Arrhythmia database has become a worldwide standard for ECG signal analysis and beat detection. The MIT-BIH arrhythmia database contains 48 ECG recordings [77], each containing 30 min segment selected from 24 hrs recordings of 47 individuals studied by the BIH Arrhythmia Laboratory between 1975 and 1979. Twenty-three recordings are taken at random from a set of 4000 24 hours ambulatory ECG recordings collected from a mixed population of inpatients (about 60%) and outpatients (about 40%) at Boston's Beth Israel Hospital; the remaining 25 recordings are selected from the same set to include less common but clinically significant arrhythmias that would not be well-represented in a small random sample [77]. Each ECG signal is passed through a band pass filter at 0.1-100 Hz and sampled at 360 Hz. Four recordings of MIT-BIH ECG database contain mostly paced beats. According to the Association for the Advancement of Medical Instrumentation (AAMI) recommended practice, these paced recordings are excluded in the experimental evaluation process because these recordings do not retain sufficient signal quality for reliable processing [3], [78]. This recommended practice provides a protocol for a reproducible test with realistic clinical requirements, and emphasizes record-by-record presentation of results that reflect an algorithm's ability to detect events of clinical significance [78]. Forty four recordings from the MIT-BIH arrhythmia database are used for performance assessment. The AAMI convention is used to combine the beats into five classes of interest which is shown in Table 1.1 [2], [78]. It is observed from the

Table 1.1 that the normal beat, left bundle branch block (LBBB), right bundle branch block (RBBB), atrial escape and nodal junction escape beats belong to class N category whereas class V contains premature ventricular contraction (PVC) and ventricular escape beats. Class S consists of atrial premature (AP), aberrated premature (aAP), nodal junction premature (NP) and supra-ventricular premature (SP) beats. Class F contains only fusion of ventricular and normal (fVN) beats where class Q is represented as unknown beat contains paced beat (P), fusion of paced and normal (fPN) beats and unclassified beats. As per AAMI recommendations, the number of different beats in each MIT-BIH ECG recording is shown in Table 1.2. In this thesis, 44 recordings of MIT-BIH arrhythmia database are considered for the classification of five heartbeat types as recommended by the AAMI standards. It is noticed from Table 1.2 that 7 beats of class Q and 13 beats of class F are only available in the record number 100-124 and in the record number 200-234, 8 beats of class Q are only available. It is also seen from the Table 1.2 that the number of beats in class N is comparably more than that of the other classes. As an example, five different types of AAMI recommended ECG beats are shown in Fig. 1.7.

1.7 Organization of the thesis

The thesis is organized as follows:

Chapter 1 represents the introduction which includes the motivation for the work, a review of the operation of heart anatomy and the associated terminology, different types of hear arrhythmias, an introduction of the ECG signal and its acquisition, a brief review of the ECG signal analysis, an overview on ECG beat classification, a brief literature survey, description of the databases, and an outline of the work reported in the thesis.

Chapter 2 presents the preprocessing step and also proposes a novel feature extraction technique based on S-transform. The theoretical background of the wavelet transform and S-transform and the methodology for extraction of temporal and mor-

Table 1.2: Number of different beats in each ECG recording as per AAMI recommendation.

AAMI standard						
Data(MIT-BIH)	N	S	V	F	Q	Total
100	2239	33	1			2273
101	1860	3			2	1865
103	2082	2				2084
105	2526		41		5	2572
106	1507		520			2027
108	1740	4	17	2		1763
109	2492		38	2		2532
111	2123		1			2124
112	2537	2				2539
113	1789	6				1795
114	1820	12	43	4		1879
115	1953					1953
116	2302	1	109			2412
117	1534	1				1535
118	2166	96	16			2278
119	1543		444			1987
121	1861	1	1			1863
122	2476					2476
123	1515		3			1518
124	1536	31	47	5		1619
200	1743	30	826	2		2601
201	1635	128	198	2		1963
202	2061	55	19	1		2136
203	2529	2	444	1	4	2980
205	2571	3	71	11		2656
207	1542	107	210			1859
208	1586	2	992	373	2	2955
209	2621	383	1			3005
210	2423	22	195	10		2650
212	2748					2748
213	2641	28	220	362		3251
214	2003		256	1	2	2262
215	3195	3	164	1		3363
219	2082	7	64	1		2154
220	1954	94				2048
221	2031		396			2427
222	2274	209				2483
223	2029	73	473	14		2589
228	1688	3	362			2053
230	2255		1			2256
231	1568	1	2			1571
232	398	1382				1780
233	2230	7	831	11		3079
234	2700	50	3			2753

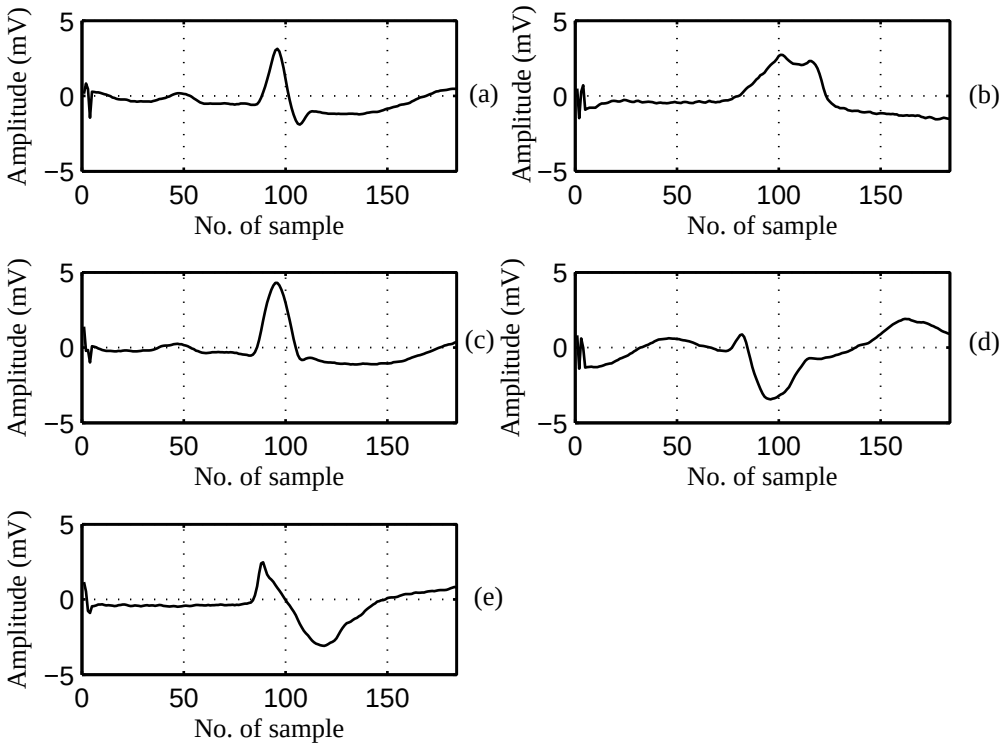

Figure 1.7: Five different types of ECG beats as per AAMI standard (a) Normal (N) (b) Supra ventricular ectopic (S) (c) Ventricular ectopic (V) (d) Fusion (F) (e) Unknown (Q), respectively.

phological features are also discussed in this chapter. Experimental results are presented and discussed in detail.

Chapter 3 presents the ECG beat classification using multi-class SVM. Theoretical background of SVM, multi-class SVM, LMS algorithm is discussed here. In addition, LMS based multi-class SVM is also proposed in this chapter to improve the performance of the ECG beat classification. The experimental results are shown and finally the measured results are presented and compared with previously reported techniques.

Chapter 4 discusses the reduction of features using Bacteria Foraging Optimization (BFO) technique. The BFO algorithm is presented in this chapter. The utility of BFO in optimizing the feature vector is presented in detail in this chapter. The performance of ECG beat classification using BFO is also mentioned in this chapter.

Chapter 5 shows the ECG signal enhancement technique using S-transform. The description of different types of noise like channel noise, muscle artifacts, electrode motion and baseline wander that are generally embedded with ECG signals during acquisition and transmission are shown in this chapter. The methodology for S-transform based ECG enhancement technique is described in detail in this chapter. Experimental results are evaluated and compared with earlier reported techniques. The enhanced signal is also applied for ECG beat classification.

Chapter 6 draws the principal conclusions on the work and discusses the scope of future work in the same and further improvements.

CHAPTER 2

Preprocessing and Feature Extraction of ECG Signal

2.1 Introduction

Electrocardiogram (ECG) is a non-invasive tool and is widely used to diagnose cardiac abnormalities. Feature extraction is an important step in designing the classification system since even the best classifier will not give an optimal performance if efficient features are not selected. Therefore, performance of ECG beat classification system is also very much dependent on the extracted feature vectors. A feature is a distinctive or characteristic measurement, transform, structural component which is extracted from a segment of a pattern. Features are used to represent patterns without losing the important information. Feature extraction is the generation of a feature or a feature vector from a pattern or object. Feature extraction is mainly based on either (1) best representation of a given class of signals, or (2) best distinction between classes [57]. Different types of features like temporal, frequency, statistical etc. which represent the ECG signal, can give the basic idea of the underlying heart condition. A number of ECG beat classification techniques have been reported by earlier researchers using different types of features [23], [29], [33], [42], [57], [58] and [79]. Most of the researchers have used wavelet transform in time-frequency domain for feature representation of ECG signal [23], [29], [33], [57], [58] and [79]. In [57], discrete wavelet transform (DWT) based features are used for the experimental study to obtain the effects of pulsed electromagnetic field (PEMF) at extremely low frequency (ELF) in response to photoplethysmographic (PPG), ECG and electroencephalographic (EEG) activity. In [23], wavelet transform and timing interval based feature extraction techniques are used to classify the three classes of ECG beats such as normal, premature ventricular contraction and other beats and achieved an average accuracy of 95.2%. Senhadji *et al.* [33] reported DWT based features for ECG signal classification technique where 25 beats for training and 28 beats for testing are used and achieved a performance accuracy of 98%. Shyu *et al.* [29] classified PVC beat using DWT based feature vectors and achieved 97.04% performance accuracy. Four types of ECG beats are classified using wavelet coefficients based feature set in [79]. A comparative study of DWT, continuous wavelet

transform (CWT) and discrete cosine transform (DCT) on ECG arrhythmia classification for a limited number of ECG beats are presented in [58]. These techniques do not follow any internationally recommended standard. These approaches are not applicable to clinical use due to their inconsistent performance when classifying a new patient's ECG waveform.

Thus, the wavelet transform so far, has remained popular in extracting feature vectors from ECG signal because of its ability to characterize time-frequency information which is important in this context [29]. Sometimes, the interpretation of the wavelet can also be counter intuitive for ECG signal analysis. For example, to define a change occurring locally in an ECG signal, one must look for the result in the high frequency range of the signal, for higher the frequency the more localized the basic wavelet will be. If a local event occurs only in the low frequency range of the ECG signal, one will still be forced to look for its effect in the high frequency range of the signal. Such interpretation will be difficult to analyze an ECG signal from a wavelet based method [80]. Another difficulty of wavelet analysis is its non-adaptive nature. Once the basic wavelet is selected, one needs to use it to analyze all the ECG data.

In this chapter, a novel feature extraction technique based on S-transform (ST) is proposed to classify the ECG beat [81]. Here, two types of features are extracted from the ECG signal: (i) temporal feature, (ii) morphological feature. The temporal features are extracted directly from the time series of ECG signal whereas morphological features are extracted from ST due to its ability to characterize the time-frequency domain information [82]. The proposed feature extraction technique combines the ST based morphological feature set and temporal feature set as pre-RR interval, post-RR interval, average RR interval and local RR interval. DWT based morphological features with one temporal feature as direct RR interval are used to classify the ECG beats in reported literature [3]. One temporal feature like direct RR interval is not enough for classification of ECG beats. Two arrhythmias may have similar morphology and direct RR time interval but other temporal information like pre-RR interval, post-RR interval, average RR interval and local RR interval may be different. For example, the

morphological structure and timing information as direct RR-interval of fusion beat closely resembles than normal beat but other timing information like pre-RR interval, post-RR interval, average RR interval and local RR interval are different with normal beat [23]. Therefore, different types of temporal features such as pre-RR interval, post-RR interval, local RR interval and average RR interval are required for better ECG beat classification. In [57], ECG beats are classified using DWT based features. This reported technique uses Daubechies-2 wavelet decomposition upto fourth level. Thus, four sets of detail coefficient-D1, D2, D3 and D4 as well as one set of approximation coefficients– A4, are taken. The reported literature [3] took the detail coefficient D4 (frequency range 4 Hz-22 Hz) as the only morphological feature where only QRS complex energy lies in that decomposition level. The normal and abnormal ECG signal frequency lies between 0.5 Hz to 200 Hz. Morphological pattern of P-wave and T-wave is also important for ECG beat classification. Therefore, in addition to detail coefficient D4 other decomposition coefficients are also required for ECG beat classification. Another drawback of the reported literature [57] is that they did not take any timing information as a feature. The timing information is also necessary with the morphological information for proper ECG beat classification [23]. For example, the atrial premature beat in the S class has same morphology as that of the normal beat but their timing information such as pre-RR interval, post-RR interval, local RR interval and average RR interval are different. Another example is that the Wenckebach-type AV block waveform of S beat is similar morphology with normal beats where their timing information is different [23]. Hence, timing information is also necessary for ECG beat classification. Therefore, in this work a combined feature set is proposed based on S-transform based morphological features along with four temporal features– pre-RR interval, post-RR interval, local RR interval and average RR interval to classify the ECG beats. The ST has the following advantages compared to wavelet transform (WT): (i) absolutely referenced phase information, (ii) frequency invariant amplitude response, and (iii) progressive resolution. In addition, ST represents the signal in the time-frequency domain, rather than the time-scale axis used in wavelet [82]. Therefore, interpretation of the frequency information in the ST is

more straightforward than that in the WT. This will be beneficial for the extraction of important features from ECG signal. The combinational of four dimensional temporal features with 180 morphological features is used to classify the five types of ECG beats as per AAMI standards and recommendation [78]. As recommended in the AAMI standards, the different types of ECG arrhythmia beats from the MIT-BIH database are divided into five classes.

The combined proposed feature set is applied as input to the classifier. In this chapter, MLP-BP neural network is used as a classifier because it has the following advantages: (i) complex class distributed features can be easily mapped by neural network, (ii) it can be easily applied on a hardware platform due to its simple structure, (iii) it has the ability to approximate functions and automatic similarity based generalization property, (iv) it can be used to generate likelihood-like scores that are discriminative in the state level [83]. To verify our proposed feature set, the wavelet based set as reported in [57] is compared with our proposed method and also our classification performance is compared with other reported wavelet based feature set [3] in Chapter 4. Experimental results are evaluated on several normal and abnormal ECG signals from 44 recordings of the MIT-BIH arrhythmia database [77]. The experimental results demonstrate that the proposed feature extraction technique shows better performance than commonly used WT feature extraction technique.

2.1.1 Organization of the chapter

The rest of this chapter is organized as follows: Section 2.2 describes the basic concepts of discrete wavelet transform and S-transform. The proposed methodology is explained in Section 2.3. Experimental results and discussion are described in the Section 2.4. Finally, conclusions are drawn in Section 2.5.

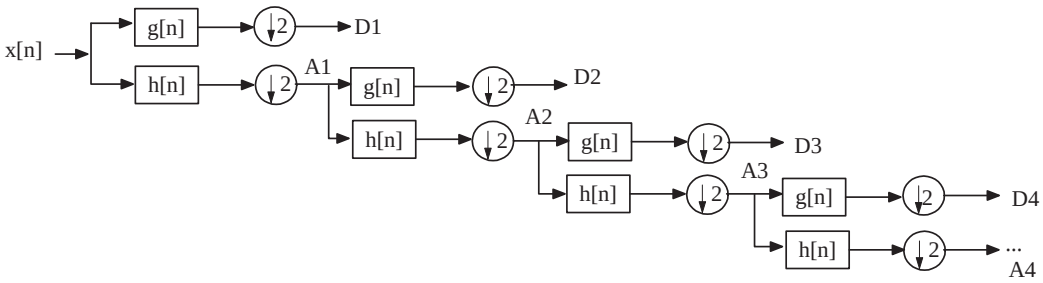

Figure 2.1: Subband decomposition using discrete wavelet transform.

2.2 Theoretical Background

2.2.1 Discrete Wavelet transform

The continuous wavelet transform (CWT) of a signal $x(t)$ is defined by [84]

$$CWT(a,b) = \int_{-\infty}^{\infty} x(t) \frac{1}{\sqrt{|a|}} \psi\left(\frac{t-b}{a}\right) dt \tag{2.1}$$

where, ψ, a and b are wavelet function, scaling and shifting parameters respectively [85]. At every possible scale, wavelet coefficients calculation is computationally very complex task. The wavelet analysis will be much more efficient if the positions and scales are chosen based on dyadic position and scales i.e based on powers of two [85]. Such analysis is obtained from the discrete wavelet transform (DWT) which can be defined as follows [85],

$$DWT(j,k) = \frac{1}{\sqrt{|2^j|}} \int_{-\infty}^{\infty} x(t) \psi\left(\frac{t-2^j k}{2^j}\right) dt, \qquad j,k \in Z \tag{2.2}$$

where, $a = 2^j$ and $b = k2^j$. Note that the translation step depends on the dilation, since smaller wavelets are advanced by small steps, and longer ones by long steps [84]. Mallat [85] has implemented this scheme by passing the signal through a series of low pass filter (LP) and high pass (HP) filter pairs. This scheme is known as decomposition. The multi-resolution decomposition of a signal $x[n]$ is shown in Fig. 2.1. The decomposition of signal at every level consists of two digital filters, the first filter g[.] which is high-

pass in nature, is known as discrete mother wavelet, and the second one, h[.] which is low-pass in nature, is the mirror version of first filter. Two down samplers that down sample the resulting signals by 2 are used [57]. The down sampled output of the high pass filter yields the detail coefficient, D1 and the down sampled output of the low pass filter provides the approximation coefficient, A1. The first approximation, A1 is further decomposed and this process is continued.

All wavelet transform can be described in terms of low-pass filter (h[.]) which satisfies the following standard quadrature mirror filter condition [84], [86]:

$$H(z)H(z^{-1}) + H(-z)H(-z^{-1}) = 2 \tag{2.3}$$

where, $H(z)$ indicates the z-transform of the filter (h[.]). The high pass filter which is complementary to the low pass filter, is defined as

$$G(z) = z * H(-z^{-1}) \tag{2.4}$$

A sequence of filters with increasing length (indicated by i) can be obtained [57]:

$$\begin{aligned} H_{i+1}(z) &= H(z^{2^i})H_i(z) \\ G_{i+1}(z) &= G(z^{2^i})H_i(z), \qquad i = 0, ..., (I-1) \end{aligned} \tag{2.5}$$

with the initial condition $H_0(z) = 1$ and I is the length of decomposition level, it can be expressed as a two-scale relation in time domain

$$\begin{aligned} h_{i+1}(n) &= [h]_{\uparrow 2^i} * h_i(n) \\ g_{i+1}(n) &= [g]_{\uparrow 2^i} * h_i(n) \end{aligned} \tag{2.6}$$

where, subscript $[.]_{\uparrow m}$ denotes the up-sampling by a factor of m and n indicates the equality sampled discrete time.

The normalized wavelet and scale basis functions $\varphi_{i,l}(n)$, $\psi_{i,l}(n)$ can be defined as

$$\begin{aligned} \varphi_{i,l}(n) &= 2^{\frac{i}{2}} h_i(n - 2^i l) \\ \psi_{i,l}(n) &= 2^{\frac{i}{2}} g_i(n - 2^i l) \end{aligned} \tag{2.7}$$

where, the inner product normalization is $2^{\frac{i}{2}}$; the scale and translation parameters are i and l respectively. The decomposition of DWT [57] is written as

$$\begin{aligned} a_{(i)}(l) &= x(n) * \varphi_{i,l}(n) \\ d_{(i)}(l) &= x(n) * \psi_{i,l}(n) \end{aligned} \tag{2.8}$$

where, the approximation and detail coefficients are $a_{(i)}(l)$ and $d_{(i)}(l)$ respectively at the resolution i [44].

2.2.2 Stockwell Transform

The Stockwell Transform (S-transform) is a time-frequency representation of a time series which uniquely combines a frequency dependent resolution with simultaneously localizing the real and imaginary spectra. The S-transform (ST) was developed by Stockwell [82] in 1996. It can be applied to fields that requires the calculation of event initiation such as biomedical engineering [87,88], genomic signal processing, power transformer protection [89–91] and geophysics [92,93]. Continuous S-transform of a function $u(t)$ is defined as

$$S(\tau, f) = \int_{-\infty}^{\infty} u(t) \frac{|f|}{\sqrt{2\pi}} e^{-\frac{(\tau - t)^2 f^2}{2}} e^{-i2\pi f t} dt \tag{2.9}$$

where, $u(t)$ is a time domain signal. A "voice" is a one dimensional function of time for a constant frequency f_0 and is denoted as $S(\tau, f_0)$. It represents how the amplitude and phase for this exact frequency changes over time. A "local spectrum" $S(\tau_0, f)$ is defined as a one dimensional function of frequency for a constant time t_0.

S-transform can be written as a convolution of two functions over the variable t

$$S(\tau, f) = \int_{-\infty}^{\infty} p_1(t, f) g(\tau - t, f) dt \tag{2.10}$$

or

$$S(\tau, f) = p_1(\tau, f) * g(\tau, f) \tag{2.11}$$

where,

$$p_1(\tau, f) = u(\tau) e^{-i2\pi f\tau} \tag{2.12}$$

and

$$g(\tau, f) = \frac{|f|}{\sqrt{2\pi}} e^{-\frac{\tau^2 f^2}{2}} \tag{2.13}$$

Let $B_1(\tau, f)$ be the Fourier transform of the S-transform $S(\tau, f)$. According to the convolution theorem, the convolution in the τ (time) domain becomes a multiplication in the α (frequency) domain.

$$B_1(\alpha, f) = P_1(\alpha, f) G_1(\alpha, f) \tag{2.14}$$

where $P_1(\alpha, f)$ and $G_1(\alpha, f)$ are the Fourier transform of $p_1(\tau, f)$ and $g(\tau, f)$, respectively.

$$B_1(\alpha, f) = U(\alpha + f) e^{-\frac{\alpha^2 2\pi^2}{f^2}} \tag{2.15}$$

where, $U(\alpha + f)$ is the Fourier transform of (2.12), and the exponential term is the Fourier transform of the Gaussian function in (2.13). Thus, S-transform is the inverse Fourier transform of the above equation (for f≠0).

$$S(\tau, f) = \int_{-\infty}^{\infty} U(\alpha + f) e^{-\frac{\alpha^2 2\pi^2}{f^2}} e^{i2\pi\alpha\tau} dt \tag{2.16}$$

The exponential function in (2.16) is the frequency dependent localizing window and is called the Voice Gaussian [93]. This window is centered around the zero frequency and thus plays the role of a low pass filter for each particular voice. This is in contrast to a

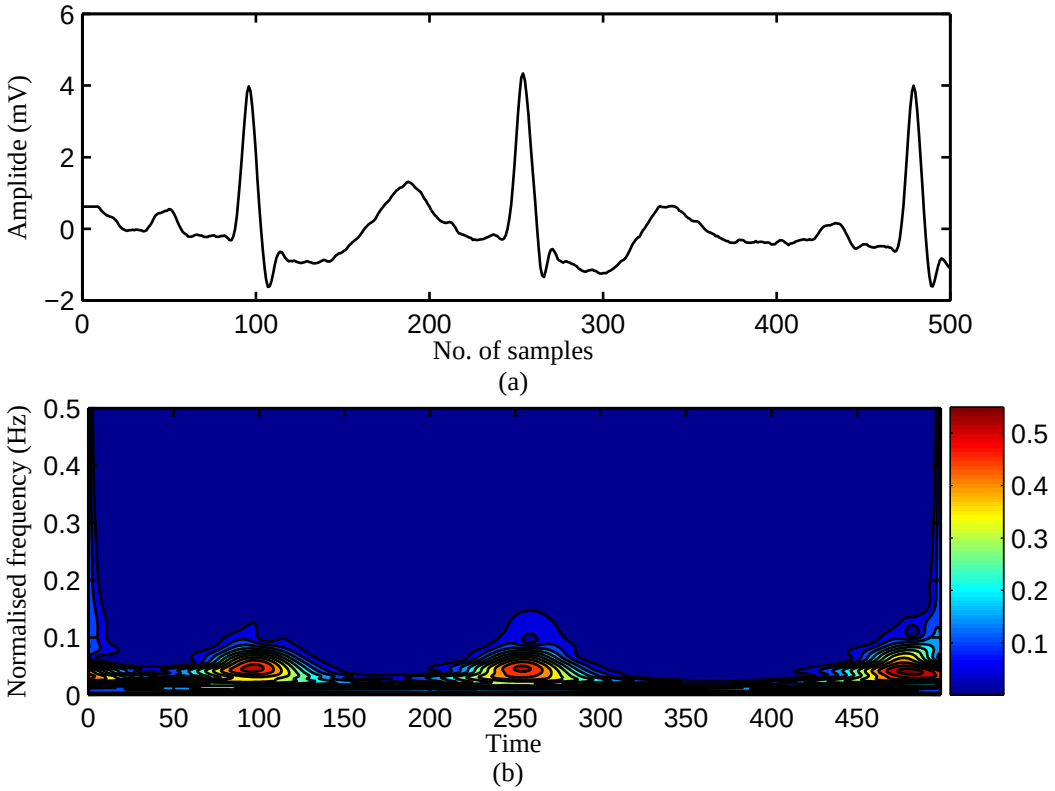

Figure 2.2: (a) ECG signal (b) ST of ECG signal, for normal beats of tape no. # 200.

wavelet transform (WT) or band pass filtered approach to calculate the voices of a time frequency representation [94]. ST provides a time frequency representation instead of the time scale representation given by the WT. Fig. 2.2(a) represents the ECG signal for normal beats of tape no. # 200 and its time-frequency domain representation using ST is shown in Fig. 2.2(b). The time and frequency locations of the ECG signal in the time frequency plane can be directly read out from the Fig. 2.2(b) plot [94, 95].

2.2.2.1 Discrete S-Transform

S-transform of a discrete time series $u[kT]$ is written as [95]

$$S\left[jT, \frac{n}{NT}\right] = \sum_{m=0}^{N-1} U\left[\frac{m+n}{NT}\right] e^{-\frac{2\pi^2 m^2}{n^2}} e^{\frac{i2\pi mj}{N}} \tag{2.17}$$

where, j, n and m =0, 1,...,$(N-1)$. N is length of the time series. Note that, $U\left[\frac{n}{NT}\right]$ is the Fourier transform of time series $u[kT]$, is expressed as

$$U\left[\frac{n}{NT}\right] = \frac{1}{N}\sum_{k=0}^{N-1} u\left[kT\right]e^{-\frac{i2\pi nk}{N}}. \tag{2.18}$$

The Discrete S-transform algorithm is illustrated in Algorithm 2.1.

Algorithm 2.1: : Algorithm of the discrete S-transform.

1: Assume the fast Fourier transform of signal $u[k]$ is $U[m]$ with sample interval T and length is N.
2: Calculate the localizing Gaussian function, $G[n, m]$.
3: Shift the signal spectrum $U[m]$ to $U[m+n]$ for the frequency n.
4: Multiply the shifted signal $U[m+n]$ with the Gaussian function $G[n, m]$. The multiplication output is denoted as $B_1[n, m]$.
5: Compute the inverse of the Fourier transform of $B_1[n, m]$.

2.3 Methodology

This chapter clearly describes the methodology followed for preprocessing, QRS complex detection and feature extraction. In the feature extraction stage, ST based combined feature is also proposed in this work. Different stages for ECG beat classification are given as follows.

2.3.1 Preprocessing

Pre-processing step for ECG signal analysis towards beat classification involves the following two sub-stages:

2.3.1.1 Normalization

It normalizes the amplitude of the ECG signals to zero mean and standard deviation of unity which reduces the DC offset and eliminates the amplitude variance for each ECG signal. Let, x be a raw ECG signal taken from the MIT-BIH arrhythmia database. The

standard deviation of the signal is defined as

$$\sigma = \sqrt{\frac{1}{(N-1)} \sum_{i=1}^{N} (x_i - m)^2} \tag{2.19}$$

σ is the standard deviation of the signal and m is the mean value of the signal. Then the normalized signal is determined as

$$S_n = \frac{(x - m)}{\sigma} \tag{2.20}$$

where, S_n is the normalized signal. This normalized signal is applied as input to R-peak detection.

Algorithm 2.2: Pan-Tompkin's algorithm [30] for R-peak detection

1: Filtering : Select the desired passband frequency range 5-15 Hz to remove the noises.
2: Differentiation : Differentiation is carried out to provide the QRS complex slope information.
3: Squaring : Point by point squaring of the differentiated signal is taken to make all data points positive and to emphasize the higher frequencies of the signal that are mainly due to the QRS complex.
4: Moving-Window Integration : This process extracts features in addition to the slope of the R wave. The width of the window should be approximately the same as the widest possible QRS complex.
5: Adaptive Thresholding : R peak is then detected using an upward and downward threshold. The thresholds are calculated using running estimates of signal peak and noise peak [30].

2.3.1.2 R-peak detection

The determination of R peak helps to extract the features from ECG signal [30]. The QRS complex detection i.e. locating the R-peak for each beat of the signal is an important step towards feature extraction. Once the R-peak is determined, all other important peaks of the ECG signal are determined with respect to the R-peak. Thus, QRS complex detection of the ECG signal is a valuable task for ECG signal analysis.

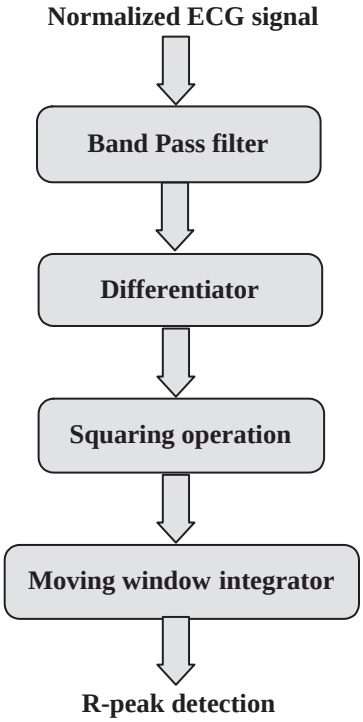

Figure 2.3: Block diagram of the Pan-Tompkin's algorithm for R-peak detection.

The commonly used real-time QRS complex detection algorithm [30] developed by J. Pan and W. J. Tompkins is followed in this work. Figure 2.3 illustrates the block diagram of the R-peak detection algorithm. This algorithm includes a series of steps that performs bandpass filtering, differentiation, squaring operation, moving window integration and adaptive thresholding. A brief description of Pan-Tompkin's algorithm [30] is in Algorithm 2.2.

2.3.2 Feature Extraction Process

A feature is a distinctive or characteristic measurement, transform, structural component extracted from a segment of a pattern. Features are used to represent patterns with the goal of minimizing the loss of important information. Features are selected based on either (1) best representation of a given class of signals, or (2) best distinction between classes [57]. Features are extracted from each ECG beat which consists of P,

Q, R, S, and T wave of one ECG cardiac cycle. The details of wavelet transform based feature extraction technique [57] and proposed feature extraction technique are given as follows.

Algorithm 2.3: Wavelet based feature extraction procedure

1: Select a window of -250 ms to +250 ms around the R-peak as found in the QRS detection algorithm, i.e. 180 samples are selected around the R-peak.
2: Convert the time domain signal into wavelet domain selecting the level of decomposition and also choose commonly supported orthogonal wavelet bases function.
3: Calculate the following features of each subband. F1: Maximum value of the wavelet coefficients. F2: Mean value of the wavelet coefficients, F3: Minimum value of the wavelet coefficients, F4: Standard deviation of the wavelet coefficients.
4: Obtain the wavelet based feature set by appending the all estimated subband features.

2.3.2.1 Wavelet transform based feature extraction method

The choice of appropriate wavelet and the number of decomposition levels are very crucial in the analysis of ECG signals using discrete wavelet transform (DWT) [57]. The decomposition levels are selected based on the maximum frequency components of the signal. The decomposition levels are taken such that those parts of the signal correlate well with the wavelet coefficients. The wavelet based feature extraction method is briefly described in Algorithm 2.3 as reported in [57]. The decomposition levels are taken as 4 as reported in referenced work [57]. Thus, four detail coefficients D1-D4 and one approximation coefficient A4 are extracted from the ECG signal as shown in Fig. 2.1. In the reported work [57], the Daubechies wavelet of order 2 (db2) is chosen due to its similar morphological structure with the ECG signals. The wavelet coefficients give a compact representation of the signal that indicates the distribution of signal energy in time and frequency domain. The computed detail and approximation wavelet coefficients of the ECG signals of each record are used as the feature vectors representing the ECG signal. For each ECG cardiac cycle, a window of -250 ms to +250 ms around the R-peak is chosen to extract the efficient features. Since each MIT-BIH

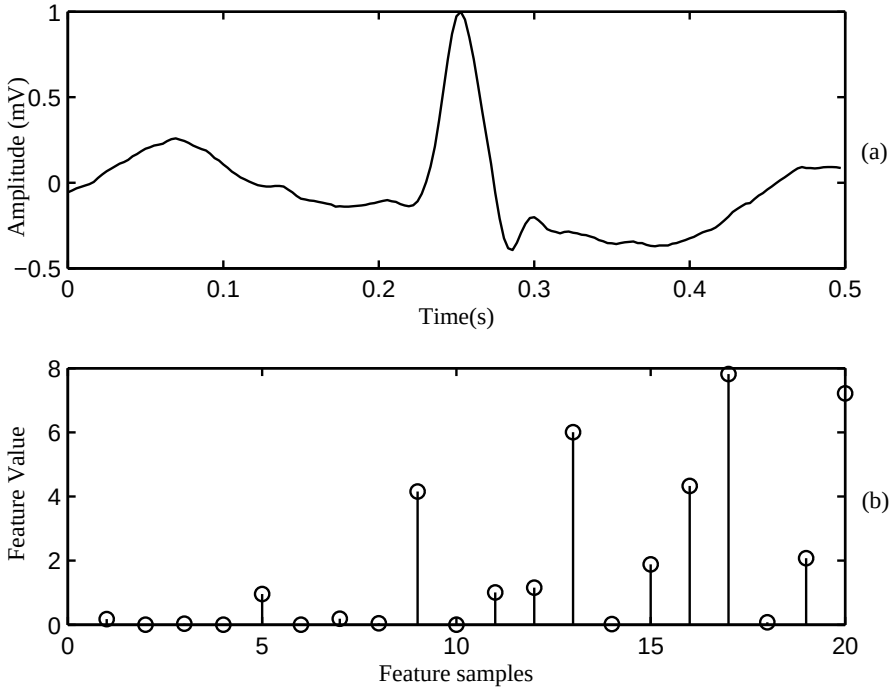

Figure 2.4: (a) ECG signal of selected samples, (b) wavelet transform based feature set for normal beat of tape no. # 200.

ECG signal is sampled at 360 Hz, therefore, the extracted number of DWT coefficients at a specific level for each ECG beat is the same. For each ECG beat, the number of detail coefficients are computed at the first, second, third and fourth levels as 91, 47, 25 and 14, respectively whereas the number of approximation coefficients at fourth level are computed as 14. Thus, a total of 191 wavelet coefficients are obtained from each ECG beat. In order to reduce the dimensionality of the extracted features, statistics over the set of the wavelet coefficients are used as [57]. The following statistical features are extracted using DWT to represent the ECG signal in time-frequency domain [96]. Assume, S_{dk} and S_{ak} are the wavelet detail and approximation coefficients extracted from ECG signal respectively, where k is the level of decomposition, d and a indicate detail and approximation, respectively.

$F1_{dk}$ and $F1_{ak}$ are the maximum of detail and approximation coefficients at k^{th}

level.

$$F1_{dk} = \max(S_{dk}) \quad where, k = 1, 2, 3, 4.$$
$$F1_{ak} = \max(S_{ak}) \quad where, k = 4.$$

$F2_{dk}$ and $F2_{ak}$ are the minimum of detail and approximation coefficients at k^{th} level.

$$F2_{dk} = \min(S_{dk}) \quad where, k = 1, 2, 3, 4.$$
$$F2_{ak} = \min(S_{ak}) \quad where, k = 4.$$

$F3_{dk}$ and $F3_{ak}$ are the mean of detail and approximation coefficients at k^{th} level.

$$F3_{dk} = \frac{1}{N}\sum_{i=1}^{N} S_{dk} \quad where, k = 1, 2, 3, 4.$$
$$F3_{ak} = \frac{1}{N}\sum_{i=1}^{N} S_{ak} \quad where, k = 4$$

N is the total number of coefficients.

$F4_{dk}$ and $F4_{ak}$ are the standard deviation of detail and approximation coefficients at k^{th} level.

$$F4_{dk} = \sqrt{\frac{1}{(N-1)}\sum_{i=1}^{N} (S_{dk} - F3_{dk})^2} \quad where, k = 1, 2, 3, 4.$$
$$F4_{ak} = \sqrt{\frac{1}{(N-1)}\sum_{i=1}^{N} (S_{ak} - F3_{ak})^2} \quad where, k = 4.$$

Therefore, 20 dimensional features are extracted from each ECG beat. As an example, wavelet based feature vector is shown in Fig. 2.4 for a normal (N) beat of MIT-BIH ECG data tape no. # 200.

2.3.2.2 Proposed feature extraction method

Two different types of features: (i) temporal feature and (ii) morphological feature are extracted using the proposed feature extraction technique.

(i) **Temporal feature**

Following temporal information [2] from each ECG beat is taken to compute temporal features:

(a) pre-RR interval: defined as the RR-interval between a given heartbeat and the

previous heartbeat,

(b) post-RR interval: between a given heartbeat and the following heartbeat,

(c) average RR-interval: the mean of the RR-intervals for a recording and is considered as the same value for all heartbeats in a recording and

(d) local average RR-interval: determined by averaging the RR-intervals of the ten RR-intervals surrounding a heartbeat.

(ii) **Morphological feature**

Morphology is a branch of biology dealing with the study of the form and structure of organisms and their specific structural features. This includes aspects of the outward appearance (shape, structure, color, pattern) as well as the form and structure of the internal parts. In this work, the morphological feature extraction technique is proposed using S-transform based method. The proposed morphological features extraction technique is briefly described in Algorithm 2.4.

Algorithm 2.4: Morphological feature extraction

1: Select a window of -250 ms to +250 ms around the R-peak as found in the QRS detection algorithm, i.e. 180 samples are selected around the R-peak.
2: Apply S-transform on the selected ECG signal to represent in time-frequency domain.
3: Select the frequency band (3-20 Hz) from the time-frequency representation of ECG signal [30] because most of the QRS complex energy and least amount of high and low frequency noises exist in this frequency range. The S-transform of selected ECG is depicted in Fig. 2.6.
4: Obtain the morphological feature from each sample by averaging its frequency from time-frequency domain of the ECG signal.

Block diagram of proposed features extraction technique is also shown in Fig. 2.5. The time-frequency domain represented ECG signal is evaluated using the following equation.

$$S\left[jT, \frac{n}{NT}\right] = \sum_{m=0}^{N-1} H\left[\frac{m+n}{NT}\right] e^{\frac{-2\pi^2 m^2}{n^2}} e^{\frac{i2\pi mj}{N}} \tag{2.21}$$

where, $H\left[\frac{n}{NT}\right]$ is the Fourier transform of time series of the ECG signal and j, m, $n = 0$,

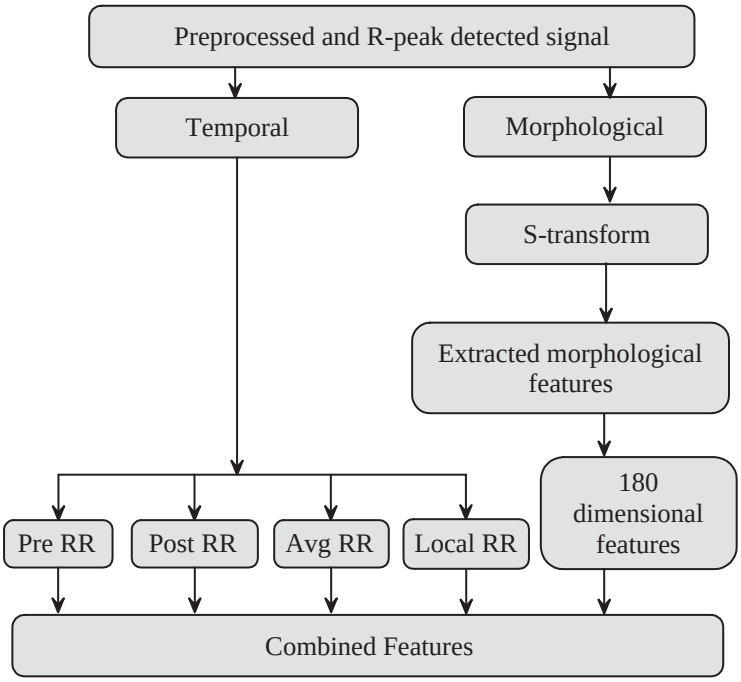

Figure 2.5: Block diagram of proposed features extraction technique.

1,..., $(N-1)$ [82]. Fig. 2.6(a) and 2.6(b) indicate the time domain ECG signal and time-frequency domain represented ECG signal respectively. The QRS complex energy and least amount of high and low frequency noises are laid in the band of frequency (3-20 Hz) [30]. Assume, $V1$ is the S-transform based morphological feature vector and T_1, T_2, T_3, T_4 are the temporal features. The morphological feature vector $V1$ is represented as

$$V1 = [F_1, F_2, F_3, ..., F_{180}].$$

The total combined features set 'M' is represented as

$$M = [T_1, T_2, T_3, T_4, F_1, F_2, F_3, ..., F_{180}].$$

The proposed combined feature vector is generated by coupling of 180 dimensional morphological features with 4 dimensional temporal features. The temporal and morphological features are shown in Fig. 2.7(a) and 2.7(b) respectively. Figure 2.7(c) indicates a

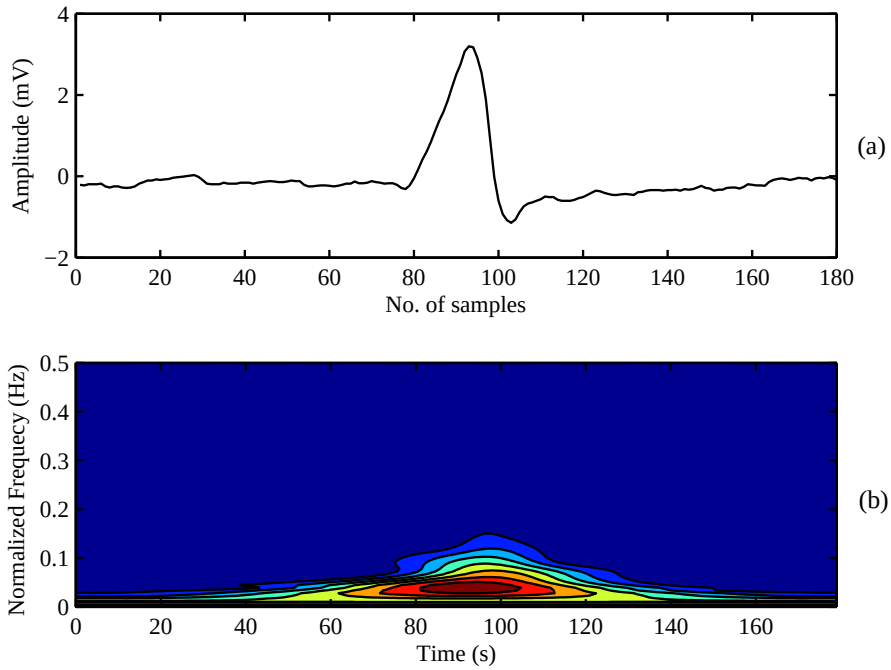

Figure 2.6: (a) ECG signal of selected samples (b) ST of selected ECG signal for normal beat of tape no. # 200.

combined feature set where the temporal feature set is appended with the morphological feature set.

2.3.3 Artificial Neural Network

Multi-layer perceptron neural network (MLP-NN) with a single hidden layer is used in this work to classify the ECG beat from extracted feature vectors. MLP-NN [1] is trained with the error back propagation learning algorithm. The input of MLP-NN is driven separately by the WT based feature set [57] and proposed S-transform based combined feature set. As an example, the schematic diagram of MLP-NN classifier with single hidden layer is shown in Fig. 2.8. In this chapter, MLP-NN classifier is used as a classifier because (i) it can be used to generate likelihood-like scores that are discriminative in the state level, (ii) it can be easily applied on a hardware platform because of its simple structure, (iii) it has the ability to approximate functions and has automatic similarity based generalization property, (iv) complex class distributed

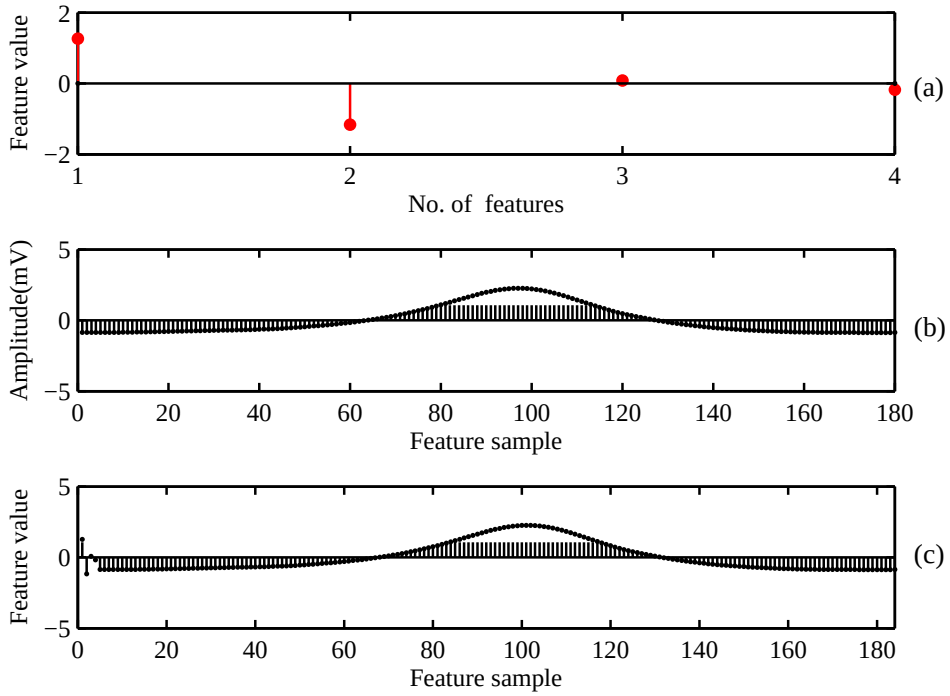

Figure 2.7: Features extracted from Fig. 2.6 (a) ECG signal of selected samples (a) temporal feature set (b) morphological feature set (c) combined set of temporal and morphological features.

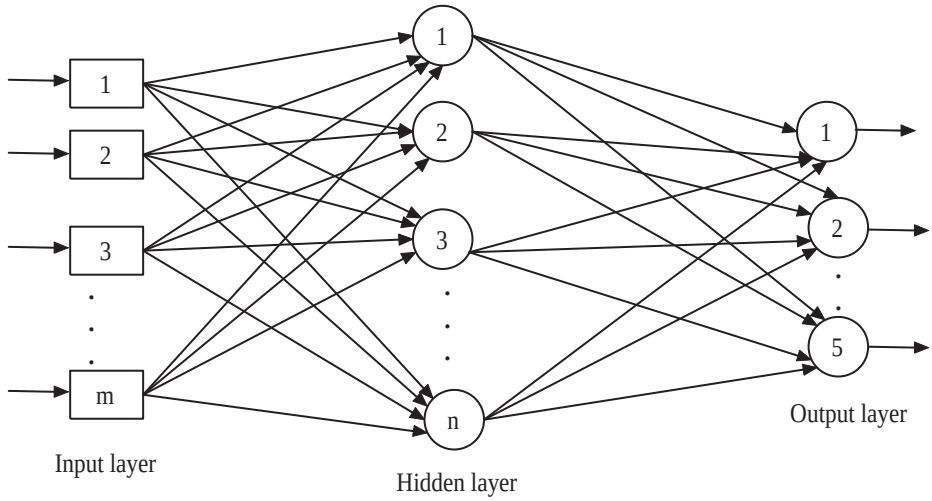

Figure 2.8: Schematic diagram of MLP-NN classifier with a single hidden layer.

features can be easily mapped by neural network [83]. The output layer has five neurons, which is equal to the number of ECG beat types to be classified. The number of input

nodes are equal to the number of input features. The back propagation training with generalized delta learning rule is an iterative gradient algorithm designed to minimize the root mean square error between the actual output of a multi layered feed-forward neural network and a desired output. Each layer is fully connected to the previous layer, and has no other connection. Many activation functions such as logistic function, hyperbolic tangent function and identity function can be used in the MLP-NN classifier. The hyperbolic tangent function is taken empirically in this application. The weight and bias values in the MLP-NN are updated with a learning rate of 0.5 which is chosen empirically.

2.4 Performance Evaluation

In this chapter, 44 recordings of MIT-BIH arrhythmia database are considered for the classification of five heartbeat types as per recommendation by the AAMI standards. The four paced recordings (102, 104, 107, 217) of MIT-BIH arrhythmia database are excluded in the dataset due to their poor signal quality [78]. The performance evaluation is quantified using the most common metrics such as accuracy (Acc), sensitivity (Sen), specificity (Spe) and positive predictivity (Ppr) [3]. The common metrics are defined using true positive (TP), true negative (TN), false positive (FP) and false negative (FN). Classification accuracy is defined as the ratio of the number of correctly classified patterns to the total number of pattern classified.

$$Acc = \frac{TP + TN}{TN + FN + TP + FP}$$

Sensitivity is the rate of correctly classified events among all events.

$$Sen = \frac{TP}{TP + FN}.$$

Specificity is the rate of correctly classified non-events among all non events.

$$Spe = \frac{TN}{TN + FP}.$$

Positive predictivity is the rate of correctly classified events in all detected events.

$$Ppr = \frac{TP}{TP + FP}.$$

For example, the calculation of accuracy, sensitivity, specificity and positive predictivity of V and S class are illustrated in Table 2.1. In the present chapter, classification

Table 2.1: Performance Measures used in this study [2]

Reference Model \ Algorithm Label	**n**	**v**	**s**	**f**	**q**
N	Nn	Nv	Ns	Nf	Nq
V	Vn	Vv	Vs	Vf	Vq
S	Sn	Sv	Ss	Sf	Sq
F	Fn	Fv	Fs	Ff	Fq
Q	Qn	Qv	Qs	Qf	Qq

$$TN_V = Nn + Ns + Nf + Nq + Sn + Ss + Sf + Sq + Fn + Fs + Ff + Fq + Qn + Qs + Qf + Qq$$
$$FN_V = Vn + Vs + Vf + Vq$$
$$TP_V = Vv$$
$$FP_V = Nv + Sv + Fv + Qv$$
$$VEB\ Acc = \frac{TP_V + TN_v}{TN_v + FN_V + TP_V + FP_V}$$
$$VEB\ Se = \frac{TP_V}{TP_V + FN_V}$$
$$VEB\ Spe = \frac{TN_v}{TN_v + FP_V}$$
$$VEB\ Ppr = \frac{TP_V}{TP_V + FP_V}$$

Reference Model \ Algorithm Label	**n**	**v**	**s**	**f**	**q**
N	Nn	Nv	Ns	Nf	Nq
V	Vn	Vv	Vs	Vf	Vq
S	Sn	Sv	Ss	Sf	Sq
F	Fn	Fv	Fs	Ff	Fq
Q	Qn	Qv	Qs	Qf	Qq

$$TN_S = Nn + Nv + Nf + Nq + Vn + Vv + Vf + Vq + Fn + Fv + Ff + Fq + Qn + Qv + Qf + Qq$$
$$FN_S = Sn + Sv + Sf + Sq$$
$$TP_V = Ss$$
$$FP_V = Ns + Vs + Fs + Qs$$
$$SVEB\ Acc = \frac{TP_S + TN_S}{TN_S + FN_S + TP_S + FP_S}$$
$$SVEB\ Se = \frac{TP_S}{TP_S + FN_S}$$
$$SVEB\ Spe = \frac{TN_S}{TN_S + FP_S}$$
$$SVEB\ Ppr = \frac{TP_S}{TP_S + FP_S}$$

performances are evaluated using two approaches. The first approach uses the wavelet based feature set [57] and the second approach uses the proposed combined feature set which couples the morphological and temporal feature set. These feature sets from two approaches are separately classified using MLP-NN classifier. The first one method is indicated as WT-NN method (wavelet based feature set with MLP-NN classifier) and

second method is represented as ST-NN method (original combined feature set with MLP-NN classifier).

2.4.1 Experimental results for wavelet based feature set

A common training dataset, which contains a total of 245 representative beats, including 75 from each type of N, S and V beats, and all (13) type F and all (7) type Q beats, is developed in this thesis [3]. These beats are randomly selected from the first 20 recordings (picked from the range 100-124 i.e 100, 101, 103, 105, 106, 108, 109, 111, 112, 113, 114, 115, 116, 117, 118, 119, 121, 122, 123, 124)). Each record in the MIT-BIH database is of about 30 min. The classifier is trained with 245 common training beats and first 5 min of the patient specific ECG record. The remaining 25 min beats of each of 24 records (picked from the range 200-234, i.e. 200, 201, 202, 203, 205, 207, 208, 209, 210, 212, 213, 214, 215, 219, 220, 221, 222, 223, 228, 230, 231, 232, 233, 234) are completely new to the classifier and are used as test patterns for performance evaluation. The training and testing data sets are represented in Fig. 2.9 using a tree diagram. Table 2.3 presents the confusion matrix of the beat-by-beat classification performance for 24 records of the MIT-BIH ECG database. The left side of Table 2.3 represents the confusion matrix of the beat-by-beat classification performance using wavelet based feature set. The beat-by-beat classification performance based on wavelet based feature set is summarized in the left side of Table 2.4 for 24 records of the MIT-BIH database. In WT-NN method, the sensitivity of N, V, S, F and Q classes are 95.12%, 84.75%, 50.55%, 54.74% and 0.00% respectively and the accuracy of N, V, S, F and Q classes are 92.23%, 96.80%, 95.39%, 98.99% and 99.59% respectively for 24 ECG records.

For evaluation of the 20 records in range of 100-124 recordings, the classifier is trained with 245 common training beats and first 5 min of the patient specific beats. These recordings are tested on the rest of the beats of these ECG recordings in patient-specific way. On the other hand, the confusion matrix and classification performance are shown at the left side of Table 2.5 and Table 2.6, respectively for total 44 ECG

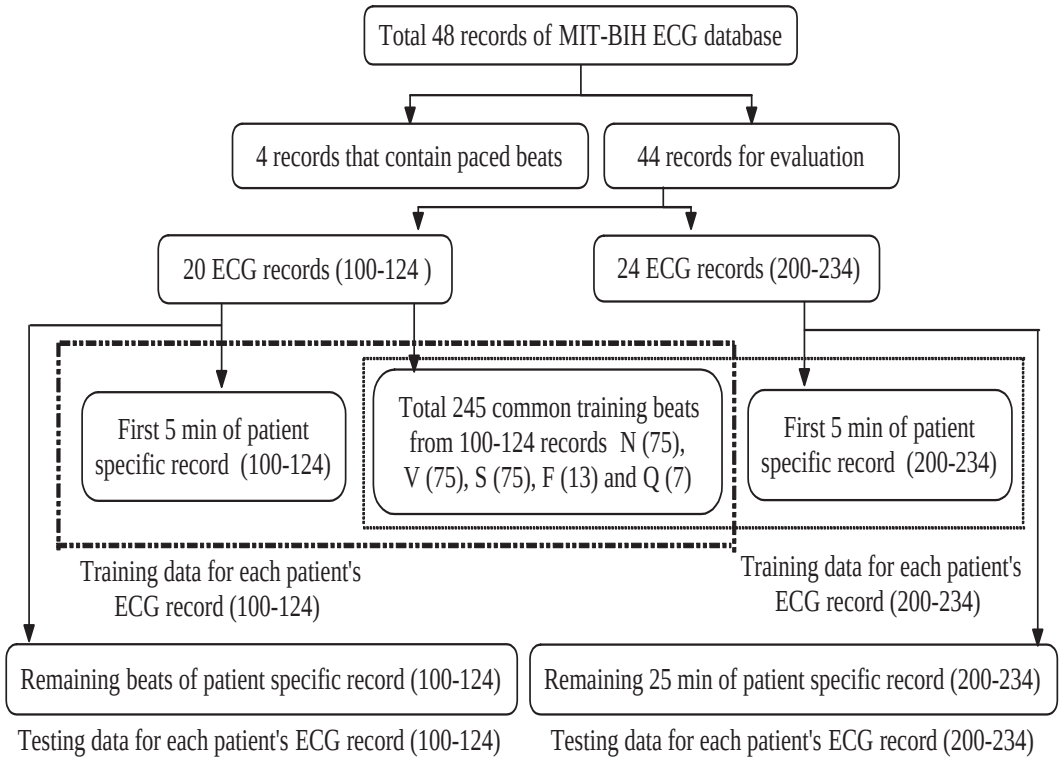

Figure 2.9: Tree diagram of 44 ECG recordings used as training and testing data in proposed method.

records (20 records in range of 100-124 recordings and 24 ECG records in range of 200-234 recordings) of the MIT-BIH database. For 44 ECG records, the sensitivity of N, V, S, F and Q classes are 94.30%, 82.30%, 48.76%, 54.74% and 0.00% respectively and the accuracy of N, V, S, F and Q classes are 92.48%, 96.35%, 95.95%, 99.30% and 99.59% respectively using WT-NN method. In this experiment, MLP neural network is used as the classifier. A neural network with a small number of neurons may not be sufficiently powerful to model a complex function of [42]. On the other hand, a neural network with too many neurons may lead to over fitting of the training sets and lose its ability to generalize which is the primary desired characteristic of a neural network [42]. The performance of the classifier mostly depends on the selection of nodes for the hidden layer. There is no technique available for the exact selection of hidden nodes [83]. In this chapter, hidden nodes in the hidden layer are selected empirically. As an example, for record no. # 234, the variation of the classification performance with respect to

hidden nodes using wavelet based feature set is shown in Fig. 2.10. It is seen from this figure that the best classification performance is achieved when the number of hidden node is 25 in the hidden layer of two layer MLP-NN structure. Column 2 and column 5 of the Table 2.2 represent the size of the ANN used in WT-NN method for beat-by-beat ECG classification.

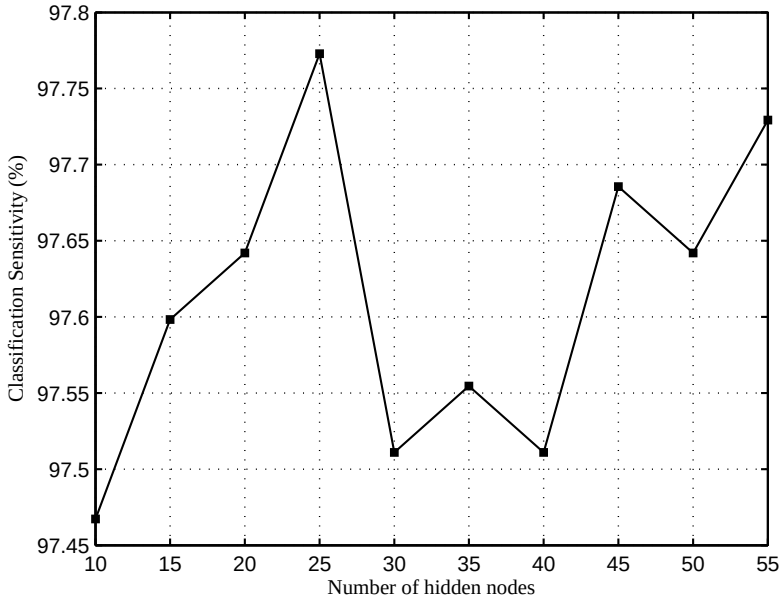

Figure 2.10: Performances of the wavelet based feature extraction method for tape no. # 234 ECG record when different hidden nodes are used in MLP neural network.

2.4.2 Experimental results for proposed combined feature set

Right side of the Table 2.3 represents the confusion matrix for the beat-by-beat classification performance for 24 ECG records using combined S-transform based feature set. The classification performance is tabulated at the right side of the Table 2.4 for 24 records of the MIT-BIH database. In ST-NN method, the sensitivity of N, V, S, F and Q classes are 96.97%, 84.92%, 62.39%, 63.24%, and 12.50%, respectively and the accuracy of N, V, S, F and Q classes are 95.10%, 97.12%, 96.09%, 99.29%, and 99.88%, respec-

Table 2.2: The size of MLP-NN used in WT-NN method and ST-NN method for beat-by-beat classification

Tape No.	WT-NN	ST-NN	Tape No.	WT-NN	ST-NN
200	20-25-5	184-100-5	215	20-40-5	184-150-5
201	20-25-5	184-125-5	219	20-30-5	184-150-5
202	20-30-5	184-150-5	220	20-20-5	184-125-5
203	20-35-5	184-150-5	221	20-25-5	184-125-5
205	20-45-5	184-150-5	222	20-30-5	184-130-5
207	20-35-5	184-125-5	223	20-45-5	184-125-5
208	20-35-5	184-125-5	228	20-35-5	184-100-5
209	20-30-5	184-150-5	230	20-50-5	184-125-5
210	20-25-5	184-125-5	231	20-30-5	184-200-5
212	20-45-5	184-125-5	232	20-50-5	184-125-5
213	20-25-5	184-150-5	233	20-30-5	184-150-5
214	20-45-5	184-150-5	234	20-25-5	184-225-5

Table 2.3: Confusion matrix for beat-by-beat classification performance using WT-NN method and proposed ST-NN method for 24 ECG records of MIT-BIH database

Method	WT-NN					ST-NN				
Class	N	V	S	F	Q	**N**	**V**	**S**	**F**	**Q**
N	39802	621	1052	199	168	**40575**	**448**	**758**	**45**	**16**
V	652	4075	72	9	0	**344**	**4083**	**266**	**83**	**32**
S	1001	115	1187	17	28	**690**	**191**	**1465**	**1**	**1**
F	158	115	4	335	0	**126**	**62**	**31**	**387**	**6**
Q	5	3	0	0	0	**2**	**4**	**1**	**0**	**1**

Table 2.4: Performance comparison of the WT-NN method and proposed ST-NN method for 24 ECG records of MIT-BIH database

Method	WT-NN					ST-NN				
Class	N	V	S	F	Q	**N**	**V**	**S**	**F**	**Q**
Acc	92.23	96.80	95.39	98.99	99.59	**95.10**	**97.12**	**96.09**	**99.29**	**99.88**
Sen	95.12	84.75	50.55	54.74	0.00	**96.97**	**84.92**	**62.39**	**63.24**	**12.50**
Spe	76.65	98.09	97.61	99.54	99.60	**85.06**	**98.43**	**97.77**	**99.74**	**99.89**
Ppr	95.64	82.67	51.27	59.82	0.00	**97.22**	**85.28**	**58.11**	**75.00**	**1.79**

tively for 24 ECG records. For 44 ECG records, the confusion matrix and classification performance are shown at the right side of Table 2.5 and Table 2.6, respectively. Using ST-NN method, the sensitivity of N, V, S, F and Q classes are 97.10%, 86.88%, 63.94%,

Table 2.5: Confusion matrix for beat-by-beat classification performance using WT-NN method and proposed ST-NN method for 44 ECG records of MIT-BIH database

Method	WT-NN					ST-NN				
Class	N	V	S	F	Q	**N**	**V**	**S**	**F**	**Q**
N	70630	1760	2004	284	218	**72724**	**820**	**1253**	**62**	**37**
V	807	4841	131	13	90	**363**	**5110**	**283**	**93**	**33**
S	1074	138	1198	17	30	**686**	**198**	**1571**	**1**	**1**
F	158	115	4	335	0	**126**	**62**	**31**	**387**	**6**
Q	5	3	0	0	0	**2**	**4**	**1**	**0**	**1**

Table 2.6: Performance comparison of WT-NN method and proposed ST-NN method for 44 ECG records of MIT-BIH database

Method	WT-NN					ST-NN				
Class	N	V	S	F	Q	**N**	**V**	**S**	**F**	**Q**
Acc	92.48	96.35	95.95	99.30	99.59	**96.01**	**97.79**	**97.07**	**99.55**	**99.90**
Sen	94.30	82.30	48.76	54.74	0.00	**97.10**	**86.88**	**63.94**	**63.24**	**12.50**
Spe	77.18	97.41	97.37	99.62	99.60	**86.86**	**98.61**	**98.07**	**99.81**	**99.91**
Ppr	97.19	70.60	35.90	51.62	0.00	**98.41**	**82.50**	**50.05**	**71.27**	**1.28**

63.24%, and 12.50%, respectively and the accuracy of N, V, S, F and Q classes are obtained as 96.01%, 97.79%, 97.07%, 99.55% and 99.90%, 97.79%, 97.06%, 99.55%, and 99.90% respectively. In ST-NN method, the nodes in the hidden layer are also selected empirically. As an example, the variation in classification performance with respect to hidden nodes using proposed combined feature set for record no. # 234 is shown in Fig. 2.11. Column 3 and column 6 of the Table 2.2 represent the size of the ANN used in ST-NN method for beat-by-beat ECG classification.

It is seen from Table 2.3 and Table 2.5 that 1001 and 1074 numbers of S beats are misclassified as N beat whereas 1052 and 2004 numbers of N beats are misclassified as S beat using WT based feature set for 24 and 44 ECG records respectively. On the other hand, 690 and 686 supra-ventricular beats are misclassified as N beat and 758 and 1253 N numbers of beats are misclassified as S beat using proposed combined feature set for 24 and 44 ECG recordings respectively. It is difficult to classify between class of N beat and class of S beat because the QRS complex associated with an atrial premature beat

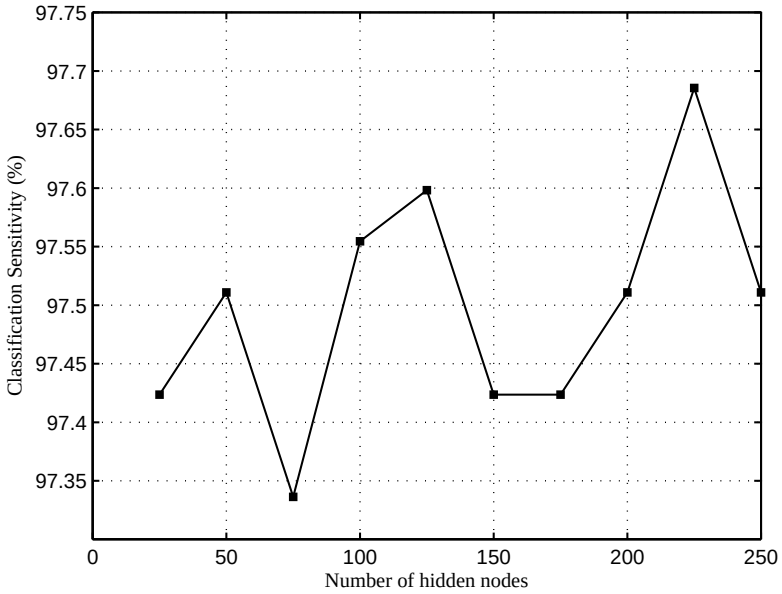

Figure 2.11: The performances of the proposed combined feature set for tape no. # 234 ECG record when different hidden nodes are used in MLP neural network.

in the class S has normal QRS duration and the same morphology as that of the N beat. Similarly, 158 F beats are misclassified as N beat and 199 N beats are misclassified as F beat using WT-NN method for 24 ECG records. In ST-NN method, 45 N beats are misclassified as F beat whereas 126 F beats are misclassified as N beat for 24 ECG records. F beats are difficult to distinguish from N beats because F beats are the union of ventricular and N beats and their morphology and timing information also closely resembles with that of N beats. The sensitivity for detection of five different classes is shown in Fig. 2.12 using bar diagram.

It is seen from the bar diagram that the detection sensitivity of F and Q beats is comparably very less than the other classes. The reason for the worse classification performance in detecting the F and Q beats is that the both classes are under-represented in the training data, and hence, more F and Q beats are misclassified as other classes. It is worthy to mention that less number of training beats are used for each patient's classifier which is approximately 2% of all beats in the training dataset. The proposed combined feature set where morphological features are extracted using S-transform tech-

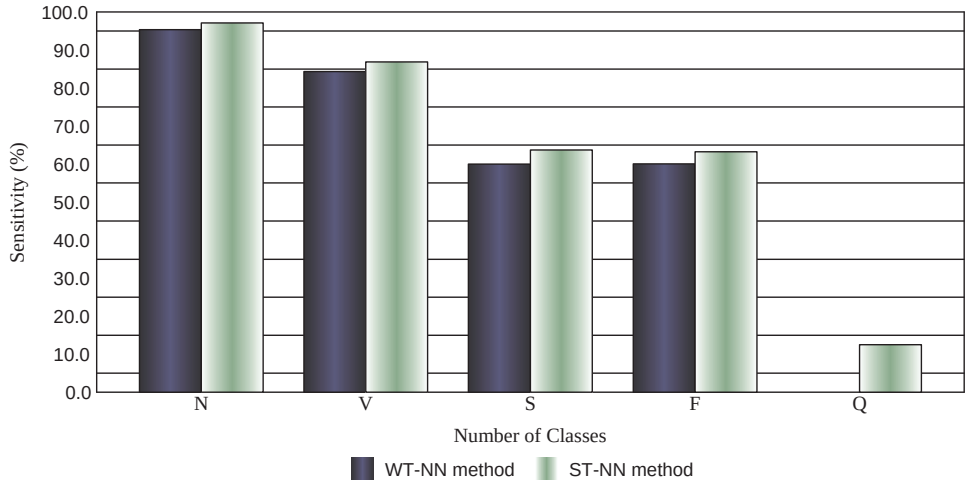

Figure 2.12: Sensitivity for detection of N, V, S, F and Q beats using WT-NN method and ST-NN method.

nique, achieves better performance over other existing methods like WT based feature extraction method [57] for all the metrics used in five different ECG beat classification.

2.5 Conclusions

This chapter proposes a novel feature extraction technique which includes temporal and morphological features. In the proposed feature extraction method, the morphological feature is extracted based on S-transform technique. A summary of the chapter is presented below:

- ST based morphological feature extraction technique is proposed to classify the ECG beats in patient specific way or by beat-by-beat basis. In the proposed technique, the ST is effectively employed to extract the significant morphological features which are combined with temporal features.

- The interpretation of the important signal information using the S-transform is more straight forward than in the WT, which will be beneficial to extract the important features from the ECG signal. These features are very useful for the detection, classification and quantification of relevant parameters of the ECG sig-

nals. A 184 dimensional combined feature vector which couples 4 dimensional temporal features with 180 dimensional S-transformed based morphological features, is generated in this work. This feature vector will serve as input to the classifier model.

- The proposed combined feature vector is compared with WT based feature vector [57] when MLP neural network is used as a classifier. Experiments are conducted on the MIT-BIH arrhythmia database for the classification of five different beats as per AAMI recommendation.

- Experimental results demonstrate that the proposed combined feature set provides better classification performance compared to the wavelet based feature set [57]. The overall performance of the proposed feature extraction method of ECG signal also shows an effective and efficient approach for computer aided diagnosis of heart diseases in a patient-specific way.

CHAPTER 3

Classification of ECG beat using LMS based SVM Classifier

3.1 Introduction

Wavelet transform and S-transform based combined feature extraction technique are described in detail in Chapter 2. In previous chapter, MLP neural network is used as a classifier to detect the five types of ECG beats as per AAMI standard [78] using these two different feature sets. The advantages of MLP-NN are also described in Chapter 2. MLP-NN classifier achieves a significant performance in the classification of ECG beats [58]. However, MLP-NN classifier suffers from slow convergence to local and global minima and from random settings of weights, initial values [97]. Another drawback of this classifier is the selection of the nodes in hidden layer. The classification performance mostly depends on the selection of hidden nodes. No method exists which allows one to decide the exact number of hidden nodes [83]. The number of hidden nodes is chosen empirically in this thesis [1].

This chapter discusses another category of universal feed forward network, known as support vector machines (SVM) which is pioneered by Vapnik [1], [98]. Like MLP neural network, SVM can be used for pattern classification and nonlinear regression. Many research work has been carried out on the survey of SVM classifier. It is seen that SVM classifiers do not trap in local minima points and need less training input therefore they are faster than ANN [58], [99]. Earlier researchers have shown that SVM classifier is better than MLP-NN classifier using the same features as input [58], [60], [100]. SVM is based on the structural risk minimization principle and therefore, it provides better generalization ability compared to traditional classification techniques [101] that use empirical risk minimization methods.

In this work, first a multi-class SVM is developed to detect the five different ECG beats of MIT-BIH arrhythmia database. Next, a least mean square (LMS) based multi-class SVM classifier is proposed to improve the performance of the ECG beat classification system [102]. The goal of this method is to project the data into higher dimensional feature space where the different classes become linearly separable to reconstruct an optimal separating hyper plane. The performance of the ECG classification decreases due

to misclassifications. Here, the classification error is represented by the minimum distance of data points from the margin of the separation region for those data points which fall inside the region of separation or make misclassification. The proposed technique relies that in order to improve the performance of the multi-class SVM classifier, the pattern separability or margin between the clusters needs to be increased. The idea is to update the adjustable weight vector at the training phase in such way that all the data points fall outside the separation region and to enlarge the width of separation boundary [1], [103]. It is seen from the definition of LMS algorithm that it adjusts the filter coefficients so as to minimize the cost function. To implement this idea, LMS algorithm is adopted here to update the adjustable weights at the training phase such that the classification error will be minimized and width of the separation region between the clusters will be increased. LMS has been successfully used in binary SVM in the context of modeling and detection [103]. If the system is an adaptive linear combiner, and if the input vector and the desired response are available, the LMS algorithm is generally the best choice because of its simplicity, ease of computation and it does not require off-line gradient estimations or repetitions of data. LMS algorithm also provides stable and robust performance against different signal conditions. Here, the classification error is represented by the minimum distance of data points from the margin of the separation region for those data points which fall inside the region of separation or make misclassification. As the number of iterations of LMS algorithm increases, weight vector performs a random walk about the solution of optimal hyperplane having maximal margin that minimizes the error and increases the classification accuracy. Experiment is conducted on 44 recordings of MIT-BIH database to classify five different beats as per AAMI standard. Experimental results demonstrate that the multi-class SVM classifier achieves a better performance compared to MLP-NN classifier when two different features– wavelet based and proposed combined features, are used as input to the classifier. The combined feature couples the four different temporal features with S-transform based morphological features. Again, the proposed LMS based multi-class SVM classifier performs better than the standard multi-class SVM classifier when the two different features mentioned

above are used separately for the detection of ECG beats.

3.1.1 Organization of the chapter

This chapter is organized as follows: Section 3.2 describes the basic idea behind a support vector machine (SVM) and least mean square algorithm (LMS). The proposed methodology is illustrated in Section 3.3. Performance evaluation of the classification is presented in Section 3.4. Finally, the chapter concludes with some remarks in Section 3.5.

3.2 Theoretical Background

3.2.1 Support Vector Machine

Support vector machine (SVM) concept originated from statistical learning theory [98]. It is found in a wide range of applications like various pattern recognition problems such as bio-informatics [104], image recognition [105], brain computer interface [106] and text classification [107] etc. The role of the SVM classifier is to project the data points into higher dimensional feature space where the different classes become linearly separable and to construct an optimal separating hyperplane in this space [1]. This requires solving a quadratic programming problem and is done by using kernel functions [103]. Many kernel functions such as polynomials, splines, radial basis functions (RBF) and sigmoid can be used in the SVM classifier. SVM is based on the structural risk minimization principle and therefore, it provides better generalization ability compared to traditional classification techniques [101] that use empirical risk minimization methods. The quality and complexity of the SVM solution do not depend directly on the dimensionality of the input space [98].

Assume, a training set of N data points $\{x_i, d_i\}_{i=1}^{N}$ are given where vector $x_i \in R^n$ denotes a pattern to be classified and scalar $d_i \in R$ is the output pattern. If the training patterns are linearly separable, SVM determines a hyperplane that separates the data in the feature space, which can be represented as

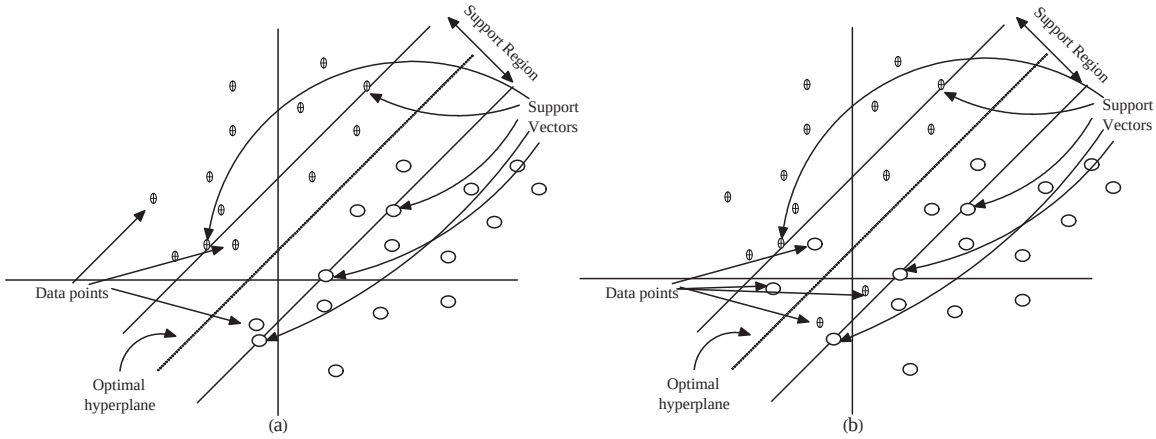

Figure 3.1: (a) Few data point inside the region, but the correct side (free from error) of the hyper plane and (b) few data point falls in the wrong side of the hyperplane [1].

$$f(x) = w^T x + b = 0 \tag{3.1}$$

where, w is an adjustable weight vector, and b is a bias. The SVM classifier finds the hyperplane that maximizes the separating margins between two classes [108]. This hyperplane can be found by minimizing the following cost function:

$$J(w) = \frac{1}{2} w^T w = \frac{1}{2} \|w\|^2 \tag{3.2}$$

subjects to the constraints

$$d_i \left[w^T x_i + b \right] \geq 1 \qquad i = 1, ..., N. \tag{3.3}$$

The constrained optimization problem is also called the primal problem. The primal problem is characterized as follows: (i) the cost function is a convex function and (ii) the constraints are linear [1]. The constrained optimization problem is solved using the method of Lagrange multiplier. The Lagrangian function is constructed as:

$$J(w, b, \alpha) = \frac{1}{2} w^T w - \sum_{i=1}^{N} \alpha_i \left[d_i (w^T x_i + b) - 1 \right] \tag{3.4}$$

where, α_i are called Lagrange multipliers which are auxiliary nonnegative variables. By the saddle point of the Lagrangian function, the solution to the constrained optimization problem is calculated. It is minimized with respect to the weight w and bias b and also maximized with respect to the Lagrange multiplier α. Following two conditions of optimality are obtained after differentiating $J(w, b, \alpha)$ with respect to w and b and equating the results to zero.

$$\text{Condition 1: } \frac{\partial J(w,b,\alpha)}{\partial w} = 0$$
$$\text{Condition 2: } \frac{\partial J(w,b,\alpha)}{\partial b} = 0$$

Weight w is obtained after applying the condition 1 in (3.4)

$$w = \sum_{i=1}^{N} \alpha_i d_i x_i \tag{3.5}$$

On the other hand, apply the condition 2 in (3.4), we get

$$\sum_{i=1}^{N} \alpha_i d_i = 0 \tag{3.6}$$

The primal problem deals with linear constraints and a convex cost function. Given such a constrained optimization problem, it is possible to construct another problem called the dual problem. The dual problem is same as primal problem, but with the Lagrange multipliers giving as optimal solution. The duality theorem is stated as follows [1]: (i) the dual problem has an optimal solution which is equal to the optimal solution of primal problem. (ii) w_0 is a optimal solution of the primal problem whereas the optimal dual solution is α_0 [1]. It is necessary and sufficient that w_0 is feasible for the primal problem, and $\phi(w_0) = J(w_0, b_0, \alpha_0) = \min_w J(w, b_0, \alpha_0)$.

The Lagrange function [1] in (3.4) can be rewritten in the following form

$$J(w, b, \alpha) = \frac{1}{2} w^T w - \sum_{i=1}^{N} \alpha_i d_i w^T x_i - b \sum_{i=1}^{N} \alpha_i d_i + \sum_{i=1}^{N} \alpha_i \tag{3.7}$$

Apply the optimality condition in (3.7), using (3.5) we get

$$w^T w = \sum \alpha_i d_i w^T x_i = \sum_{i=1}^{N} \sum_{j=1}^{N} \alpha_i \alpha_j d_i d_j x_i^T x_j \tag{3.8}$$

According to duality problem $J(w, b, \alpha) = Q(\alpha)$, (3.7) is written as

$$Q(\alpha) = \sum_{i=1}^{N} \alpha_i - \frac{1}{2} \sum_{i=1}^{N} \sum_{j=1}^{N} \alpha_i \alpha_j d_i d_j x_i^T x_j \tag{3.9}$$

Now, Lagrange multipliers which are solved for the dual problem of (3.2) using the following expression.

$$\max\{Q(\alpha) = \sum_{i=1}^{N} \alpha_i - \frac{1}{2} \sum_{i=1}^{N} \sum_{j=1}^{N} \alpha_i (d_i d_j x_i^T x_j) \alpha_j\} \tag{3.10}$$

subject to the constraints

$$\alpha_i \geq 0, \quad \sum_{i=1}^{N} \alpha_i d_i = 0 \tag{3.11}$$

If the training data is not completely separable by a hyperplane, a new set of nonnegative scalar variables is introduced as ξ_i, slack variable, $\xi_i \geq 0, \;\; i = 1, ..., N$ that represents the amount by which the linearity constraint is violated [108].

$$d_i \left[w^T x_i + b \right] \geq 1 - \xi_i \tag{3.12}$$

$$\xi_i \geq 0, \qquad i = 1, ..., N. \tag{3.13}$$

The slack variable is measured by the deviation of a data point from the ideal condition of pattern separability. For $0 \leq \xi_i \leq 1$, the data points fall inside the separation region but on the correct side (error free) of the optimal hyperplane, as shown in Fig. 3.1(a). For $\xi_i > 1$, it falls on the wrong side of the separating hyperplane, as illustrated in Fig. 3.1(b). In this case, the cost function in (3.2) is modified due to the extent of the

constraint violations [108]. Hence, the cost function to be minimized becomes

$$\min_{w,\xi} P_1(w,\xi) = \frac{1}{2}w^T w + C\sum_{i=1}^{N}\xi_i \tag{3.14}$$

subject to the constrains in (3.12) and (3.13). Where, C is the regularization parameter which controls the trade off between complexity of the machine and the number of non separable points [1].

Using the method of Lagrange multipliers and proceeding in similar way explained for linearly separable case, the dual problem may be formulated for non-separable pattern as

$$\max\{Q(\alpha) = \sum_{i=1}^{N}\alpha_i - \frac{1}{2}\sum_{i=1}^{N}\sum_{j=1}^{N}\alpha_i(d_i d_j x_i^T x_j)\alpha_j\} \tag{3.15}$$

subject to the constrains

$$\sum_{i=1}^{N}\alpha_i d_i = 0, \quad 0 \le \alpha_i \le C. \tag{3.16}$$

The weight w is computed using (3.5) and bias b is calculated from $d_i(wx_i + b) = 1$. The optimal decision function of pattern x can be expressed as

$$f(x) = sign\left(\sum_{i=1}^{N}(\alpha_i d_i x_i^T x + b)\right). \tag{3.17}$$

For nonlinear decision surface, the original input space can always be mapped to higher-dimensional feature space where the training data set is linearly separable. In that case, the training data may be mapped on to a high-dimensional feature space through a mapping function φ. The optimization problem for the new point becomes

$$\min_{w,\xi} P_1(w,\xi) = \frac{1}{2}w^T w + C\sum_{i=1}^{N}\xi_i \tag{3.18}$$

subject to the constraints

$$d_i(w^T\varphi(x_i) + b) \ge 1 - \xi_i, \quad \xi_i \ge 0, \quad i = 1, 2, ..., N. \tag{3.19}$$

The dual problem may be formulated for nonlinear decision surface, by replacing x by $\varphi(x)$ in (3.15)

$$\max\{Q(\alpha) = \sum_{i=1}^{N} \alpha_i - \frac{1}{2} \sum_{i=1}^{N} \sum_{j=1}^{N} \alpha_i (d_i d_j \varphi^T(x_i)\varphi(x_j))\alpha_j\} \tag{3.20}$$

subject to the constraints $\sum_{i=1}^{N} \alpha_i d_i = 0, \quad 0 \leq \alpha_i \leq C.$

In a high dimensional space the computation of $\varphi^T(x_i)\varphi(x_j)$ is expensive and is reduced by using a kernel $k(x_i, x_j)$ which satisfies the Mercer's theorem [1]. The kernel function is defined as

$$k(x_i, x_j) = \varphi^T(x_i)\varphi(x_j). \tag{3.21}$$

Finally, the dual problem to be solved is

$$\max_{\alpha} [\sum_{i=1}^{N} \alpha_i - \frac{1}{2} \sum_{i,j=1}^{N} \alpha_i \alpha_j d_i d_j k(x_i, x_j)] \tag{3.22}$$

subjects to the constraints [1]

$$w = \sum_{i=1}^{N} d_i \alpha_i \varphi(x_i) \tag{3.23}$$

and

$$\sum_{i=1}^{N} \alpha_i d_i = 0, \quad 0 \leq \alpha_i \leq C \quad \forall i. \tag{3.24}$$

Thus, the decision function for pattern x becomes

$$f(x) = \text{sgn}\left(\sum_{i=1}^{N} d_i \alpha_i k(x, x_i) + b\right). \tag{3.25}$$

3.2.2 Multi-Class Support Vector Machine

Support vector machine is first designed by Vapnik [98] for binary classification. Multi-class SVM is decomposed into a series of binary class analysis which can be ad-

dressed with a binary SVM by a one-against-all technique (OAA), one against one (OAO) and directed acyclic graph SVM (DAGSVM). In this work, OAA SVM classifier is used for the classification of ECG beats. OAA approach is very simple and is extremely powerful and produces effective performance [109]. One against all SVM classifier constructs K SVM models, where K is the number of patterns. Assume, a training set of N data points $\{(x_i, d_i)\}_{i=1}^{N}$ is given, where $x_i \in R^n$ is the pattern to be classified and assigned class labels $d_i \in \{1, ..., k\}$. In the high-dimensional feature space the input data x can be represented as $\varphi(x)$. The i^{th} SVM is trained with all the data of i^{th} class with positive labels and all other data with negative labels. The i^{th} SVM solves the following problem [110].

$$\begin{aligned} &\min_{w^i, b^i, \xi^i} P_1(w, \xi) = \tfrac{1}{2}(w^i)^T w^i + C \sum_{j=1}^{N} {\xi_j}^i \\ &subject\,to\ (w^i)^T \varphi(x_j) + b^i \geq 1 - \xi_j^i \quad , \quad if\ d_j = i \\ &\qquad\qquad (w^i)^T \varphi(x_j) + b^i \leq -1 + \xi_j^i \quad , \quad if\ d_j \neq i \\ &\qquad\qquad \xi_j^i \geq 0, \quad j = 1, ..., N \end{aligned} \tag{3.26}$$

After solving (3.26), we get the following k number of decision functions

$$(w^1)^T \varphi(x) + b^1$$

$$.$$

$$.$$

$$(w^k)^T \varphi(x) + b^k$$

We can say x is in the class which has the largest value of the decision function as

$$class\ of\ x\ \equiv \arg \max_{i=1,....,k} \left((w^i)^T \varphi(x) + b^i \right)$$

Practically, the dual problem of (3.26) whose number of variables is the same as the number of the data in (3.26) is solved. Hence kN-variable quadratic programming problems are solved.

3.2.3 Least Mean Square (LMS) Algorithm

To derive the LMS algorithm [1], cost function is defined as

$$\mathcal{E}(\mathbf{w}) = \frac{1}{2}E^2(k) \tag{3.27}$$

where, $E(k)$ measures the error signal at time k. $\mathcal{E}(w)$ is differentiated with respect to the weight vector w

$$\frac{\partial \mathcal{E}(\mathbf{w})}{\partial \mathbf{w}} = E(k)\frac{\partial E(k)}{\partial \mathbf{w}} \tag{3.28}$$

The LMS algorithm works according to the least square filter. The error signal is defined as

$$E(k) = d(k) - \mathbf{x}^T(k)\mathbf{w} \tag{3.29}$$

Therefore,

$$\frac{\partial E(k)}{\partial \mathbf{w}} = -\mathbf{x}(k) \tag{3.30}$$

$$\frac{\partial \mathcal{E}(\mathbf{w})}{\partial w(k)} = -\mathbf{x}(k)E(k) \tag{3.31}$$

According to the steepest decent algorithm [1], we can write the following equation

$$\mathbf{w}(k+1) = \mathbf{w}(k) - \eta g(k) \tag{3.32}$$

where, η indicates a positive constant called the step-size or learning rate parameter. The gradient vector $g(k)$ is written as $g(k) = \frac{\partial \mathcal{E}(\mathbf{w})}{\partial \mathbf{w}(k)} = -\mathbf{x}(k)E(k)$. The LMS algorithm is defined as follows [1]:

$$\mathbf{w}(k+1) = \mathbf{w}(k) + \eta \mathbf{x}(k)E(k) \tag{3.33}$$

3.3 Proposed Framework: LMS based SVM classifier

The procedure for the development of LMS based SVM classifier is as follows:

Step 1: Let us first consider, for the simplicity, a supervised binary classification problem. Assume, a training set consists of N data points $(x_i, d_i)_{i=1}^N$ where $x_i \in \Re^m$ is the

i^{th} input pattern and $d_i \in \Re$ is the i^{th} output pattern. Input patterns are mapped by $\varphi : x_i \rightarrow \varphi(x_i)$ from the input space to a feature space.

For nonlinear decision surface, the decision function may be defined for input pattern x as

$$f(x) = \text{sgn}\left(\sum_{i=1}^{N} d_i \alpha_i k(x, x_i) + b\right). \tag{3.34}$$

Step 2: It is seen from (3.34) that the decision function depends on desired outputs d_i, Lagrange multiplier α_i, kernel function $k(x, x_i)$ and bias b where d_i and b are constant. The following fixed radial basis function kernel is used in this work, which is taken empirically.

$$k(x, x_i) = \exp\left(\frac{-(\|x - x_i\|^2)}{2\gamma^2}\right) \tag{3.35}$$

where, γ is width of the kernel function. The value of the γ is empirically chosen as 10 in this work.

Now, decision function changes with changing the Lagrange multiplier. It is noticed from (3.23) that the weight vector w depends on three variable parameters d_i, α_i and $\varphi(x_i)$. Now, weight vector w changes with change in α_i which in turn modifies the decision function. In this work, α_i is modified using LMS algorithm to find out the optimal hyperplane with maximum separating margin between the classes such that classification error is minimized at the training phase and width of the separation region between the clusters will be increased. Those data points which fall inside the region of separation or show misclassified data at the training phase are taken to determine the classification error. The mean square error (MSE) is calculated as $MSE = \frac{1}{N_e} \sum_{j=1}^{N_e} E(j)^2$. where, $E(j)$ is the misclassification error and N_e is the number of data points that result in misclassification. The LMS algorithm is applied as (3.36) to update α_i which in turn reduces the MSE.

$$\alpha(n+1) = \alpha(n) + \eta k(x_i, x_j) E(n) \tag{3.36}$$

where, n is the number of iteration and η is the learning rate parameter. It is seen from the experiments that about all data points are outside of the boundary of the separation

region after weight vector modification. It is also noted that the region of separation between the clusters is enlarged for the proposed technique relative to the region of separation obtained using standard SVM technique. Therefore, data classification is more comfortable in case of the proposed technique compared to standard SVM technique.

Step 3: The classification of ECG beats involves simultaneous discrimination of multiple classes. Therefore, the OAA approach of multi-class SVM is applied for a K-class classification problem, where K is an independent binary classifier, each trained with distinguished training samples for one class with regard to the remaining class. In the multi-class SVM classifier, the Lagrange multiplier of each K independent binary classifier is modified which in turn modifies the weight vector using Step 2.

Step 4: The updated weights are stored based on modified Lagrange multipliers of each independent binary classifier and are used for testing purpose.

3.4 Performance Evaluation

The performance of the proposed method is evaluated on the MIT-BIH dataset as described in chapter 2. In the present chapter, classification performances are evaluated using two approaches. The first approach uses wavelet based feature set [57] and the second approach uses the combined feature set which couples the ST based morphological feature and temporal feature. These feature sets from two approaches are separately classified using SVM and proposed LMS-SVM classifier. The wavelet based feature set with SVM classifier and LMS based SVM classifier are denoted here as WT-SVM method and WT-LMS-SVM method respectively. The combined feature set with SVM classifier and the proposed LMS based SVM classifier are indicated here as ST-SVM and ST-LMS-SVM classifier respectively.

3.4.1 Experimental results for wavelet based feature set

Classification experiments are performed on 44 records of the MIT-BIH arrhythmia database. In this work, a common training data set is constructed in the same way as

discussed in Chapter 2. The classifier is trained with a total of 245 common training beats and first 5 min of each patient specific record (picked from the range 200-234) [3]. The remaining 25 min of each record is used for testing purpose for performance evaluation. Table 3.1 represents the confusion matrix for beat-by-beat classification

Table 3.1: Confusion matrix for beat-by-beat classification performance using WT-SVM method and WT-LMS-SVM method for 24 ECG records of the MIT-BIH database [Kernel width (γ)=10]

Method	WT-SVM					WT-LMS-SVM				
Class	N	V	S	F	Q	**N**	**V**	**S**	**F**	**Q**
N	40043	619	952	130	98	**40143**	**601**	**903**	**122**	**73**
V	598	4094	23	72	21	**501**	**4199**	**22**	**52**	**34**
S	906	117	1262	11	52	**890**	**110**	**1293**	**17**	**38**
F	138	95	27	352	0	**132**	**89**	**11**	**380**	**0**
Q	6	1	1	0	0	**5**	**3**	**0**	**0**	**0**

Table 3.2: Performance comparison of the WT-SVM method and WT-LMS-SVM method for 24 records of the MIT-BIH database [Kernel width (γ)=10]

Method	WT-SVM					WT-LMS-SVM				
Class	N	V	S	F	Q	**N**	**V**	**S**	**F**	**Q**
Acc	93.05	96.88	95.79	99.05	99.64	**93.50**	**97.15**	**95.99**	**99.15**	**99.69**
Sen	95.70	85.15	53.75	57.52	0.00	**95.94**	**87.33**	**55.07**	**62.09**	**0.00**
Spe	78.81	98.14	97.88	99.57	99.66	**80.35**	**98.21**	**98.02**	**99.61**	**99.71**
Ppr	96.05	83.11	55.72	62.30	0.00	**96.33**	**83.95**	**58.01**	**66.55**	**0.00**

performance of 24 ECG records using wavelet based feature set with SVM classifier and LMS based SVM classifier respectively. In a multi-class classification problem, the confusion matrix shows the outcome achieved by a classifier and a detailed distribution of the misclassified events. The classification evaluation is quantified using the most common metrics such as accuracy (Acc), sensitivity (Sen), specificity (Spe) and positive predictivity (Ppr) found in the literature [3]. These common metrics are defined using true positive (TP), true negative (TN), false positive (FP) and false negative (FN) which are clearly mentioned in chapter 2. The beat-by-beat classification performance based on WT-SVM method and WT-LMS-SVM method is summarized in Table 3.2 for 24

records of the MIT-BIH database. WT-SVM method achieves a sensitivity of 95.70%, 85.15%, 53.75%, 57.52% and 0.00% for the classes N, V, S, F and Q respectively and accuracy of 93.05%, 96.88%, 95.79%, 99.05% and 99.64% for the classes N, V, S, F and Q respectively using 24 ECG records whereas the WT-LMS-SVM method shows a sensitivity of 95.94%, 87.33%, 55.07%, 62.09% and 0.00% and accuracy of 93.50%, 97.15%, 95.99%, 99.15% and 99.69% for the classes N, V, S, F and Q respectively.

Table 3.3: Confusion matrix for beat-by-beat classification performance using WT-SVM method and WT-LMS-SVM method for 44 records of the MIT-BIH database

Method	WT-SVM					WT-LMS-SVM				
Class	N	V	S	F	Q	**N**	**V**	**S**	**F**	**Q**
N	71465	1730	1392	162	147	**71717**	**1602**	**1308**	**146**	**123**
V	662	5078	31	81	30	**541**	**5122**	**113**	**60**	**46**
S	967	121	1263	51	55	**971**	**112**	**1296**	**37**	**41**
F	138	95	27	352	0	**132**	**89**	**11**	**380**	**0**
Q	6	1	1	0	0	**5**	**3**	**0**	**0**	**0**

Table 3.4: Performance comparison of the WT-SVM method and WT-LMS-SVM method for 44 records of the MIT-BIH database

Method	WT-SVM					WT-LMS-SVM				
Class	N	V	S	F	Q	**N**	**V**	**S**	**F**	**Q**
Acc	93.79	96.72	96.85	99.34	99.71	**94.24**	**96.94**	**96.91**	**99.43**	**99.74**
Sen	95.42	86.33	51.40	57.52	0.00	**95.76**	**87.08**	**52.75**	**62.09**	**0.00**
Spe	80.21	97.50	98.22	99.65	99.72	**81.59**	**97.68**	**98.24**	**99.71**	**99.75**
Ppr	97.58	72.28	46.54	54.49	0.00	**97.75**	**73.93**	**47.51**	**61.00**	**0.00**

For evaluation of the range of 100-124 recordings, the classifier is trained with 245 common training beats and first 5 min of the patient specific beats. These recordings are tested on rest of the beats of these ECG recordings in a patient-specific way. The confusion matrix and classification performance are shown in Table 3.3 and Table 3.4, respectively for 44 ECG records (20 records in range of 100-124 recordings and 24 records in range of 200-234 recordings) of MIT-BIH database. For 44 ECG records, WT based feature set with multi-class SVM classifier (WT-SVM) method yields a detection

sensitivity of 95.42%, 86.33%, 51.40%, 57.52% and 0% for the classes N, V, S, F and Q respectively and accuracy of 93.79%, 96.72%, 96.85%, 99.34% and 99.71% for the same classes respectively, whereas WT based feature set with proposed LMS based multi-class SVM classifier (WT-LMS-SVM) method shows a detection sensitivity of 95.76%, 87.08%, 52.75%, 62.09% and 0% for the classes N, V, S, F and Q respectively and accuracy of 94.24%, 96.94%, 96.91%, 99.43% and 99.74% for the same classes respectively.

3.4.2 Experimental results for S-transform based combined feature set

Table 3.5: Confusion matrix for beat-by-beat classification performance using ST-SVM method and ST-LMS-SVM method for 24 ECG records of the MIT-BIH database [Kernel width (γ)=10]

Method	ST-SVM					ST-LMS-SVM				
Class	N	V	S	F	Q	**N**	**V**	**S**	**F**	**Q**
N	40874	345	577	33	13	**40936**	**303**	**538**	**50**	**15**
V	304	4265	148	70	21	**273**	**4327**	**122**	**72**	**14**
S	672	147	1497	25	7	**640**	**84**	**1612**	**3**	**9**
F	125	61	33	390	3	**127**	**67**	**22**	**393**	**3**
Q	2	5	0	0	1	**3**	**3**	**0**	**0**	**2**

Table 3.6: Performance comparison of the ST-SVM method and ST-LMS-SVM method for 24 records of the MIT-BIH database [Kernel width (γ)=10]

Method	ST-SVM					ST-LMS-SVM				
Class	N	V	S	F	Q	**N**	**V**	**S**	**F**	**Q**
Acc	95.83	97.78	96.76	99.29	99.90	**96.07**	**98.11**	**97.14**	**99.31**	**99.91**
Sen	97.69	88.71	63.76	63.73	12.50	**97.83**	**90.00**	**68.65**	**64.22**	**25.00**
Spe	85.82	98.75	98.40	99.74	99.91	**86.59**	**98.98**	**98.56**	**99.74**	**99.92**
Ppr	97.37	88.43	66.39	75.29	2.22	**97.52**	**90.45**	**70.27**	**75.87**	**4.65**

Table 3.5 and Table 3.6 represent the confusion matrix and classification performance matrix respectively for 24 ECG records using ST-SVM method and ST-LMS-SVM method. ST-SVM method shows a sensitivity of 97.69%, 88.71%, 63.76%, 63.73% and 12.50% for the classes N, V, S, F and Q respectively, and accuracy of 95.83%, 97.78%, 96.76%, 99.29% and 99.90% for the same classes respectively whereas the ST-LMS-SVM method gives a sensitivity of 97.83%, 90.00%, 68.65%, 64.22% and 25.00%

for the classes N, V, S, F and Q respectively and accuracy of 96.07%, 98.11%, 97.14%, 99.31% and 99.91% for the same classes respectively for 24 ECG records. For 44 ECG records, the confusion matrix and classification performance matrix are shown in Table 3.4 and Table 3.7 respectively using ST-SVM method and ST-LMS-SVM method. For 44 ECG recordings, ST-SVM method achieves a detection sensitivity of 97.95%, 89.70%, 64.96%, 63.73% and 12.50% for the classes N, V, S, F and Q respectively and accuracy of 96.83%, 98.34%, 97.65%, 99.56% and 99.92% for the same classes respectively. On the other hand, ST-LMS-SVM method yields a sensitivity of 97.97%, 90.79%, 69.96%, 64.22% and 25.00% for the classes N, V, S, F and Q respectively and accuracy of 96.92%, 98.50%, 97.87%, 99.57% and 99.92% for the same classes respectively using the same 44 ECG records. Thus, the proposed LMS based multi-class SVM classifier shows better

Table 3.7: Confusion matrix for beat-by-beat classification performance using ST-SVM method and proposed ST-LMS-SVM method for 44 ECG records of the MIT-BIH database

Method	ST-SVM					ST-LMS-SVM				
Class	N	V	S	F	Q	**N**	**V**	**S**	**F**	**Q**
N	73360	567	901	50	18	**73373**	**562**	**878**	**61**	**22**
V	326	5276	178	73	29	**294**	**5340**	**152**	**74**	**22**
S	671	152	1596	26	12	**638**	**84**	**1719**	**4**	**12**
F	125	61	33	390	3	**127**	**67**	**22**	**393**	**3**
Q	2	5	0	0	1	**3**	**3**	**0**	**0**	**2**

Table 3.8: Performance comparison of the ST-SVM method and ST-LMS-SVM method for 44 records of the MIT-BIH database

Method	ST-SVM					ST-LMS-SVM				
Class	N	V	S	F	Q	**N**	**V**	**S**	**F**	**Q**
Acc	96.83	98.34	97.65	99.56	99.92	**96.92**	**98.50**	**97.87**	**99.57**	**99.92**
Sen	97.95	89.70	64.96	63.73	12.50	**97.97**	**90.79**	**69.96**	**64.22**	**25.00**
Spe	87.45	98.99	98.63	99.82	99.93	**88.15**	**99.08**	**98.71**	**99.83**	**99.93**
Ppr	98.49	87.05	58.94	72.36	1.59	**98.57**	**88.18**	**62.04**	**73.87**	**3.28**

performance compared to the standard multi-class SVM classifier for both wavelet based feature set and ST based combined feature set for all the metrics used in N, V, S, F and

Q beat detection.

In WT-SVM method, it is seen from the Table 3.1 that 906 number of S beats are misclassified as N beat and 952 beats of N class are misclassified as S class. It is also noticed from the Table 3.1 that 890 number of S beats are misclassified as N beat and 903 number of N beats are misclassified as S beat using the WT-LMS-SVM technique for 24 ECG records. For 44 ECG records, it is seen from the Table 3.3 that 1029 number of S beats are misclassified as N beat and 1392 number of N beats are misclassified as S beat using the WT-SVM method whereas 1001 number of S beats are misclassified as N beat and 1308 number of N beats are misclassified as S beat using the WT-LMS-SVM method.

On the other hand, it is seen from the Table 3.7 that 901 and 878 numbers of S beats are misclassified as N beat and 671 and 638 numbers of N beats are misclassified as S beat for 44 records using the ST-SVM and ST-LMS-SVM methods respectively. As shown in Table 3.5 for 24 ECG records, 672 number of S beats are misclassified as N beat and 577 number of N beats are misclassified as S beat using the ST-SVM method whereas 640 number of S beats are misclassified as N beat and 538 number of N beats are misclassified as S beat using the ST-LMS-SVM method. It is difficult to classify between N beat class and S beat class because the QRS complex associated with an atrial premature beat in the S class has normal QRS duration and the same morphology as that of the N beat. Therefore, more S beats are misclassified as N beat and vice versa.

Similarly, it is also seen from the Table 3.3 and Table 3.7 that 162 number of N beats are misclassified as F beat using the WT-SVM method whereas 50 number of N beats are misclassified as F beat using the ST-SVM method for 44 ECG records. On the other hand, for the same 44 ECG records, 146 number of N beats are misclassified as F beat using the WT-LMS-SVM method and 61 number of N beats are misclassified as F beat using the ST-LMS-SVM method. F beats are very difficult to distinguish from N beats because F beats are the union of ventricular and N beats and their morphology and timing information also closely resembles with that of N beats. It is also seen from the

Table 3.4 and 3.8 that the classifier performance in detecting the S beats and F beats are worse because S beats and F beats are less in number compared to V beats and N beats in the training data and hence, more S beats and F beats are misclassified as N beats.

3.5 Conclusions

The principal conclusions for this chapter are as follows:

- The LMS based multi-class SVM classifier is proposed in this work to classify the ECG beats in a patient-specific way.
- The primary aim of the SVM is to construct a hyperplane as the decision surface such that the margin of separation between two classes is maximized. In this work, the Lagrange multiplier is modified based on LMS algorithm, which in turn modifies the weight vector to minimize the classification error at training phase and these updated weights are used during the testing phase to classify ECG beats.
- The experiments are conducted on benchmark of the MIT-BIH arrhythmia database as recommended by AAMI standards. The classification results show that the proposed LMS based multi-class SVM technique achieves better performance compared to the standard multi-class SVM method for ECG beat detection.

CHAPTER 4

Feature Vector Optimization for ECG beat Classification

4.1 Introduction

Reduction of feature dimensionality is one of the most important tasks for pattern recognition [111], classification [112] and data mining [113]. A major problem associated with pattern recognition is the "curse of dimensionality" in which the number of the features is larger than the number of patterns that leads to the large number of classifier parameters (e.g., weights in a neural network) [114]. Therefore, the dimensionality reduction through feature subset selection carries several advantages for a classification system employed for a specific task: (i) a reduction in the cost of acquisition of the data, (ii) improvement of comprehensibility of the final classification model, (iii) a faster induction of the final classification mode, (iv) an improvement in classification accuracy [36].

The basic idea of *Feature Selection* (FS) is to reduce the computation at the time of testing while achieving the best performance through the chosen optimal set of features. It involves the definition of the most informative and discriminative features of the original data for classification. This can be performed by eliminating the redundant, uninformative, and noisy features. In this chapter, an optimization technique using bacteria foraging optimization algorithm (BFO) is applied to reduce the number of features [102]. The goal of the feature selection is to choose a subset of available features by eliminating the unnecessary features. The length of the combined feature set which couples the morphological and temporal features, is reduced here by BFO algorithm which removes the redundant and irrelevant features. The advantage of the BFO is that it converges quickly in order to reach the global minimum solution [56]. Another advantage is that it involves less computational complexity [56]. In this chapter, 44 ECG recordings of the MIT-BIH arrhythmia database are used for the classification of five types of ECG beats recommended by the AAMI standards. A common training and testing dataset as described in the Chapter 2, is used for performance evaluation. The combined feature set of each record is optimized individually by BFO algorithm [115]. The resultant optimized feature subset is applied to the input of the LMS based SVM

classifier which is discussed in the previous chapter. The experimental results show that the proposed technique achieves significant reduction of features and improves the performance of ECG beat classification.

4.1.1 Organization of the chapter

The rest of the chapter is organized as follows. The theoretical background of the BFO technique is discussed in Section 4.2. The methodology of the feature reduction is thoroughly described in Section 4.3. This is followed by detailed experimental results shown in Section 4.4. Finally, Section 4.5 presents the conclusions for this chapter.

4.2 Theoretical Background

4.2.1 Bacteria Foraging Optimization (BFO)

Natural selection tends to eliminate animals with poor foraging strategies (methods for handling, locating and ingesting food) and favor the propagation of genes of animals with successful foraging behavior since they are more likely to enjoy reproductive success (they obtain enough food to enable them to reproduce) [116]. Bacterial foraging optimization (BFO) is a novel evolutionary algorithm based on the social foraging behavior of *E. coli* bacteria. *E. coli* and *Salmonella* are two motile bacteria which propel themselves by rotating their flagella. During foraging of the real bacteria, locomotion is achieved by a set of tensile flagella. Two basic operations performed by a bacterium during foraging are tumbling and swimming. Each flagellum pulls on the cell during clockwise rotation of flagella, as a result of which bacterium tumbles. The tumbling frequency of bacteria is less in a nutrient rich medium and more in case of harmful environment so as to quickly find a nutrient environment. On the other hand, during counter-clockwise movement of the flagella, bacteria swim at a rapid rate. Bacteria generally travel longer distances in a friendly environment and always avoid a noxious environment, preferring instead to move towards a favourable environment [117, 118]. BFO mimics the four basic principal mechanisms observed in bacteria : i) chemotaxis,

ii) swarming, iii) reproduction and iv) elimination-dispersal.

4.2.2 Chemotaxis

It is a very vital step towards the bacteria foraging method. The movement of bacteria is decided depending upon the rotation of the flagella. During foraging time it has two modes of operation (i) tumbling, (ii) swimming. In the predefined direction, it always swims for a period of time or it tumbles to avoid the noxious environment. Assume $\theta^k(l,m,n)$ indicates the location of the k^{th} bacterium at l^{th} chemotaxis, m^{th} reproductive, and n^{th} elimination-dispersal step. $C(k)$ is the step size taken in a random direction at the time of tumbling (run length unit). At the time of chemotaxis the bacterium movement can be expressed in the following equation

$$\theta^k(l+1,m,n) = \theta^k(l,m,n) + C(k)\frac{\Delta(k)}{\sqrt{\Delta^T(k)\Delta(k)}} \tag{4.1}$$

where, $\Delta(k)$ is a vector in the random direction whose elements lie in [-1, 1].

4.2.3 Swarming

When a bacterium searches an optimum path for foraging, it attracts other bacteria to that direction so that they can together reach the optimum path swiftly. Swarming causes the collective movement of the bacteria to the food. If $P(l,m,n) = \theta^k(l,m,n)$, is a set of bacteria locations, where $k = 1, 2, ..., S1$ then swarming can be represented as:

$$\begin{aligned} J_{cc}(\theta, P(l,m,n) &= \sum_{k=1}^{S1} J_{cc}^k(\theta, \theta^k(l,m,n)) \\ &= \sum_{k=1}^{S1}\left[-d1_{attract}\exp\left(-w1_{attract}\sum_{t=1}^{p}(\theta_t - \theta_t^k)^2\right)\right] \\ &\quad + \sum_{i=1}^{S1}\left[h1_{repellent}\exp\left(-w1_{repellent}\sum_{t=1}^{p}(\theta_t - \theta_t^k)^2\right)\right] \end{aligned} \tag{4.2}$$

where, $J_{cc}(\theta, P1(k,l,m))$ indicates the time-dependent function which depends on the collective movement of bacteria and $J(k,l,m,n)$ is integrated to the cost function. Therefore, the bacteria begin to find food and avoid areas with less food while attracting

each other; but they never get too close to each other. $S1$ represents the total number of bacteria and $P1$ is the bacterium position in the p-dimensional space which is to be optimized in this work. $d1_{attract}, h1_{repellent}, w1_{attract}$ and $w1_{repellent}$ are coefficients that must be given a proper value depending on the problem [119–121].

4.2.4 Reproduction

Half of the bacteria die due to low nutrient concentration and of the remaining half consisting of healthy bacteria, each bacterium splits into two bacteria, which are placed in the same previous location. This process keeps the population of bacteria constant [121].

4.2.5 Elimination-Dispersal

The bacteria population may be gradually unadaptable to the environment which causes a group of bacteria to be killed or dispersed into a new location due to the sudden change in the local environment or food consumption. The purpose of the elimination-dispersal event is to avoid being stuck in a local optimal solution and search for a new individual which is much closer to the global optimal solution.

4.3 Proposed Methodology

The length of the extracted combined features are reduced using BFO algorithm which removes the redundant and irrelevant features. It converges quickly in order to reach the global minimum solution [56]. The resulting optimized feature subset is applied to the input of the classifier to detect the ECG beats. The position of each bacteria denotes one possible solution for feature subset selection which is important for ECG beat classification. The number of dimensions of search space is equal to the length of the combined feature vector extracted from S-transform based morphological features and temporal features. The position of the bacteria is represented by 1 or 0 for each dimension of search space, where the selected feature is represented by 1 and

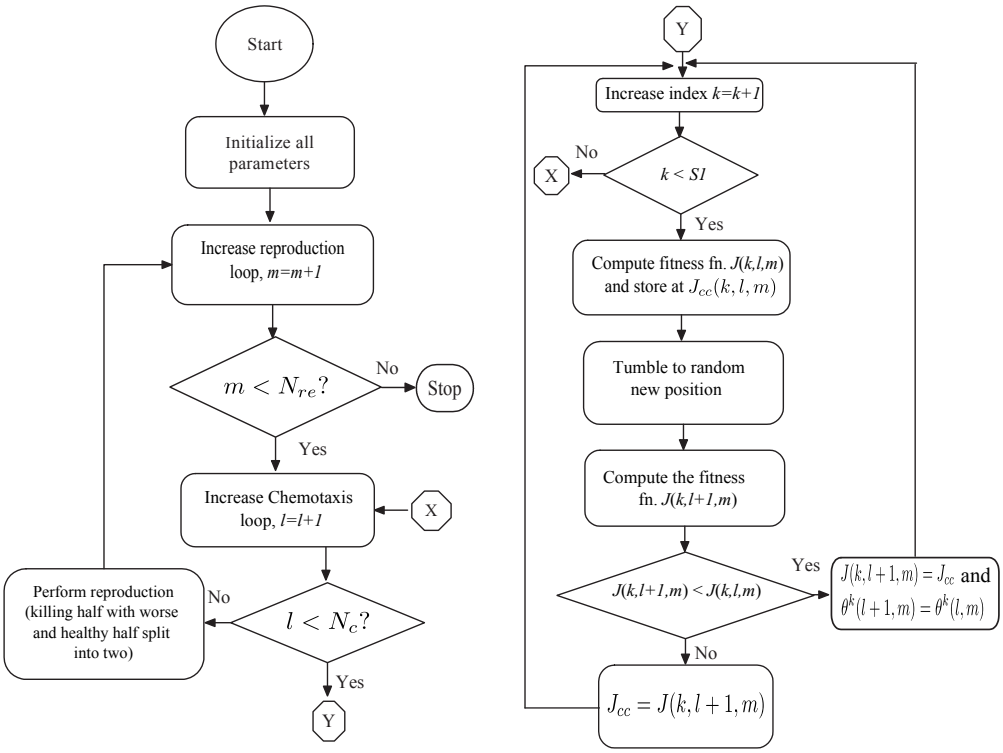

Figure 4.1: Flow chart of the feature reduction technique using BFO algorithm.

the non-selected feature is represented by 0. Each bacteria tumbles to the new random position in each iteration of chemotaxis [56], [122]. In every generation, the fitness value of each bacteria is evaluated by a fitness function. This evolution is driven by the fitness function J [115]. Let $c_1, c_2, ..., c_L$ and $N_1, N_2, ..., N_L$ denote the classes and number of samples within each class, respectively. Let M_k be the mean of the k^{th} class in the feature space, where $k = 1, 2, ..., L$ and L is the number of class. Then M_k can be calculated as

$$M_k = \frac{1}{N_k} \sum_{j=1}^{N_k} C_j^{(k)} \tag{4.3}$$

where, $C_j^{(k)}$, j=1,2,...,N_k represents the samples from class c_k, N_k represents the number of samples in the k^{th} class and total mean M_0 is defined as

$$M_o = \frac{1}{n1} \sum_{k=1}^{L} N_k M_k \tag{4.4}$$

where, $n1$ is the total number of samples for all classes. The fitness function J is computed using the following equation

$$J = \sqrt{\sum_{k=1}^{L} (M_k - M_0)^T (M_k - M_0)} \tag{4.5}$$

The flow chart of the feature reduction procedure using BFO algorithm is clearly shown in Fig. 4.1.

The detailed feature reduction procedure using BFO algorithm is illustrated as follows.

Step 1: Assume, p is the dimension of search space. The number of dimensions of search space is equal to the length of the proposed combined feature. The position of the bacteria is represented by 1 or 0 for each dimension of search space which indicates the each possible solution of optimized feature. Let, $S1$, N_c, N_{re} are the total number of bacteria in the population, number of chemotaxis steps and the number of reproduction steps respectively.

Step 2: Select randomly the position of k^{th} bacteria in l^{th} chemotaxis and m^{th} reproduction step as $\theta^k(l,m) = F_1F_2.....F_p$. F_z =1 or 0 $(z = 1, 2, .., p)$ depending upon whether z^{th} feature will be selected or not for the next iteration.

Step 3: (Reproduction loop) For $m = m + 1$.

Step 4: (Chemotaxis loop) For $l = l + 1$.

(a): (Bacteria fitness value calculation loop) For $k = k + 1$.

(b): Compute the fitness function of k^{th} bacteria for position $\theta^k(l,m)$ using (4.3), (4.4) and (4.5).

(c): *Tumble:* Tumble to random new position, $\theta^k(l+1,m)$ as defined in Step 2, i.e. $\theta^k(l,m) = F_1F_2.....F_p$.

(d): *Move:* After tumbling, move the bacteria to new position $\theta^k(l+1,m)$.

(e): Compute the fitness function $J(k,l+1,m)$ for new position $\theta^k(l+1,m)$ using (4.3), (4.4) and (4.5).

(f): If current fitness function $J(k,l+1,m)$ is less than previous fitness function $J(k,l,m)$, then move bacteria back to its previous position: $\theta^k(l+1,m) = \theta^k(l,m)$ and

simultaneously update the fitness function $J(k, l+1, m) = J(k, l, m)$.

(g): If $k < S1$, go to (b). In this case, compute fitness function for next bacteria until fitness function values for all bacteria are not computed.

Step 6: If $l < N_c$, go to Step 4. At this step we go for chemotaxis process until specific number of chemotaxis step is reached.

Step 7: *Reproduction:* For given m and for each k=1,2,...,$S1$, Assume, $J^k_{health} = \sum_{l=1}^{N_c+1} J(k, l, m)$ is the health of bacteria. Then the health of bacteria is sorted according to descending order of J_{health} (highest cost means highest health). The bacteria with $S_r = S1/2$ lowest J_{health} values die. Each bacterium of the remaining bacteria with best J_{health} values splits in two bacteria which are placed in the same previous location. This process keeps the population of bacteria constant.

Step 8: The position of bacteria is selected according to $max(J_{health})$ value. This position represents the best selected feature subset out of the complete feature set.

There are certain variations in this above BFO algorithm from original one. Firstly, the bacteria moves back to its previous position if the current position is less suitable which is verified by the fitness function. Secondly, the bacteria may get stuck in a local optima. The elimination-dispersal step removes bacteria from its current position and moves it to a random new position. In this algorithm, the position of bacteria is decided randomly in each iteration. Hence, the elimination-dispersal step is not used in this feature reduction algorithm [56], [122].

4.4 Performance Evaluation

In this thesis, 44 recordings of the MIT-BIH arrhythmia database are considered for the classification of five types of heartbeats as per AAMI standards and recommendations. A common training dataset [3], which contains a total of 245 representative beats, including 75 beats from each of classes N, S and V and 13 beats of class F and 7 beats of class Q, is described in Chapter 2. The LMS based SVM classifier is trained with 245 common training beats and first 5 min of the patient specific ECG record. The

remaining 25 min beats of each 24 records (in the range of 200-234) out of 44 recordings are completely new to the classifier and are used as test patterns for performance evaluation. The classification evaluation is quantified using the most common metrics such as accuracy (Acc), sensitivity (Sen), specificity (Spe) and positive predictivity (Ppr) found in the literature [3]. In Chapter 3, the performance of a standard multi-class SVM classifier is compared with the LMS based SVM classifier for ECG beat classification using both wavelet based feature and combined feature based on S-transform. In this work, the feature set of each record is optimized individually using BFO algorithm. It is found from the BFO output that the optimized feature length of each record is different to achieve the optimum solution, which is approximately 50% of the original feature length. The beat-by-beat optimized feature length is shown in Table 4.1. In this chapter, classification performances are evaluated using two approaches. The first approach uses the BFO based reduced wavelet feature set whereas second approach is based on BFO based reduced combined feature set. These feature sets from two approaches are separately classified using LMS based multi-class SVM classifier. The first one approach is indicated as WT-BFO-LMS-SVM method, and second approach as ST-BFO-LMS-SVM method.

4.4.1 Experimental results for wavelet based feature set

The confusion matrix and classification performance for beat-by-beat evaluation of 24 ECG records are shown in Table 4.2 and Table 4.3 respectively based on WT-LMS-SVM method and WT-BFO-LMS-SVM method. For 24 ECG records, using WT-LMS-SVM method the sensitivities for classification performance of N, V, S, F and Q classes are achieved as 95.94%, 87.33%, 55.07%, 62.09% and 0.00% respectively whereas the WT-BFO-LMS-SVM method yields the sensitivities of N, V, S, F and Q classes as 96.80%, 87.98%, 61.08%, 64.71% and 0.00% respectively. The accuracies of classification obtained for the classes N, V, S, F and Q are 93.50%, 97.15%, 95.99%, 99.15% and 99.69% respectively using the WT-LMS-SVM method whereas the same using the WT-BFO-LMS-SVM method are 94.43%, 97.38%, 96.73%, 99.37% and 99.78% respec-

Table 4.1: Beat-by-beat optimized feature length using BFO technique (where original features are 20 dimensional and 180 dimensional using WT based method and ST based method, respectively.)

Tape No.	Reduced feature length		Tape No.	Reduced feature length	
	WT Method	ST method		WT Method	ST method
200	10	91	215	11	91
201	10	92	219	11	90
202	11	93	220	11	84
203	12	84	221	10	91
205	10	86	222	12	97
207	10	89	223	10	95
208	11	94	228	11	84
209	10	85	230	10	95
210	11	93	231	11	96
212	11	90	232	10	83
213	10	83	233	10	91
214	10	88	234	10	97

Table 4.2: Confusion matrix for beat-by-beat classification performance using WT-LMS-SVM method and WT-BFO-LMS-SVM method for 24 ECG records of the MIT-BIH database

Method	WT-LMS-SVM					WT-BFO-LMS-SVM				
Class	N	V	S	F	Q	**N**	**V**	**S**	**F**	**Q**
N	40143	601	903	122	73	**40502**	**545**	**647**	**70**	**78**
V	501	4199	22	52	34	**488**	**4230**	**43**	**27**	**20**
S	890	110	1293	17	38	**825**	**82**	**1428**	**2**	**1**
F	132	89	11	380	0	**103**	**94**	**19**	**396**	**0**
Q	5	3	0	0	0	**6**	**1**	**1**	**0**	**0**

tively for 24 ECG records. Table 4.4 and Table 4.5 represent the confusion matrix and classification performance respectively for 44 ECG records of the MIT-BIH database. The sensitivities obtained for the classes N, V, S, F and Q are 95.76%, 87.08%, 52.75%, 62.09% and 0.00% respectively using WT-LMS-SVM method whereas the same using the WT-BFO-LMS-SVM method are 96.07%, 88.20%, 57.17%, 64.04% and 0.00% respectively using 44 ECG records. From the evaluation results of 44 ECG records, it is seen that accuracies obtained for the classes N, V, S, F and Q are 94.24%, 96.94%, 96.91%, 99.43% and 99.74% respectively using the WT-LMS-SVM method whereas the

Table 4.3: Performance Comparison of the WT-LMS-SVM method and WT-BFO-LMS-SVM method for 24 records of the MIT-BIH database

Method	WT-LMS-SVM					WT-BFO-LMS-SVM				
Class	N	V	S	F	Q	**N**	**V**	**S**	**F**	**Q**
Acc	93.50	97.15	95.99	99.15	99.69	**94.43**	**97.38**	**96.73**	**99.37**	**99.78**
Sen	95.94	87.33	55.07	62.09	0.00	**96.80**	**87.98**	**61.08**	**64.71**	**0.00**
Spe	80.35	98.21	98.02	99.61	99.71	**81.69**	**98.39**	**98.50**	**99.80**	**99.80**
Ppr	96.33	83.95	58.01	66.55	0.00	**96.61**	**85.42**	**66.79**	**80.00**	**0.00**

same using the WT-BFO-LMS-SVM method are 94.54%, 97.23%, 97.16%, 99.52% and 99.77% respectively.

Table 4.4: Confusion matrix for beat-by-beat classification performance using WT-LMS-SVM method and proposed WT-BFO-LMS-SVM method for 44 ECG records of the MIT-BIH database

Method	WT-LMS-SVM					WT-BFO-LMS-SVM				
Class	N	V	S	F	Q	**N**	**V**	**S**	**F**	**Q**
N	71717	1602	1308	146	123	**71953**	**1460**	**1196**	**137**	**150**
V	541	5122	113	60	46	**540**	**5186**	**93**	**28**	**35**
S	971	112	1296	37	41	**963**	**82**	**1408**	**2**	**2**
F	132	89	11	380	0	**106**	**86**	**20**	**399**	**1**
Q	5	3	0	0	0	**6**	**1**	**1**	**0**	**0**

Table 4.5: Performance Comparison of the WT-LMS-SVM method and WT-BFO-LMS-SVM method for 44 records of the MIT-BIH database

Method	WT-LMS-SVM					WT-BFO-LMS-SVM				
Class	N	V	S	F	Q	**N**	**V**	**S**	**F**	**Q**
Acc	94.24	96.94	96.91	99.43	99.74	**94.54**	**97.23**	**97.16**	**99.52**	**99.77**
Sen	95.76	87.08	52.75	62.09	0.00	**96.07**	**88.20**	**57.17**	**64.04**	**0.00**
Spe	81.59	97.68	98.24	99.71	99.75	**81.85**	**97.91**	**98.39**	**99.79**	**99.78**
Ppr	97.75	73.93	47.51	61.00	0.00	**97.77**	**76.15**	**52.28**	**69.27**	**0.00**

4.4.2 Experimental results for S-transform based feature set

Table 4.6 and Table 4.7 represent the confusion matrix and classification performance respectively for beat-by-beat evaluation of 24 ECG records using ST-LMS-SVM method and ST-BFO-LMS-SVM method. For 24 ECG records, ST-LMS-SVM method yields a

detection sensitivity of 97.83%, 90.00%, 68.65%, 64.22% and 25.00% for the classes N, V, S, F and Q respectively and accuracy of 96.07%, 98.11%, 97.14%, 99.31% and 99.91% for the same respectively whereas ST-BFO-LMS-SVM method shows a detection sensitivity of 98.12%, 91.37%, 73.64%, 66.99% and 25.00% for the classes N, V, S, F and Q respectively and accuracy of 96.64%, 98.38%, 97.50%, 99.40% and 99.91% for the same respectively. Table 4.8 and Table 4.9 show the confusion matrix and classification performance respectively for evaluation of 44 ECG records based on ST-LMS-SVM method and ST-BFO-LMS-SVM method. For 44 ECG records, the ST-LMS-SVM method gives a detection sensitivity of 97.97%, 90.79%, 69.96%, 64.22% and 25.00% for the classes N, V, S, F and Q respectively and accuracy of 96.92%, 98.50%, 97.87%, 99.57% and 99.92% for the same respectively whereas the ST-BFO-LMS-SVM method yields a detection sensitivity of 98.14%, 91.74%, 74.73%, 66.99% and 25.00% for the classes N, V, S, F and Q respectively and accuracy of 97.25%, 98.56%, 98.17%, 99.60% and 99.95% for the same respectively.

Table 4.6: Confusion matrix for beat-by-beat classification performance using ST-LMS-SVM method and ST-BFO-LMS-SVM method for 24 ECG records of the MIT-BIH database

Method	ST-LMS-SVM					ST-BFO-LMS-SVM				
Class	N	V	S	F	Q	**N**	**V**	**S**	**F**	**Q**
N	40936	303	538	50	15	**41056**	**222**	**525**	**27**	**12**
V	273	4327	122	72	14	**248**	**4393**	**82**	**68**	**17**
S	640	84	1612	3	9	**522**	**86**	**1729**	**2**	**9**
F	127	67	22	393	3	**107**	**80**	**13**	**410**	**2**
Q	3	3	0	0	2	**3**	**3**	**0**	**0**	**2**

It is seen from the performance Table 4.2 - 4.9 that the average beat classification sensitivity of the proposed BFO-LMS-SVM method is better than the LMS-SVM method for both WT based and ST based combined feature set. In WT-LMS-SVM method, 1001 number of S beats are misclassified as N beat for WT-LMS-SVM method whereas for WT-BFO-LMS-SVM method, 963 number of S beats are misclassified as N beat. Table 4.8 represents that 638 and 521 numbers of S beats are classified as N beat for ST-LMS-

Table 4.7: Performance Comparison of the ST-LMS-SVM method and ST-BFO-LMS-SVM method for 24 records of the MIT-BIH database

Method	ST-LMS-SVM					ST-BFO-LMS-SVM				
Class	N	V	S	F	Q	**N**	**V**	**S**	**F**	**Q**
Acc	96.07	98.11	97.14	99.31	99.91	**96.64**	**98.38**	**97.50**	**99.40**	**99.91**
Sen	97.83	90.00	68.65	64.22	25.00	**98.12**	**91.37**	**73.64**	**66.99**	**25.00**
Spe	86.59	98.98	98.56	99.74	99.92	**88.68**	**99.13**	**98.69**	**99.80**	**99.92**
Ppr	97.52	90.45	70.27	75.87	4.65	**97.90**	**91.83**	**73.61**	**80.87**	**4.76**

Table 4.8: Confusion matrix for beat-by-beat classification performance using ST-LMS-SVM method and ST-BFO-LMS-SVM method for 44 ECG records of the MIT-BIH database

Method	ST-LMS-SVM					ST-BFO-LMS-SVM				
Class	N	V	S	F	Q	**N**	**V**	**S**	**F**	**Q**
N	73373	562	878	61	22	**73501**	**546**	**782**	**59**	**8**
V	294	5340	152	74	22	**279**	**5396**	**116**	**70**	**21**
S	638	84	1719	4	12	**521**	**89**	**1836**	**2**	**9**
F	127	67	22	393	3	**107**	**80**	**13**	**410**	**2**
Q	3	3	0	0	2	**3**	**3**	**0**	**0**	**2**

SVM and ST-BFO-LMS-SVM methods respectively. It is also seen from the Table 4.5 and 4.9 that the sensitivities of S beat detection for the WT-BFO-LMS-SVM technique is comparatively very less than the proposed ST-BFO-LMS-SVM technique because of large number of N beats are misclassified as S beat in the case of the WT-BFO-LMS-SVM method. The atrial escape beat of N class is difficult to distinguish from atrial premature beat of S class due to similar morphological characteristics. Similarly, from

Table 4.9: Performance Comparison of the ST-LMS-SVM method and ST-BFO-LMS-SVM method for 44 records of the MIT-BIH database

Method	ST-LMS-SVM					ST-BFO-LMS-SVM				
Class	N	V	S	F	Q	**N**	**V**	**S**	**F**	**Q**
Acc	96.92	98.50	97.87	99.57	99.92	**97.25**	**98.56**	**98.17**	**99.60**	**99.95**
Sen	97.97	90.79	69.96	64.22	25.00	**98.14**	**91.74**	**74.73**	**66.99**	**25.00**
Spe	88.15	99.08	98.71	99.83	99.93	**89.84**	**99.08**	**98.88**	**99.84**	**99.95**
Ppr	98.57	88.18	62.04	73.87	3.28	**98.78**	**88.26**	**66.84**	**75.79**	**4.76**

Table 4.4 it is seen that in the WT-BFO-LMS-SVM method, 137 beats of N class are misclassified as F class and 106 beats of F class are misclassified as N class. For the

proposed ST-BFO-LMS-SVM method, 59 number of N beats are misclassified as F beat whereas 107 number of F beats are misclassified as N beat as represented by Table 4.8. From the performance statistics, it is seen that the sensitivity of S beat detection is not as good as V beat detection due to deficiency of class S patterns in the training phase and also intra-variation of patterns makes its detection complex [63]. Therefore, more S beats are misclassified as N beat. F beats are difficult to distinguish from N beat because F beats are the union of V and N beats and their morphology and timing information also closely resembles those of N beat. However, the beat detection performance of all classes of beats is comparably more than earlier reported techniques.

Table 4.10: Classification performance (in %) of Ince *et al.* [3] and the proposed methods for 24 recordings of the MIT-BIH arrhythmia database

Methods	Ince et al.					Proposed				
Class	N	V	S	F	Q	**N**	**V**	**S**	**F**	**Q**
Acc	95.0	97.6	96.1	99.2	99.9	**96.6**	**98.4**	**97.5**	**99.4**	**99.9**
Sen	97.0	83.4	62.1	61.4	0.0	**98.1**	**91.4**	**73.6**	**67.0**	**25.0**
Spe	84.1	98.1	98.5	99.7	99.9	**88.7**	**99.1**	**98.7**	**99.8**	**99.9**
Ppr	97.0	87.4	56.7	73.4	0.0	**97.9**	**91.8**	**73.6**	**80.9**	**4.8**

Table 4.10 compares the classification performance of ST-BFO-LMS-SVM method with recently reported Ince *et al.* method [3]. In Ince *et al.* method, the detection sensitivities are 97.0%, 83.4%, 62.1%, 61.4% and 0.0% for the classes N, V, S, F and Q respectively whereas the proposed ST-BFO-LMS-SVM yields the sensitivities of 98.1%, 91.4%, 73.6%, 67.0% and 25.0% for the classes N, V, S, F and Q respectively using 24 ECG records. The positive predicitivities are obtained as 97.9%, 91.8%, 73.6%, 80.9% and 4.8% respectively for the classes N, V, S, F and Q using proposed ST-BFO-LMS-SVM method whereas the Ince *et al.* [3] achieves the positive predicitivities of 97.0%, 87.4%, 56.7%, 73.4% and 0.0% for the classes N, V, S, F and Q respectively. It is noticed from the performance table that the performance of the proposed method is better than reported Ince *et al.* [3] method. For comparing the performance results, the detection of V and S beats are shown in Table 4.11. The performance results of V beat detections are based on 11 test recordings (200, 202, 210, 210, 212, 213, 214, 219, 221, 222, 228, 231,

Table 4.11: Performance comparison (in percent) of ventricular and supra-ventricular beat detections

Methods	Recordings	V				S			
		Acc	Sen	Spe	Ppr	Acc	Sen	Spe	Ppr
Hu *et al.* [31]	200, 202, 210, 213, 214, 219, 221, 228	94.8	78.9	96.8	75.8	N/A	N/A	N/A	N/A
Chazal *et al.* [62]	231, 233, 234 for V beat detection and 200,	96.4	77.5	98.9	90.6	92.4	76.4	93.2	38.7
Jiang *et al.* [63]	202, 210, 212, 213, 214, 219, 221, 222,	98.8	94.3	99.4	95.8	97.5	74.9	98.8	78.8
Ince *et al.* [3]	228, 231, 232, 233, 234 for S beat detection	97.9	90.3	98.8	92.2	96.1	81.8	98.5	63.4
Proposed		**99.0**	**95.7**	**99.6**	**96.3**	**98.2**	**84.9**	**98.9**	**82.6**
Ince *et al.* [3]	44 recordings of MIT-BIH	98.3	84.6	98.7	87.4	97.4	63.5	99.0	53.7
Proposed	arrhythmia database	**98.6**	**91.7**	**99.1**	**89.3**	**98.2**	**74.7**	**99.0**	**66.9**

232, 233, and 234) that are common to other existing methods as shown in the Table 4.11. For S beat detection, comparison results are based on 14 common recordings (200, 202, 210, 210, 213, 214, 219, 221, 228, 231, 233, and 234) between proposed method and all other existing methods except Hu *et. al* [31] method. In the proposed ST-BFO-LMS-SVM method, the sensitivity, accuracy, specificity and positive predictivity of V beat detection are 95.7%, 99.0%, 99.6%, and 96.3% respectively, whereas the Ince *et al.* [3] method achieves sensitivity, accuracy, specificity and positive predictivity as 90.3%, 97.9%, 98.8%, and 92.2% respectively for selected 11 ECG records. For S beat detection, the proposed ST-BFO-LMS-SVM technique shows the sensitivity, accuracy, specificity and positive predictivity as 84.9%, 98.2%, 98.9%, and 82.6% respectively, whereas the Ince *et al.* [3] technique provides 81.8%, 96.1%, 98.5%, and 63.4%, respectively for 14 ECG records. From the performance statistics, it is seen that the sensitivity of S beat detection is not as good as V beat detection due to a deficiency in S beat patterns during the training phase and also because the intra-variation of patterns makes it complex to detect. It is difficult to classify between N beat and S beat because the QRS complex associated with an atrial premature beat in the S beat has normal QRS duration and the same morphology as that of the N beat. Therefore, more S beats are misclassified as N beat. An overall average sensitivity of 74.7% and specificity of 99.0% are achieved for S beat detection and an average sensitivity of 91.7% and specificity of 99.1% are achieved for V beat detection using proposed ST-BFO-LMS-SVM method over all 44 patient-recordings of the MIT-BIH arrhythmia database. These results show that a significant improvement is achieved in case of the proposed ECG heartbeat classification method

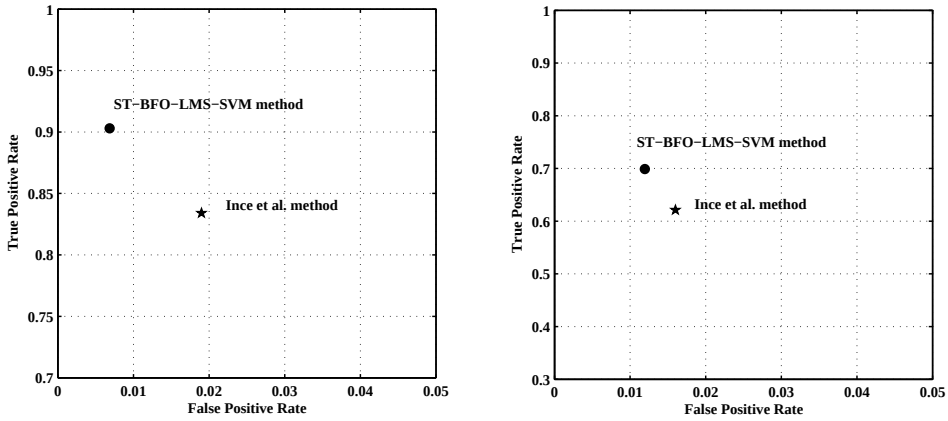

Figure 4.2: Comparison of true positive rate and false positive rate for two techniques in terms of (a) V beat detection (b) S beat detection.

compared to existing methods.

The relationship between sensitivity and specificity are described by the receiver operating characteristic (ROC) curve which alleviates improved analysis in terms of the classification performance of a diagnostic technique [4]. Fig. 4.2 is marked as a ROC curve of V beat and S beat detection for 44 ECG records where the X-axis represents the false positive rate (FPR) and the Y-axis represents the true positive rate (TPR). For accurate classification, TPR=1 and FPR=0 corresponds to the upper left corner of the ROC curve. Therefore, the combination of TPR-FPR is considered better when it is nearer to the upper left corner. It is observed that for V beat and S beat detection, proposed ST-BFO-LMS-SVM method provides a higher TPR but lower FPR compared to the Ince *et al.* [3] method which only reported testing results for 44 ECG records.

4.5 Conclusions

The salient points covered in this chapter are:

- In this chapter, BFO technique is adopted to optimize the features for ECG beat classification.
- Length of the combined features are reduced in this work by removing the redundant and irrelevant features using BFO algorithm.

- An automatic ECG beat classification experiment is conducted on the benchmark MIT-BIH arrhythmia database based on AAMI standards and recommendations. The classification performances show that the proposed BFO-LMS-SVM technique achieves better average specificities and sensitivities compared to existing methods. Experimental results also show that a significant improvement is achieved for proposed heartbeat classification method compared to existing methods.

CHAPTER 5

ECG Signal Enhancement based on S-transform

5.1 Introduction

Electrocardiogram (ECG) is a noninvasive technique that is used as a diagnostic tool for cardiovascular diseases [67]. Since ECG is widely used as a fundamental tool for patient monitoring, examination, and diagnosis of cardiac disorders, it is important to be able to reliably and quickly detect the cardiac disorders. ECG would be much more useful as a diagnostic tool if unwanted noise embedded in the signal is removed. For wireless and telecardiology applications, the transmission of noise free ECG signal over telephone lines or mobile communication is very important. During acquisition and transmission, ECG signals are generally affected by the different noises like channel noise, muscle artifacts, electrode motion and baseline wander [68], [123]. Muscle artifacts are introduced due to muscle activity and electrode motion is caused by a shift in electrode location [68]. Baseline wander is the variation in the isoelectric line of ECG which can occur during respiration. Poor channel conditions can also introduce noise in the ECG signal during its transmission [68]. All these noises can corrupt the signal and make the signal analysis difficult and error prone. Hence, for further processing, noisy ECG signals should be enhanced by removing the noise components from signals.

Various techniques have been reported in the literature for the enhancement of ECG signals [67,70,123–129] including techniques like fuzzy multi-wavelet denoising [124], independent component analysis [125], wavelet denoising [70], [126] and least mean square (LMS) algorithm based adaptive filter [123]. However, most of these reported techniques generally concentrated only on one kind of noise [67,70,123–129]. A few reported techniques [68,123] show significant performance in case of ECG signals embedded with different types of noises. However, these techniques require prior information of the signal to work efficiently such as position of the R-peak for empirical mode decomposition (EMD) based technique [68] and a reference signal for the LMS algorithm based method [123]. This kind of information is difficult to obtain when the noise level is very high. The wavelet transform (WT) based techniques [70,124,126] are more popular and widely used because of its ability to characterize time-frequency domain information of a

time domain signal. Ercelebi [126] reported an ECG signal enhancement technique based on 4th level decomposition coefficients of Daubechies wavelet with soft thresholding when the ECG signal is corrupted with base line wander, muscle artifact and electrode motion noises. In another reported literature, Poornachandra [70] proposed an ECG signal enhancement technique using 3rd level decomposition coefficients of Daubechies wavelet with subband dependent thresholding. This reported work is applied on baseline wander, muscle artifact, electrode motion and Gaussian noises. However, the amplitude of the wavelet transform is dependent on the frequency. Wavelet transform also has other limitations [95] such as having better frequency resolution and poor time resolution for low frequencies and vice versa for high frequencies. It also has locally referenced phase.

In this chapter, a novel method for ECG signal enhancement is proposed using S-transform to overcome the aforementioned limitations [130]. This method can be applied to enhance the ECG signal from different noises which often get embedded with ECG the signal during its acquisition and transmission [68]. During acquisition of ECG signal in real time environment, different types of noises such as channel noise, muscle artifacts, electrode motion, and base line wander are often embedded with ECG signal. Muscle artifacts are due to the movement of muscle between skin and electrode. Motion artifacts are transient baseline changes caused by changes in the electrode-skin impedance with electrode motion. Base line drift may be caused in chest-lead ECG signals due to coughing and breathing and the resulting movement of the chest, and because of movement of arms/legs in case of limb-lead ECG acquisition. This work proposes an automatic and generalized approach for ECG signal enhancement technique. Besides this, the proposed method does not require any prior information like R-peak position or reference signal as auxiliary signal. S-transform (ST), derived by Stockwell *et al.* [82], is closely related to the wavelet transform (WT) and short time Fourier transform (STFT). ST has a similar form to the STFT except that the width of window varies with frequency [95]. S-transform has three characteristics that distinguishes it from wavelet transform: (i) frequency invariant amplitude response (ii) progressive resolution and (iii) absolutely referenced phase information. Besides these, ST uses

time-frequency axis rather than the time-scale axis used in the WT [95]. Therefore, the interpretation on the frequency information in the ST is more straight forward than in the WT, which is beneficial for removing noise components. ST is used to represent the noisy ECG signal in time-frequency domain. An automatic mask window and morphological filtering technique is applied to this time-frequency domain represented noisy signal for removing the noise. The proposed algorithm is evaluated for different types of noise like white Gaussian noise, muscle artifact, electrode motion, and baseline wander [130]. Performance of the proposed algorithm is evaluated by means of signal to noise ratio (SNR) and root mean square error (RMSE). Experimental results show that the proposed method [130] yields superior performance compared to the commonly used wavelet transform with soft thresholding (WT-Soft) [126] and wavelet transform with subband thresholding (WT-Subband) based techniques [70]. The performance of different ECG enhancement techniques at 1.25 dB input SNR level is also compared using analysis of variance (ANOVA) based statistical evaluation method to quantify the significant difference among all methods, and the proposed method yields superior performance compared to other methods. The performance of R-peak detection for denoised ECG signal in terms of sensitivity and positive predictivity using proposed enhancement method is also better than WT-Soft, WT-Subband based methods and it validates the superior performance of the proposed method. An ECG beat classification experiment is also presented here to evaluate the quality of the preserved features in the recovered ECG signal. It is observed that the recognition performance for the denoised ECG signal using proposed enhancement scheme is better compared to the WT-Soft, WT-Subband based methods.

5.1.1 Organization of the chapter

The rest of the chapter is organized as follows. In Section 5.2 provides the fundamental information on different types of noises. WT based ECG enhancement techniques are briefly explained in Section 5.3. The proposed methodology is presented in Section 5.4. In Section 5.5, experimental results and performance comparisons are shown. Section

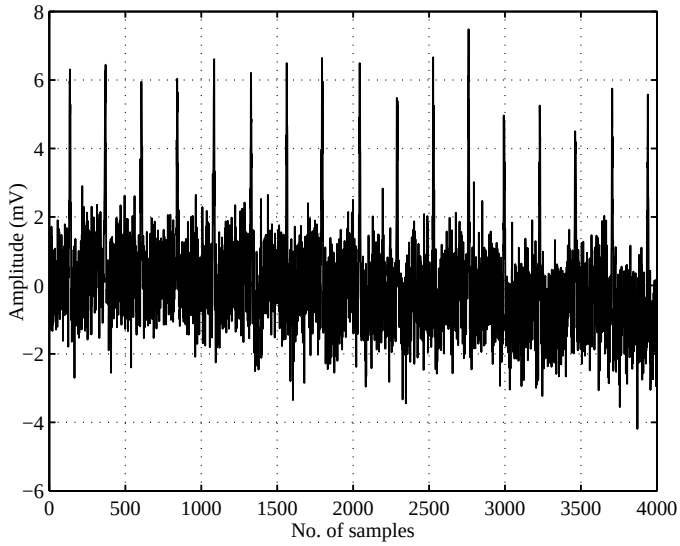

Figure 5.1: ECG signal corrupted with Gaussian noise at an SNR of 1.25 dB.

5.6 discusses the significant results and comparison is made with earlier reported works. Finally, the chapter concludes with some final remarks in Section 5.7.

5.2 Different types of noises

Generally, noises are embedded with ECG signals during its acquisition and transmission. There are four different types of noises within the frequency band of the ECG signal that may contaminate it and may change its characteristics. These are as follows: (i) Gaussian noise (ii) Muscle artifacts (MA) (iii) Electrode motion (EM) and (iv) Baseline wander (BW).

5.2.1 Gaussian noise

During the acquisition and transmission in real time environment, ECG signals are often embedded with Gaussian noise which is random in nature. Poor channel conditions can also introduce Gaussian noise in ECG signals during the transmission [68]. Gaussian noise corrupted ECG signal at an SNR of 1.25 dB is shown in Fig. 5.1.

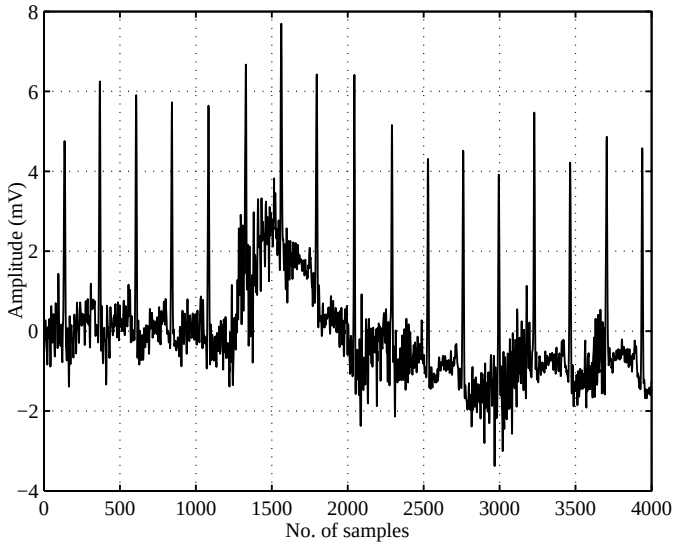

Figure 5.2: ECG signal corrupted with muscle artifacts (MA) noise at an SNR of 1.25 dB.

5.2.2 Muscle artifacts (MA) noise

Generally muscle contraction appears due to electrical activity in the muscles. The signals resulting from muscle contraction are assumed to be transient bursts of zero-mean band-limited Gaussian noise. Elecrtomyogram (EMG) interferences generate rapid fluctuation which is faster than the ECG wave. Its frequency lies between 0 to 10 kHz and duration is 50 ms [131]. MA noise corrupted ECG signal at an SNR of 1.25 dB is shown in Fig. 5.2.

5.2.3 Electrode motion (EM) noise

During the acquisition of ECG signal in real time environment, the EM noise is often embedded with ECG signal due to the transient baseline change between electrode skin impedance and electrode motion. The loss of contact can be permanent, or can be intermittent, as would be the case when a loose electrode is brought in and out of contact with the skin as a result of movements and vibration. It can generate larger amplitude signals in ECG waveform. The peak amplitude of this artifact may sometimes rise upto 500 percent of peak to peak ECG amplitude and its duration is about 100-500 ms [131]. ECG signal corrupted by real EM noise at an SNR of 1.25 dB is shown in Fig.

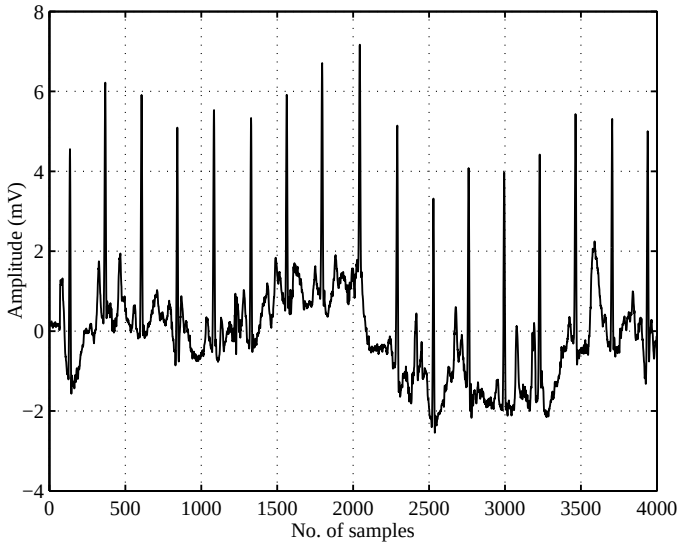

Figure 5.3: ECG signal corrupted with electrode motion (EM) noise at an SNR of 1.25 dB.

5.3.

5.2.4 Baseline wander (BW) noise

Base-line drift may be caused in chest-lead ECG signals by coughing or breathing with large movement of the chest, or movement of arms or legs in case of limb-lead ECG acquisition [77]. In most of the ECG recordings, the respiration, electrode impedance change due to perspiration and increased body movements are the main causes of base-line wandering [132]. Base-line drift can sometimes be caused by variations in temperature and bias in the instrumentation and amplifiers. Baseline wander noise lies between 0.15 Hz and 0.5 Hz [133]. Fig. 5.4 shows the ECG signal corrupted with baseline wander noise at an SNR of 1.25 dB.

5.3 Wavelet transform based ECG signal enhancement methods

In this section, two types of ECG denoising techniques [70], [126] are briefly described i.e, (i) wavelet transform with soft-thresholding [126] and (ii) wavelet transform with

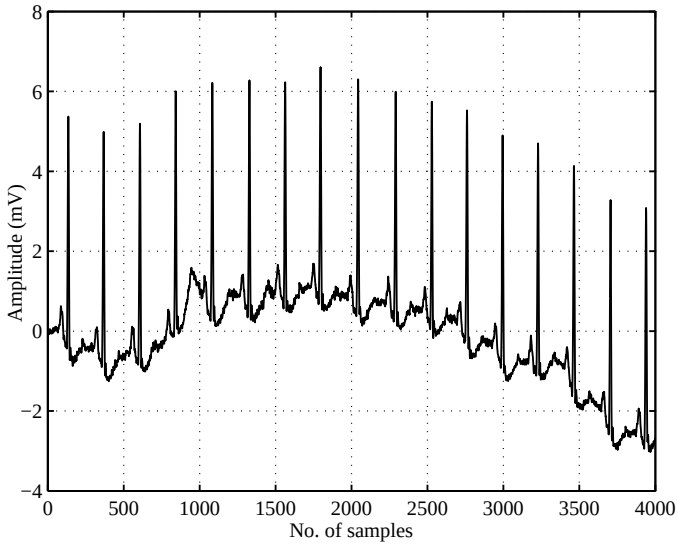

Figure 5.4: ECG signal corrupted with baseline wander (BW) noise at an SNR of 1.25 dB.

subband thresholding [70]. The wavelet transform with soft-thresholding is indicated as WT-soft method whereas wavelet transform with subband thresholding is represented as WT-subband method.

5.3.1 Wavelet transform with soft thresholding based (WT-soft) method

In this method [126], wavelet transform (WT) is applied on the noisy ECG signal to represent the signal in time-frequency domain. Next, a threshold is applied in this domain to remove the noise components from the signal and inverse transform is used on the denoised wavelet coefficients to get the enhanced signal. In the reported technique [126], the denoised ECG signal is obtained by applying the threshold at each level of decomposition. In the reported work [126], the decomposition level is taken as 4. Thresholding is a decision process that discriminates between ECG signal components and noise components.

The choice of thresholding functions and threshold values are critical in denoising schemes. Donoho proposed the following universal threshold (or 'thr') [134] for denosing.

$$thr = \sqrt{2\log_2(N)} \tag{5.1}$$

where, N is the length of the data sample. Wavelet coefficients are normalized using the following equation.

$$scale = \frac{median(|\gamma^j|)}{0.6745} \tag{5.2}$$

$$\gamma_n^j = \frac{\gamma^j}{scale} \tag{5.3}$$

where, γ^j is wavelet coefficient and γ_n^j is the normalized value of wavelet coefficient at decomposition level j. Each WT coefficient is then either soft or hard-thresholded. Soft thresholding removes all coefficients below a predefined threshold and reduces all remaining coefficients by that threshold. Soft-thresholded wavelet coefficients [126] can be represented as

$$\tilde{\gamma}_n^j(k) = \begin{cases} sign(\gamma_n^j(k))(|\gamma_n^j(k) - thr|) & if\ \gamma_n^j(k) > thr, \\ 0 & if\ \gamma_n^j(k) \leq thr. \end{cases} \tag{5.4}$$

Hard-thresholding keeps or zeros the absolute value of all the transform coefficients compared to the fixed threshold. Equation (5.5) represents the hard-thresholded wavelet coefficients [134], [126].

$$\tilde{\gamma}_n^j(k) = \begin{cases} \gamma_n^j(k) & if\ \gamma_n^j(k) > thr, \\ 0 & if\ \gamma_n^j(k) \leq thr. \end{cases} \tag{5.5}$$

5.3.2 Wavelet transform with subband thresholding based (WT-subband) method

In [70], a WT based denoising technique is reported for the enhancement of the ECG signal which is contaminated with white additive Gaussian noise and other real noises. In this reported technique, as S-median threshold, which is a level dependent threshold, is used for the WT based denoising technique. It also employs the spatial adaptivity of the WT and at the same time preserves the noise-reduced reconstruction property. The threshold also reduces the mean square error (MSE) value and outperforms the universal threshold in the process. Subband level dependent median threshold (S-median) is

expressed as

$$t_{l,n} = \frac{\sigma_n \sqrt{2\log(k)}}{(S_{l,n} + b)}, \quad n = 1, 2, ..., l \tag{5.6}$$

where, subband level dependent parameter is S_l, n which is defined as

$$S_{l,n} = 2^{(L-N/L)} \tag{5.7}$$

where, L indicates the maximum decomposition level, l is the no. of decomposition level, k is the length of the signal, σ indicates the noise variance and N the is level at which thresholding is done (for example at level 2, N = 2). Besides spatial adaptation and optimality, subband level dependent median threshold (S-median) has another parameter-tuning factor b [70]. The tuning parameter tunes the threshold to obtain

Algorithm 5.1: ECG signal denoising using WT-subband

1: Transform the signal into wavelet domain using commonly supported orthogonal wavelet basis function and select the level of decomposition (usually 3) [70].
2: Calculate the noise in each subband using median absolute deviation (MAD) estimator.
3: Calculate the S-median threshold by calculating the 'S' value and the MAD estimator.
4: Apply soft threshold, $\delta_t(x) = \text{sgn}(x)(|x| - t)^+$ to the empirical wavelet coefficients with subband level dependent threshold $t_{l,n}$.
5: Recover the signal using inverse wavelet transform.

effective noise-free reconstruction unlike universal threshold, which over-smoothens by killing significant coefficients. The tuning factor is estimated in the following way:
(i) As per the reported technique [70], the detail coefficient of decomposition level D_3 is divided into $D_3|_{i=1}^{\frac{p}{2}}$ and $D_3|_{i=\frac{p}{2}+1}^{p}$, where p is total number of the detail coefficients D_3.
(ii) The Mean values of detail coefficient $D_3|_{i=1}^{\frac{p}{2}}$ and $D_3|_{i=\frac{p}{2}+1}^{p}$ are computed individually.
(iii) The value of tuning factor 'b' is computed from the difference between the mean values of the two detail coefficients.
If the variance of the noisy signal is unknown, then the noise variance is computed by the following equation using the median absolute deviation (MAD) estimator which was

proposed by the Donoho on all the levels.

$$\sigma_n = \frac{median\,|x|}{0.6745}, \quad n = 1, 2, ..., l \tag{5.8}$$

The denoising algorithm using WT-subband method [70] is shown in Algorithm 5.1.

5.4 Proposed Framework: S-transform based ECG signal enhancement method

The objective of the proposed algorithm is to achieve enhanced signal by selecting the required frequencies and removing the noise components. Block diagram of proposed S-Transform based ECG signal enhancement method is shown in Fig. 5.5 and the different steps are explained as follows.

Step 1: Time-frequency domain representation: S-transform [135] is used to obtain the time-frequency representation of a time domain noisy ECG signal. The continuous S-transform $S(\tau, f)$ of a noisy ECG signal $h(t)$ at time $t = \tau$ and frequency f is defined as

$$S(\tau, f) = \int_{-\infty}^{\infty} h(t) \frac{|f|}{\sqrt{2\pi}} e^{\frac{-(\tau-t)^2 f^2}{2}} e^{-i2\pi ft}\, dt \tag{5.9}$$

An ECG signal $S(\tau, f_o)$ is defined as a one dimensional function of time for a frequency f_o. If the time series h(t) is windowed (or multiplied point by point) with a window function (Gaussian function) *g(t)* then the resulting spectrum is

$$H(f) = \int_{-\infty}^{\infty} h(t) g(t)\, e^{-i2\pi ft}\, dt \tag{5.10}$$

where generalized Gaussian function is

$$g(t) = \frac{1}{\sigma\sqrt{2\pi}} e^{-\frac{t^2}{2\sigma^2}} \tag{5.11}$$

and then allowing the Gaussian to be a function of translation τ and dilation (or window

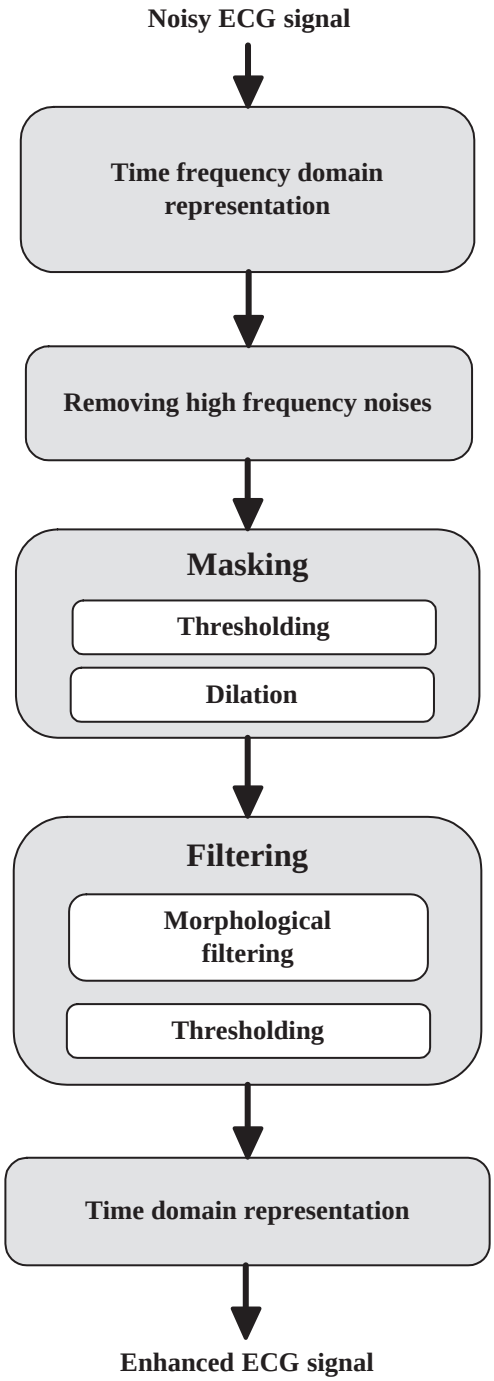

Figure 5.5: Block diagram of the proposed ECG signal enhancement technique.

width) σ.

$$S(\tau, f, \sigma) = \int_{-\infty}^{\infty} h(t) \frac{1}{\sigma\sqrt{2\pi}} e^{-\frac{(t-\tau)^2}{2\sigma^2}} e^{-i2\pi ft}\, dt \tag{5.12}$$

This is a special case of the multi-resolution Fourier transform due to its three independent variables and it is also impractical as a tool for analysis. Simplification can be achieved by adding the constraint restricting the width of the window to σ which is proportional to the period (or inverse of the frequency).

$$\sigma(f) = \frac{1}{|f|}$$

The Discrete S-transform [95] of the noisy ECG signal $h[kT]$ is given by

$$S\left[jT, \frac{n}{NT}\right] = \sum_{m=0}^{N-1} H\left[\frac{m+n}{NT}\right] e^{\frac{-2\pi^2 m^2}{n^2}} e^{\frac{i2\pi mj}{N}} \tag{5.13}$$

where $H\left[\frac{n}{NT}\right]$ is the Fourier transform of $h\left[kT\right]$ and j, m, $n = 0,1,...,(N-1)$. The time-frequency domain representation of a noisy ECG signal at an SNR of 5 dB is shown in Fig. 5.6(a).

Step 2: Remove High Frequency noises: The objective of this step is to remove high frequency noise components by applying frequency domain thresholding [136]. A clean ECG signal generally has a bandwidth of 0.05 to 100 Hz [4]. However, ECG signals of different beat types available in the MIT-BIH arrhythmia database [77] have shown that almost all the important information is present within 200 Hz. Hence a frequency domain threshold has been defined at 200 Hz such that the frequency components below 200 Hz are retained and frequency components above 200 Hz are removed. Fig. 5.6(b) shows the time-frequency domain representation (S_1) after removing high frequency noise.

Step 3: Masking: The objective of masking is to remove noise components whose frequencies are between the QRS complexes of the time-frequency domain represented S_1. Firstly, the output of the previous step, S_1 is thresholded by selecting an appropriate

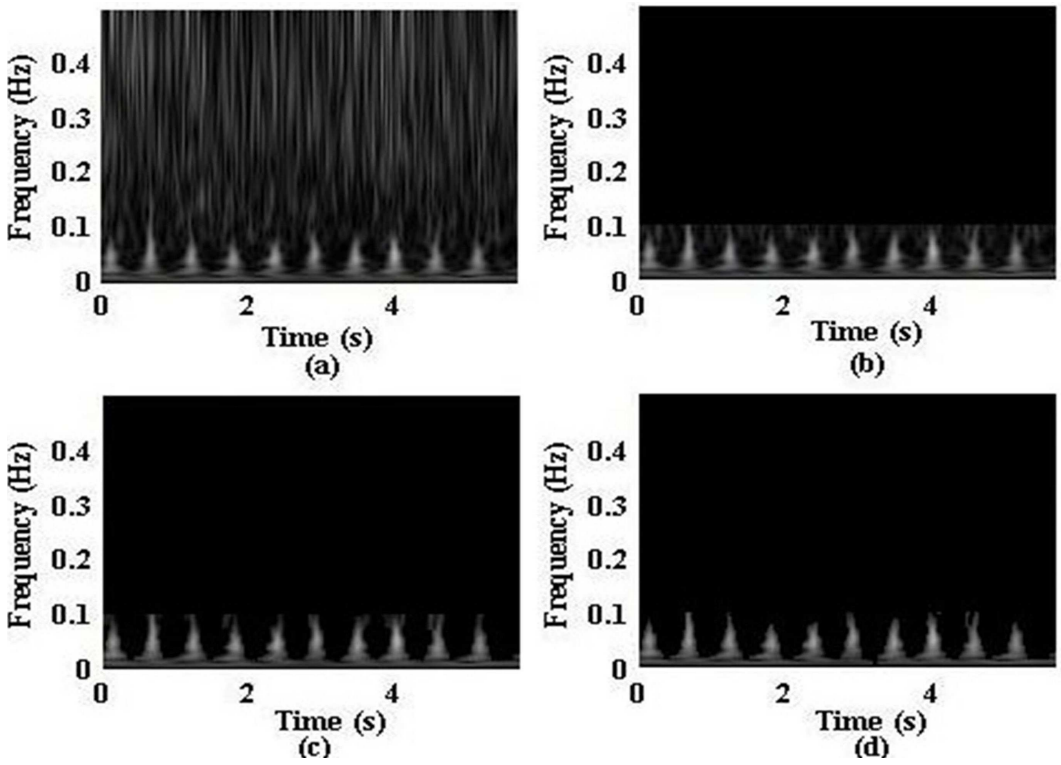

Figure 5.6: Different stages of the proposed method (a) Time-frequency domain representation of noisy ECG signal at an SNR of 5 dB (b) Time-frequency domain representation of ECG signal after removing high frequency noise (c) Time-frequency domain representation of ECG signal after masking (d) Time-frequency domain representation of ECG signal after filtering.

threshold T_m. The binary matrix B is obtained as follows

$$B[m,n] = \begin{cases} 1 & \text{if } S_1[m,n] > T_m, \\ 0 & \text{if } S_1[m,n] \leq T_m \end{cases} \tag{5.14}$$

where, m and n represent row and columns of S_1 and B respectively. T_m is the selected optimum threshold value. This threshold value T_m is selected such that the ratio of inter-class variance σ_B^2 to the total-class variance σ_T^2 [137] is maximized. These two variables can be computed as follows [138].

$$\sigma_B^2 = \omega_0(\mu_0 - \mu_T)^2 + \omega_1(\mu_1 - \mu_T)^2 \tag{5.15}$$

$$\sigma_T^2 = \sum_{i=1}^{L}(i-\mu_T)^2 P_i \tag{5.16}$$

where

$$\omega_0 = \sum_{i=1}^{T_m} P_i \quad \text{and} \quad \omega_1 = \sum_{i=T_m+1}^{L} P_i$$
$$\mu_0 = \sum_{i=1}^{T_m}(iP_i)/\omega_0 \quad \text{and} \quad \mu_1 = \sum_{i=T_m+1}^{L}(iP_i)/\omega_1$$
$$P_i = n_i/N \ (P_i \geq 0 \ ; \ \sum_{i=1}^{L} P_i = 1)$$

N is the total number of elements of S_1 matrix, n_i is the number of elements at i-th intensity level, P_i is the estimated probability at i-th intensity level, ω_0 and ω_1 are the total estimated probabilities of all intensity levels for binary classes '0' and '1' respectively, μ_0 and μ_1 are the estimated mean values of all intensity levels for binary classes '0' and '1' respectively, μ_T is the estimated total mean of intensity of S_1 matrix. The output binary matrix B is dilated using a structuring element A_1 [139] as follows.

$$B \oplus A_1 = \{x|(\hat{A_1})_x \cap B \neq \emptyset\} \tag{5.17}$$

where, A_1 and B are considered as sets in 2-D integer space Z^2, $x = \{x_1, x_2\}$, $\hat{A_1}$ is the reflection of A_1 and $\emptyset$ is an empty set. Dilation expands the boundary of the white area in the binary matrix and avoids any small break in the binary matrix. The largest connected area in this matrix is the second level mask M_1. The output of masking, $S_2 = S_1 \circ M_1$, is shown in Fig. 5.6 (c).

Step 4: Filtering: Filtering technique is used to smoothen the boundaries in time-frequency domain representation of the masked output S_2. This is done by performing the following steps [139] on S_2.

1. Initially, S_2 is dilated using the smaller structuring element A_2 for a more precise operation.

$$S_{21} = S_2 \ominus A_2 \tag{5.18}$$

Here, each element is assigned the maximum value in the neighborhood defined by the structuring element A_2.

2. The dilated output S_{21} is eroded using A_2 using the following equation. Erosion is the opposite of dilation. Here, each element is assigned the minimum value in the neighborhood defined by the structuring element A_2.

$$S_{22} = S_{21} \oplus A_2 = \{x|(A_2)_x \subseteq \emptyset\} \tag{5.19}$$

3. The eroded output S_{22} is opened by A_2. Opening is a combination of erosion and dilation. This step removes small unconnected areas and smoothens sharp peaks.

$$S_{23} = \{S_{22} \ominus A_2\} \oplus A_2 \tag{5.20}$$

4. The opened output S_{23} is closed by A_2. Closing is a combination of dilation and erosion. This step combines small breaks in the area and smoothens the boundaries.

$$S_{24} = \{S_{23} \oplus A_2\} \ominus A_2 \tag{5.21}$$

Finally the output matrix S_{24} is converted into a binary matrix (M_2) using (5.14). Filtering is performed by multiplying S_2 with the resultant binary matrix M_2. The output of filtering, $S_3 = S_2 \circ M_2$, is shown in Fig. 5.6 (d).

Step 5: Inverse S-Transform: The filtered time-frequency domain signal, S_3, is converted to the time domain using the inverse S-Transform equation as

$$\hat{h}[kT] = \frac{1}{N} \sum_{n=0}^{N-1} \{ \sum_{j=0}^{N-1} S_3 \left[\frac{n}{NT}, jT \right] \} e^{\frac{j2\pi nk}{N}} \tag{5.22}$$

where $\hat{h}[kT]$ is the enhanced ECG signal. Fig. 5.7(a) shows the noisy ECG signal and Fig. 5.7(b) shows the enhanced ECG signal.

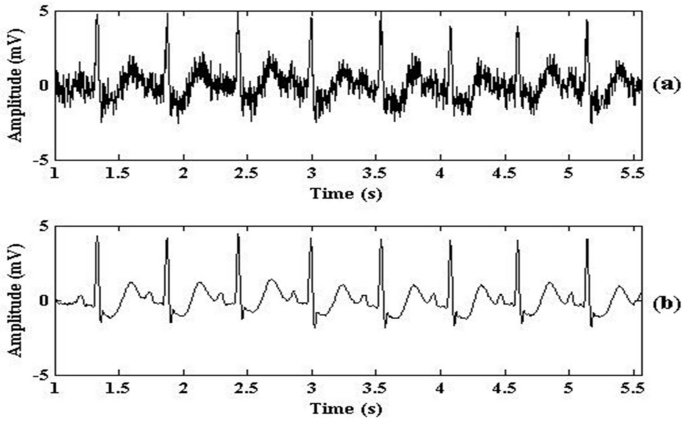

Figure 5.7: ECG signals (a) Noisy ECG signal with Gaussian noise at 5 dB SNR (b) Enhanced ECG signal.

5.5 Experimental Evaluation

The proposed algorithm is tested on the ECG data of the MIT-BIH arrhythmia database as described in Chapter 1. Noise is added to these signals that result in SNR levels of 0 dB, 1.25 dB and 5 dB. These noisy ECG signals are denoised using the proposed method. The performance of the proposed method is compared with WT-Soft [126] and WT-Subband [70] methods that are commonly used for ECG enhancement. The performance of this method is evaluated based on the SNR and RMSE [140]. The SNR can be represented as follows

$$SNR = \frac{\sum_{t=0}^{L-1} h(t)^2}{\sum_{t=0}^{L-1} n(t)^2} \tag{5.23}$$

where $h(t)$ is the ECG signal and $n(t)$ is the noise signal. In this paper, RMSE is used to evaluate the quality of the information preserved in the denoised ECG signal. RMSE is defined as follows:

$$RMSE = \sqrt{\frac{\sum_{t=0}^{L-1} (h(t) - \hat{h}(t))^2}{L}} \tag{5.24}$$

where the numerator part is the square error, $\hat{h}(t)$ is the reconstructed ECG signal and L is the length of the ECG signal.

5.5.1 Output SNR and RMSE

The proposed method is tested on different types of noise that are generally embedded with ECG signals during transmission and acquisition i.e., channel noise, muscle artifacts, electrode motion and baseline wander [130]. A multi-point low pass filter is also used in this work for enhancement of the noisy signal and the results are compared with performance of the proposed method. In this filter, to obtain the lower amplitude detail, the number of points and spacings are chosen empirically for best filter as 61 and 20 respectively. A threshold value of 2.5 mV is selected empirically and the amplitude above the threshold level is added to the lower amplitude detail for obtaining the filtered signal. The experimental results show that the performance of the proposed method is better than the multi-point low pass filter for each ECG signal of the MIT-BIH database. Both multi-point low pass filter and the proposed method are tested on noisy ECG signal at 1.25 dB SNR. The average values of SNR and MSE obtained using multi-point low pass filter are 6.06 dB and 0.511 for Gaussian noise, 1.54 dB and 0.841 for muscle artifact noise, 0.982 dB and 0.895 for electrode motion and 0.676 dB and 0.928 for baseline wander noise respectively. The SNR and MSE values obtained using the proposed method are 9.77 dB and 0.33 for Gaussian noise, 9.66 dB and 0.329 for muscle artifact, 7.01 dB and 0.45 for electrode noise motion and 11.38 dB and 0.27 for baseline wander noise respectively.

5.5.2 Experimental results with Gaussian noise

Noise due to poor channel conditions can be modeled using white Gaussian noise [68]. Hence, Gaussian noise is artificially added to ECG data available in the MIT-BIH database [136]. Fig. 5.8 represents the time-frequency representation of the enhanced ECG signal using short time Fourier transform (STFT) and Wigner-Ville transform (WVT) based method. It is clearly seen from the figures that the method reported

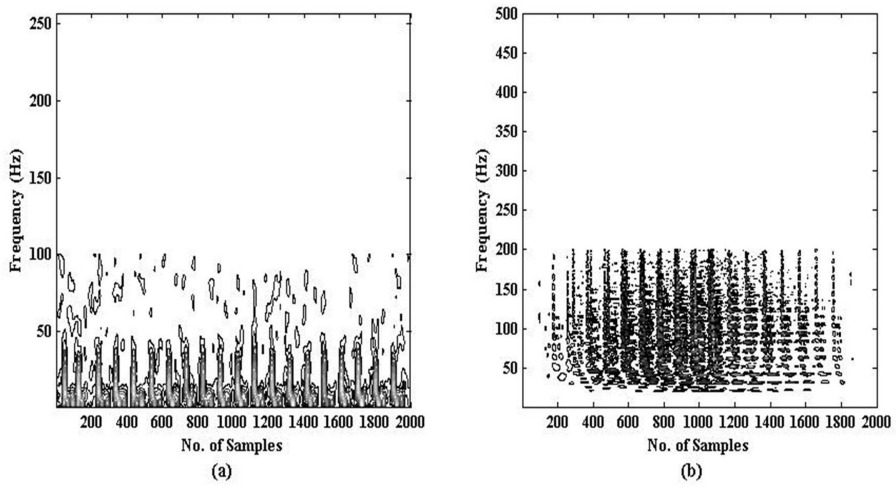

Figure 5.8: Time-frequency domain representation of enhanced ECG signal from 5 dB SNR level noisy signal using (a) short time Fourier transform (STFT) (b) Wigner-Ville transform.

in [141] is unable to enhance the ECG signal. The WVT obtains very high time and frequency resolution but presence of cross terms due to the bilinear structure makes the interpretation of the time-frequency representation difficult [141]. Therefore, at low SNR this method would not be able to denoise the signal. On the other hand, in case of STFT, the resolution depends on the length of fixed window. Thus, WVT and STFT based techniques are not able to provide significant performance for ECG signal enhancement. Fig. 5.9(a) shows the original ECG (MIT-BIH tape no. # 230) and Fig. 5.9(b) shows the ECG with added white Gaussian noise resulting in an SNR of 1.25 dB. Fig. 5.9(c), 5.9(d) and 5.9(e) depict the denoised ECG signal using WT with soft threshold (WT-Soft) [126], WT with subband dependent threshold (WT-Subabnd) [70] based techniques and the proposed method respectively. Though both methods remove majority of the noise, it can be clearly seen from Fig. 5.9(c) and 5.9(d) that WT-Soft and WT-Subband methods output have more distortions. The amplitude of the wavelet transform is dependent on the frequency whereas S-transform provides uniform amplitude response for all frequencies [95]. This effect is observed in the output of the WT-Soft and WT-Subband methods which have lower R and S peak amplitudes. Table 5.1 shows the comparison of SNR and RMSE values for WT-Soft, WT-Subband methods

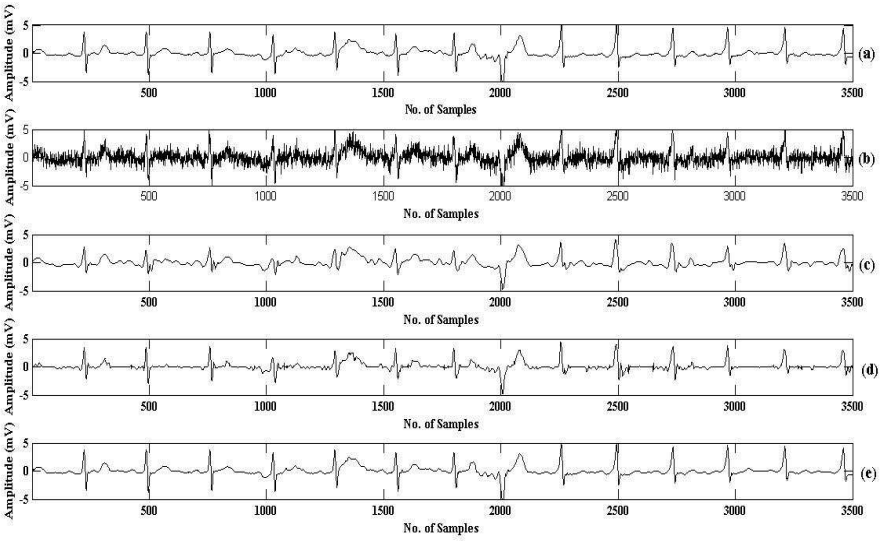

Figure 5.9: (a) Original ECG signal (MIT-BIH tape no. # 230) (b) Noisy ECG signal with Gaussian noise at an SNR of 1.25 dB. Enhancement of noisy ECG signal using (c) WT-Soft method (d) WT-Subband method (e) Proposed method.

and the proposed method. The table contains comparative results for 10 different sets of data taken from the MIT-BIH database. From the results, it is evident that the proposed method gives better performance, with a higher SNR and a lower RMSE. For example, the results using tape no # 122 shows that for an input SNR of 5 dB, WT-Soft method gives an output SNR of 9.77 dB whereas WT-Subband method gives an output SNR of 9.86 dB. Meanwhile, the proposed method output has a higher SNR of 11.42 dB. Similarly, the RMSE comparison shows that proposed method gives an RMSE of 0.268 which is lower than the RMSE of WT-Soft and WT-Subband methods output i.e., 0.325 and 0.304 respectively.

5.5.3 Experimental results with real noises

5.5.3.1 Muscle artifacts (MA) noise

Real case noises such as muscle artifacts (MA), electrode motion (EM), and baseline wander (BW) are more probable during ECG acquisition [68]. These types of noise

Table 5.1: Experimental results for Gaussian noise

MIT-BIH Tape No.			103	105	111	116	122	205	213	219	223	230
WT-Soft Method	0dB	SNR	5.84	7.35	7.04	6.63	6.69	5.45	5.91	7.25	7.35	5.73
		RMSE	0.511	0.429	0.445	0.466	0.463	0.534	0.507	0.434	0.429	0.517
	1.25dB	SNR	6.72	7.96	7.72	7.37	7.47	6.31	6.62	8.02	8.1	6.44
		RMSE	0.461	0.400	0.412	0.428	0.423	0.484	0.467	0.397	0.394	0.476
	5dB	SNR	9.66	10.22	9.62	9.65	9.77	8.57	8.74	10.36	10.87	8.85
		RMSE	0.33	0.308	0.33	0.329	0.325	0.373	0.366	0.303	0.286	0.361
WT-Subband Method	0dB	SNR	6.69	7.68	7.06	6.87	7.23	6.44	7.13	6.92	7.35	6.55
		RMSE	0.425	0.393	0.432	0.409	0.410	0.482	0.479	0.459	0.405	0.341
	1.25dB	SNR	7.77	8.65	7.78	7.83	8.50	7.55	8.08	8.45	8.32	7.63
		RMSE	0.375	0.344	0.401	0.404	0.392	0.413	0.455	0.391	0.333	0.395
	5dB	SNR	10.51	12.11	9.85	9.76	9.86	9.22	9.67	11.01	11.21	9.14
		RMSE	0.250	0.227	0.320	0.328	0.304	0.336	0.317	0.259	0.227	0.302
Proposed Method	**0dB**	**SNR**	**9.96**	**8.85**	**7.55**	**7.95**	**8.32**	**8.45**	**8.14**	**8.94**	**9.56**	**9.93**
		RMSE	**0.318**	**0.361**	**0.419**	**0.401**	**0.384**	**0.378**	**0.392**	**0.357**	**0.332**	**0.319**
	1.25dB	**SNR**	**10.95**	**9.95**	**8.71**	**8.73**	**9.32**	**9.15**	**9.42**	**10.03**	**10.81**	**11.05**
		RMSE	**0.284**	**0.318**	**0.371**	**0.366**	**0.342**	**0.349**	**0.338**	**0.315**	**0.288**	**0.28**
	5dB	**SNR**	**12.91**	**13.54**	**10.09**	**9.82**	**11.42**	**10.1**	**12.49**	**12.54**	**13.86**	**13.14**
		RMSE	**0.226**	**0.21**	**0.313**	**0.323**	**0.268**	**0.313**	**0.237**	**0.236**	**0.203**	**0.22**

are more significant during stress test. For evaluating the proposed methodology, these noises are taken from the noise stress database [77] and added to ECG data from the MIT-BIH database. Fig. 5.10 shows the experiment results for MA noise. Fig. 5.10(a) shows the original ECG (MIT-BIH tape no. # 230) and Fig. 5.10(b) shows the ECG with added MA noise resulting in an SNR of 1.25 dB. Fig. 5.10(c), 5.10(d) and 5.10(e) show the output of WT-Soft, WT-Subband and proposed techniques. Table 5.2 shows the SNR and RMSE comparison of the signal enhanced using WT-Soft and WT-Subband methods and proposed method. It is noticed from the table that WT-Soft method provides only a minor improvement in SNR and RMSE which is lower than that of the WT-Subabnd technique. For example, experiment results for tape no. # 105 show that for as input SNR of 5 dB, WT-Soft method obtains an output SNR of 5.37 dB whereas the same for the WT-Subband technique is 6.49 dB. On the other hand, the proposed method output obtains a higher output SNR of 12.76 dB. The RMSE of the proposed method output is 0.230 which is much lower than that of the other two methods. The comparative results for other data also prove that the proposed method obtains a superior performance, with a higher SNR and lower RMSE.

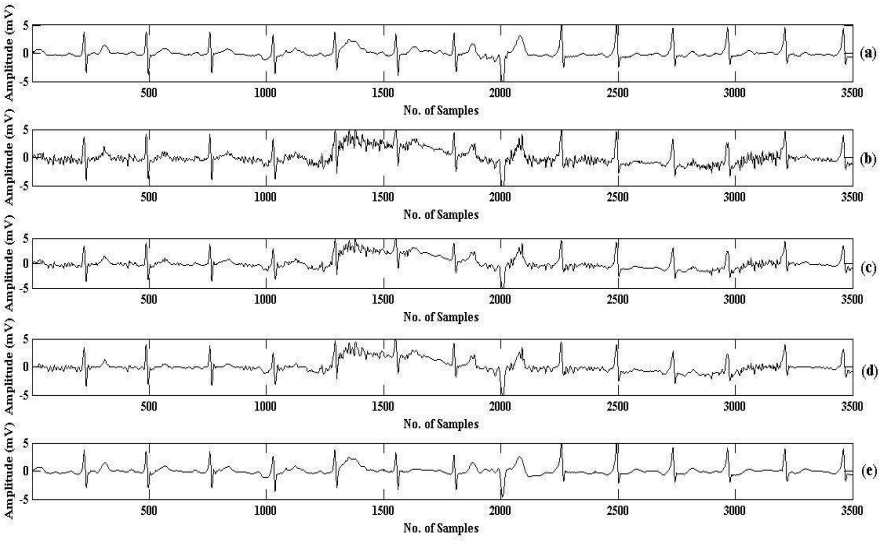

Figure 5.10: (a) Original ECG signal (MIT-BIH tape no. # 230) (b) Noisy ECG signal with muscle artifacts (MA) noise at an SNR of 1.25 dB. Enhancement of noisy ECG signal using (c) WT-Soft method (d) WT-Subband method (e) Proposed method.

5.5.3.2 Electrode motion (EM) noise

Fig. 5.11(a) - 5.11(e) shows the experimental results in case of signal corrupted by EM noise. Fig. 5.11(a) shows the original ECG (MIT-BIH tape no. # 230) and Fig. 5.11(b) shows the ECG with added EM noise resulting in an SNR of 1.25 dB. Fig. 5.11(c), 5.11(d) and 5.11(e) show the output of WT-Soft, WT-Subband and the proposed techniques. Table 5.3 compares the SNR and RMSE of the enhanced signal using WT-Soft, WT-Subband and proposed methods for EM noise. The comparative results show that both WT-Soft and WT-Subband methods fail to improve the signal quality whereas the proposed method gives a better performance. For example, the experiment results for tape no. # 230 with 5 dB input SNR shows that there is no improvement in SNR in case of WT-Soft method and WT-Subband method provides only an output SNR of 5.39 dB. Meanwhile, the proposed method gives a higher output SNR of 10.45 dB. The proposed method output also has an RMSE of 0.3 which is lower than that of any of the WT based methods.

Table 5.2: Experimental results for muscle artifacts (MA) noise

MIT-BIH Tape No.			103	105	111	116	122	205	213	219	223	230
WT-Soft Method	0dB	SNR	0.37	0.39	0.41	0.38	0.39	0.34	0.37	0.37	0.38	0.36
		RMSE	0.958	0.956	0.954	0.958	0.956	0.961	0.958	0.959	0.957	0.96
	1.25dB	SNR	1.62	1.64	1.65	1.62	1.63	1.6	1.61	1.62	1.62	1.6
		RMSE	0.83	0.828	0.827	0.83	0.829	0.832	0.83	0.829	0.829	0.831
	5dB	SNR	5.35	5.37	5.37	5.35	5.34	5.31	5.33	5.37	5.37	5.35
		RMSE	0.54	0.539	0.539	0.54	0.541	0.542	0.541	0.539	0.539	0.54
WT-Subband Method	0dB	SNR	1.62	1.67	1.49	1.55	1.64	1.72	1.42	1.64	1.68	1.67
		RMSE	0.838	0.836	0.850	0.847	0.839	0.828	0.856	0.838	0.836	0.835
	1.25dB	SNR	2.82	2.90	2.70	2.76	2.86	2.95	2.58	2.85	2.92	2.87
		RMSE	0.730	0.726	0.739	0.736	0.729	0.718	0.748	0.728	0.726	0.727
	5dB	SNR	6.40	6.49	6.17	6.29	6.49	6.54	6.02	6.44	6.56	6.49
		RMSE	0.482	0.479	0.494	0.489	0.479	0.473	0.501	0.481	0.477	0.479
Proposed Method	**0dB**	**SNR**	**10.41**	**10.02**	**8.21**	**8.19**	**9.2**	**8.32**	**8.79**	**10.05**	**9.95**	**8.7**
		RMSE	**0.302**	**0.316**	**0.389**	**0.389**	**0.347**	**0.384**	**0.363**	**0.314**	**0.318**	**0.367**
	1.25dB	**SNR**	**10.89**	**10.42**	**8.66**	**8.51**	**9.67**	**8.61**	**9.67**	**10.61**	**10.56**	**9.01**
		RMSE	**0.286**	**0.301**	**0.369**	**0.375**	**0.328**	**0.371**	**0.329**	**0.295**	**0.297**	**0.355**
	5dB	**SNR**	**12.63**	**12.76**	**9.94**	**9.75**	**11.69**	**9.91**	**12.53**	**12.89**	**13.44**	**10.15**
		RMSE	**0.234**	**0.23**	**0.318**	**0.325**	**0.26**	**0.32**	**0.236**	**0.227**	**0.213**	**0.311**

Figure 5.11: (a) Original ECG signal (MIT-BIH tape no. # 230) (b) Noisy ECG signal with electrode motion (EM) noise at an SNR of 1.25 dB. Enhancement of noisy ECG signal using (c) WT-Soft method (d) WT-Subband method (e) Proposed method.

Table 5.3: Experimental results for electrode motion (EM) noise

.

MIT-BIH Tape No.			103	105	111	116	122	205	213	219	223	230
W-SoftT Method	0dB	SNR	0.02	0.02	0.00	0.02	0.01	0.01	0.01	0.02	0.02	0.02
		RMSE	0.958	0.956	0.954	0.958	0.956	0.961	0.958	0.959	0.957	0.96
	1.25dB	SNR	1.26	1.26	1.24	1.27	1.26	1.26	1.25	1.27	1.27	1.27
		RMSE	0.864	0.865	0.867	0.864	0.865	0.865	0.865	0.864	0.864	0.864
	5dB	SNR	5.00	4.99	4.92	5.01	4.98	4.97	4.98	5.01	5.01	5.00
		RMSE	0.562	0.563	0.567	0.562	0.563	0.564	0.564	0.562	0.561	0.562
WT-Subband Method	0dB	SNR	0.26	0.27	0.30	0.41	0.01	0.57	0.37	0.13	0.13	0.26
		RMSE	0.941	0.934	0.935	0.944	0.906	0.935	0.947	0.903	0.862	0.893
	1.25dB	SNR	1.51	1.58	1.56	1.66	1.75	1.87	1.60	1.61	1.62	1.65
		RMSE	0.837	0.833	0.834	0.825	0.816	0.805	0.830	0.831	0.830	0.827
	5dB	SNR	5.29	5.30	5.30	5.42	5.53	5.76	5.26	5.39	5.42	5.39
		RMSE	0.543	0.542	0.540	0.535	0.528	0.513	0.543	0.537	0.535	0.537
Proposed Method	**0dB**	**SNR**	**6.41**	**6.13**	**5.45**	**5.47**	**5.87**	**5.59**	**5.85**	**6.05**	**6.21**	**6.29**
		RMSE	**0.478**	**0.493**	**0.534**	**0.533**	**0.509**	**0.525**	**0.51**	**0.498**	**0.489**	**0.484**
	1.25dB	**SNR**	**7.47**	**7.35**	**6.4**	**6.32**	**6.96**	**6.47**	**7.06**	**7.17**	**7.45**	**7.48**
		RMSE	**0.423**	**0.429**	**0.478**	**0.483**	**0.449**	**0.475**	**0.444**	**0.438**	**0.424**	**0.423**
	5dB	**SNR**	**10.32**	**10.4**	**8.54**	**8.32**	**9.60**	**8.55**	**10.12**	**10.04**	**10.74**	**10.45**
		RMSE	**0.305**	**0.302**	**0.374**	**0.384**	**0.331**	**0.374**	**0.312**	**0.315**	**0.290**	**0.300**

5.5.3.3 Baseline wander (BW) noise

Fig. 5.12(a) - 5.12(e) shows the experimental results for BW noise. Fig. 5.12(a) shows the original ECG (MIT-BIH tape no. # 230) and Fig. 5.12(b) shows the ECG with added BW noise resulting in an SNR of 1.25 dB. Fig. 5.12(c), 5.12(d) and 5.12(e) show the output of WT-Soft, WT-Subband and proposed techniques. Table 5.4 compares the SNR and RMSE values for WT-Soft, WT-Subband and proposed methods with baseline wander. The comparative results show that WT-Soft and WT-Subband methods fail as an enhancement technique for baseline wander. The WT-Soft method output has a slightly lesser SNR compared to the input SNR due to the distortions introduced during signal reconstruction whereas WT-Subband technique gives a higher SNR than the classical WT-Soft method. Meanwhile, the proposed method has a superior performance with a higher SNR and lower RMSE. For example, the experimental results for tape no. # 122 with 5 dB input SNR show that the output of the WT-Soft method has a degraded SNR of 4.95 dB whereas the WT-Subband method provides

Figure 5.12: (a) Original ECG signal (MIT-BIH tape no. # 230) (b) Noisy ECG signal with baseline wander (BW) at an SNR of 1.25 dB. Enhancement of noisy ECG signal using (c) WT-Soft method (d) WT-Subband method (e) Proposed method.

an output SNR of 5.42 dB. On the other hand, the proposed method gives a superior enhancement resulting in an output SNR of 12.38 dB. The RMSE of the proposed method output is 0.240 which is lower than the RMSE of WT-Soft or WT-Subband method. The performance of proposed ECG denoising technique at 1.25 dB SNR level is also compared with the performance of WT-Soft [126] and WT-Subband [70] method in Fig. 5.13 using box plot representation of statistical analysis [142], [143] to quantify the significant difference among all methods. It is clearly seen from Fig 5.13 that the performance of proposed method is better than WT-Soft [126] and WT-Subband [70] method for different types of noise that are generally embedded with ECG signal. The real case noises have frequency components in the same range as that of the original ECG signal [74]. Output signals shown in Fig. 5.10 - Fig. 5.12 proves that WT-Soft and WT-Subband fail to remove these noise components and hence do not improve the signal

Table 5.4: Experimental results for baseline wander (BW) noise

.

MIT-BIH Tape No.			103	105	111	116	122	205	213	219	223	230
WT-Soft Method	0dB	SNR	-0.01	-0.01	-0.04	-0.01	-0.01	-0.02	-0.01	0.0	0.0	-0.01
		RMSE	1.001	1.001	1.004	1.001	1.002	1.002	1.001	1.000	1.000	1.001
	1.25dB	SNR	1.24	1.23	1.2	1.24	1.23	1.22	1.23	1.24	1.25	1.24
		RMSE	0.867	0.867	0.871	0.867	0.868	0.868	0.868	0.867	0.866	0.867
	5dB	SNR	4.97	4.96	4.89	4.98	4.95	4.94	4.96	4.99	4.98	4.98
		RMSE	0.564	0.565	0.569	0.564	0.565	0.566	0.565	0.563	0.563	0.564
WT-Subband Method	0dB	SNR	0.16	0.20	0.21	0.22	0.33	0.51	0.22	0.21	0.27	0.27
		RMSE	0.981	0.977	0.974	0.974	0.962	0.942	0.973	0.976	0.969	0.969
	1.25dB	SNR	1.41	1.45	1.47	1.49	1.60	1.82	1.46	1.48	1.53	1.54
		RMSE	0.849	0.846	0.842	0.842	0.830	0.810	0.844	0.843	0.838	0.837
	5dB	SNR	5.16	5.20	5.21	5.22	5.42	5.73	5.22	5.29	5.32	5.37
		RMSE	0.551	0.549	0.546	0.548	0.534	0.515	0.546	0.544	0.542	0.538
Proposed Method	**0dB**	**SNR**	**11.4**	**11.56**	**9.22**	**9.01**	**10.58**	**9.31**	**11.57**	**11.55**	**12.14**	**11.68**
		RMSE	**0.269**	**0.264**	**0.346**	**0.354**	**0.296**	**0.342**	**0.264**	**0.265**	**0.247**	**0.261**
	1.25dB	**SNR**	**12.06**	**12.23**	**9.61**	**9.35**	**11.17**	**9.7**	**12.22**	**12.22**	**12.95**	**12.35**
		RMSE	**0.249**	**0.245**	**0.331**	**0.341**	**0.276**	**0.327**	**0.245**	**0.245**	**0.225**	**0.241**
	5dB	**SNR**	**13.54**	**13.77**	**10.41**	**10.04**	**12.38**	**10.46**	**13.77**	**13.65**	**14.81**	**13.89**
		RMSE	**0.21**	**0.205**	**0.302**	**0.315**	**0.24**	**0.3**	**0.205**	**0.208**	**0.182**	**0.202**

quality. Meanwhile, the proposed method performs time-frequency domain filtering by using an appropriate mask and hence exhibits a better enhancement in signal quality.

5.5.4 One way ANOVA results

Table 5.5 represents one way ANOVA results for different types of noise based on SNR of denoised ECG signals. This table also provides an evidence to the results mentioned above. The large value of F indicates relatively more difference between groups than within the groups. If the *'sig'* value (significance level) [142] in Table 5.5 is less than 0.05, there is a significant difference between the groups with a confidence level of 95%. This rule indicates that performance of the WT-Soft [126], WT-Subband [70] and proposed method for removal of Gaussian, muscle artifact, electrode motion, baseline wander noises from noisy ECG signal are significantly different from each other. The proposed technique is implemented using MATLAB Version 7.0.0.19920 Release 14 of Math works Inc. When executed on a Intel Core i5 computer, processor 3.20 Ghz with 4 GB RAM, Windows 7 platform and as the only application running, it takes an execution time of 0.2626 s for enhancement of the MIT-BIH tape no. # 230 noisy ECG signal at 1.25 dB SNR level corrupted with Gaussian noise, whereas WT-Soft [126] takes 0.2519 s for the

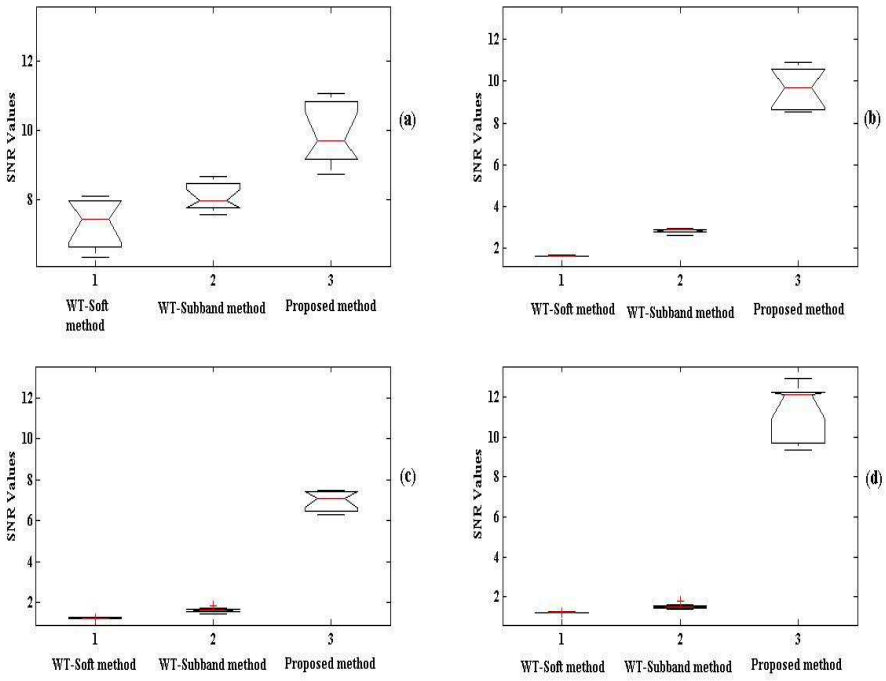

Figure 5.13: Box plot based statistical evaluation on SNR of denoised signals using different ECG signal enhancement methods when the signals are embedded with (a) Gaussian noise (b) Muscle Artifacts (MA) noise (c) Electrode Motion (EM) noise (d) Baseline Wander (BW) noise at an SNR of 1.25 dB.

same. In the same environment, 0.3932 s is required to execute the test program for aforementioned noisy ECG signal when WT-Subband [70] is used.

5.5.5 R-peak detection test

To evaluate the quality of the biology-related information preserved in the enhanced ECG signal, R-peak detection test is also conducted in addition to SNR and RMSE on the enhanced ECG signal where enhancement of ECG signal is achieved by using WT-Soft [126], WT-Subband [70] and the proposed methods individually. These biological indices are very crucial for the diagnosis of heart diseases. For the R-peak detection experiment, five ECG signals are picked up from the MIT-BIH database. In this work, R-peak detection algorithm is implemented based on Pan-Tompkin's algorithm [30] which

Table 5.5: One way ANOVA results for different types of noises

Noise Type	Source of Variation	Sum of Squares	df	Mean Squares	F	sig
Gaussian noise	Between the groups	33.81	2	16.90	35.53	0.000
	Within the groups	12.85	27	0.476		
	Total	46.66	29			
MA noise	Between the groups	376.20	2	188.1	653.13	0.000
	Within the groups	7.77	27	0.288		
	Total	383.97	29			
EM noise	Between the groups	206.96	2	103.48	1390.86	0.000
	Within the groups	2.01	27	0.074		
	Total	208.97	29			
BW noise	Between the groups	668.10	2	334.05	554.90	0.000
	Within the groups	16.25	27	0.602		
	Total	684.35	29			

Table 5.6: R-peak detection performance of enhanced ECG signal using WT-Soft, WT-Subband and proposed method

Noise Type	MIT-BIH tape no.	Enhanced ECG Signal using					
		WT-Soft method		WT-Subband method		**Proposed method**	
		Se (%)	P (%)	Se (%)	P (%)	**Se (%)**	**P (%)**
Gaussian noise	205	98.37	97.79	99.14	99.18	**99.55**	**99.51**
	213	98.34	94.26	99.00	97.02	**99.00**	**98.40**
	219	98.09	93.33	99.03	94.68	**99.91**	**99.77**
	223	96.34	96.05	98.34	96.62	**99.43**	**97.49**
	230	98.89	98.37	99.56	99.34	**99.78**	**99.82**
MA noise	205	98.44	98.04	99.18	98.99	**99.55**	**99.40**
	213	98.34	94.34	98.78	97.13	**98.96**	**98.34**
	219	98.18	93.57	98.63	94.64	**98.94**	**97.82**
	223	96.48	96.13	97.49	96.27	**97.75**	**97.64**
	230	99.73	96.44	99.87	96.20	**99.91**	**97.24**
EM noise	205	98.63	97.36	98.88	99.10	**99.59**	**99.44**
	213	98.25	96.64	98.93	97.19	**98.93**	**98.52**
	219	98.04	93.45	99.45	94.72	**99.95**	**99.86**
	223	96.55	96.20	98.34	96.48	**99.69**	**97.86**
	230	99.73	99.47	99.82	99.47	**99.87**	**99.73**
BW noise	205	99.74	97.29	99.81	98.66	**99.89**	**99.07**
	213	98.43	95.37	99.09	96.27	**99.88**	**99.72**
	219	97.73	93.73	98.94	94.31	**99.31**	**95.99**
	223	97.53	94.04	98.49	95.88	**99.43**	**97.24**
	230	99.73	99.73	99.82	99.78	**99.87**	**99.82**
Average		98.28	96.08	99.03	97.10	**99.46**	**98.63**

is briefly discussed in Chapter 2. The comparative R-peak detection performance results

that are computed based on sensitivity (Se) and positive predictivity ($+P$) [144], [145], are given in Table 5.6. These parameters are defined by (5.25) and (5.26).

$$Se = \frac{TP}{TP + FN} \tag{5.25}$$

$$+P = \frac{TP}{(TP + FP)} \tag{5.26}$$

where, TP is the true positive, FN is the false negative, and FP is the false positive. Table 5.6 also shows that the average sensitivity for the R-peak detection of enhanced ECG signal using WT-Soft [126] and WT-Subband [70] methods are 98.28% and 99.03% respectively, whereas an average sensitivity is 99.46% for the proposed method. Positive predictivity for the R-peak detection of enhanced ECG signal using the proposed method is 98.63% whereas 96.08% and 97.10% are for enhanced ECG signal using WT-Soft and WT-Subband methods respectively. Therefore, the performance of the R-peak detection of enhanced ECG signal using the proposed method is better compared to WT-Soft [126] and WT-Subband [70] methods. Thus, the proposed ECG enhancement technique performs better compared to the earlier reported WT based methods.

5.5.6 Beat detection performance evaluation

To evaluate the quality of the preserved features in the enhanced signal, ECG beat classification experiment is performed in this section. In this experiment, each type of noise is added to ECG signal that results in an SNR of 1.25 dB individually. The different test datasets are prepared after enhancement of the noisy ECG signals using WT-Soft [126] and WT-Subband [70] methods and the proposed ST based technique. Clean data is used to train the classifier while testing is done with enhanced data. As expected, the performance deteriorates for decreasing input SNR for each of the four different noisy environments. Table 5.7 represents the average sensitivity of the ECG beat classification using wavelet transform based feature set under different noisy environments. In WT-Soft method [126], the classification sensitivities of the tape no. 205, 213, 219, 223 and 230 are 86.16%, 78.37%, 89.13%, 70.24% and 85.25% respectively whereas

Table 5.7: Recognition sensitivity (Se in %) of ECG beats enhanced from 1.25 dB SNR under different noisy environments using wavelet based feature set.

Noise Type	MIT-BIH tape no	WT-soft method	WT-subband method	**Proposed method**
Gaussian noise	205	88.73	90.42	**92.49**
	213	81.18	84.76	**86.85**
	219	78.90	85.63	**91.31**
	223	70.70	73.24	**74.32**
	230	87.89	92.89	**94.57**
MA noise	205	86.28	89.70	**91.46**
	213	83.40	84.07	**87.01**
	219	77.15	82.28	**87.42**
	223	74.14	77.09	**80.80**
	230	86.21	93.66	**95.13**
EM noise	205	86.77	88.91	**92.39**
	213	85.07	85.96	**86.98**
	219	80.56	83.53	**91.24**
	223	73.32	74.90	**79.60**
	230	86.65	90.75	**94.68**
BW noise	205	86.16	91.01	**92.53**
	213	78.37	82.12	**84.81**
	219	89.13	92.24	**93.59**
	223	70.24	78.46	**86.22**
	230	85.25	90.70	**94.62**
Average		81.80	85.62	**88.90**

the classification sensitivities of the same tapes in case of the WT-subband method are 91.01%, 82.12%, 92.24%, 78.46% and 90.70% respectively under the baseline wander noisy environment. On the other hand, the classification sensitivities of 92.53%, 84.81%, 93.59%, 86.22% and 94.62% are achieved for the tape no. 205, 213, 219, 223 and 230 respectively using the proposed S-transform based enhancedment method. Similarly, if we consider the tape no. 213, the classification sensitivities are 86.85%, 87.01% and 86.98% under the Gaussian noise, MA noise and EM noise respectively using the proposed method whereas classification sensitivities for the same tape in case of WT-subband method are 84.76%, 84.07% and 85.96% respectively. On the other hand, the

Table 5.8: Recognition sensitivity (Se in %) of ECG beats enhanced from 1.25 dB SNR under different noisy environments using proposed S-transform based combined feature set.

Noise Type	MIT BIH tape no	WT-soft method	WT-subband method	**Proposed method**
Gaussian noise	205	91.61	95.50	**95.86**
	213	81.36	84.84	**87.98**
	219	83.42	86.10	**92.55**
	223	73.77	76.19	**77.89**
	230	93.43	94.84	**96.16**
MA noise	205	88.80	91.18	**95.14**
	213	83.54	85.39	**87.34**
	219	83.48	89.13	**91.27**
	223	74.14	78.91	**83.56**
	230	93.07	96.04	**96.63**
EM noise	205	91.43	93.08	**93.67**
	213	86.46	87.13	**88.52**
	219	84.12	89.76	**92.17**
	223	76.04	78.03	**83.77**
	230	91.57	93.49	**96.16**
BW noise	205	91.33	93.23	**94.30**
	213	80.52	87.26	**87.81**
	219	92.55	93.08	**94.41**
	223	73.26	78.64	**87.17**
	230	93.17	94.11	**95.79**
Average		85.35	88.30	**90.91**

WT-soft method obtains the classification sensitivities of 81.18%, 83.40% and 85.07% under Gaussian noise, MA noise and EM noise respectively for the same tape. It is also noticed from Table 5.7 that the average sensitivity of WT-soft method under all types of noisy environment is 81.80% whereas the average sensitivities for proposed enhancement method is 88.90% using wavelet based feature set. On the other hand, the WT-subband technique obtains an average sensitivity of 85.62%. Hence, the proposed enhancement technique achieves a better performance compared to other exisiting methods like WT-soft and WT-subband methods. Table 5.8 represents the average sensitivity of the ECG beat classification using proposed S-transform based combined feature set under differ-

ent noisy environments such as Gaussian noise, MA noise, EM noise and BW noise. It is seen from the table that the proposed enhancement technique is better compared to WT-soft and WT-subband methods. For example, the classification sensitivities are 91.33%, 80.52%, 92.55%, 73.26% and 93.17% are achieved for the tape no. 205, 213, 219, 223 and 230 respectively using WT-soft method under BW noise environment whereas the classification sensitivities for same tapes are obtained as 93.23%, 87.26%, 93.08%, 78.64% and 94.11% respectively using WT-subband method. On the other hand, the proposed S-transform based enhancement technique shows the sensitivities of 94.30%, 87.81%, 94.41%, 87.17% and 95.79% respectively for the same tapes. Similarly, the classification sensitivities of the tape no. 213 are 81.36%, 83.54% and 86.46% under the Gaussian noise, MA noise and EM noise respectively using the WT-soft method whereas the classification sentivities using WT-subband method are 84.84%, 85.39% and 87.13% respectively. On the other hand, the proposed method yields classification sensitivities of 87.98%, 87.34% and 88.52% under Gaussian noise, MA noise and EM noise respectively for the same tape. It is also observed from the table that the average sensitivity under all types of noise is 85.35% using WT-soft method whereas the same for WT-subband method is 88.30%. The average sensitivity of the proposed method for the same is 90.91% which is better than WT-soft and WT-subband methods. The overall performance of the ECG beat detection of enhanced ECG signal using the proposed S-transform based method is better compared to WT-Soft [126] and WT-Subband [70] methods using both under the exisiting wavelet transform and S-transform based combined feature sets.

5.6 Discussion

The experimental results show that the performance of the proposed method is always better compared to WT-Soft [126] and WT-Subband methods [70] for a broad range of ECG signals. WT-Soft [126] and WT-Subband [70] based approaches use wavelet based technique whereas, the proposed method employs S-transform based technique.

S-transform enjoys several advantages compared to wavelets like progressive resolution, frequency invariant amplitude response and absolutely reference phase information as mentioned in Section 5.1. Beside this, the proposed method contains masking and filtering technique which significantly reduces the background noise. This process may also contribute to attain a good SNR and RMSE in addition to the performance of the S transform. The masking and filtering techniques are used here to remove noise components whose frequencies lie between the frequency range of the QRS complexes. Out of four different cases of noise, it is seen that the performance of the proposed method for few beats of noisy ECG signal with motion artifact shows an attenuation of T waveforms and the smaller peak amplitude of QRS wave but it is better than any of the WT based methods. This is because the morphology of the motion artifact often resembles [146] that of P, QRS and T waves and specifically, the frequency spectrum of this noise completely overlaps that of the ECG signal. The proposed algorithm works very well under all other noisy environments as shown in Table 5.1 to 5.4 and Fig. 5.9 to 5.12. The proposed automatic ECG enhancement technique can be implemented in real-time for denoising of ECG signals. This method does not require any reference signal such as auxiliary signal or prior information like R-peak position. A frequency domain fixed thresholding remove the high frequency noise from the noisy ECG signal. The algorithm automatically adjusts the thresholds and parameters periodically to adapt to the changes in noise conditions. This adaptive approach provides the accurate use of ECG signals in real-time like, QRS morphology detection and diagnosis of heart diseases. Without affecting signal quality significantly even at low input SNR levels, the proposed technique is able to reduce the noise efficiently and reliably. The proposed algorithm also preserves the quality of the structural information in the enhanced ECG signal. During acquisition and transmission of ECG signal in real time environment, different types of noise such as channel noise, muscle artifacts, electrode motion, and baseline wander are often embedded with the ECG signal. For all types of noise the proposed algorithm performs better compared to existing WT-Soft [126] and WT-Subband methods [70].

5.7 Conclusions

- This chapter proposes an S-transform based ECG signal enhancement technique which does not require any reference signal such as auxiliary signal or prior information like R-peak position.

- The noise components are removed from the time-frequency domain represented noisy ECG signal by automatic binary masking and filtering. S-transform is used in this work to represent the noisy ECG signal in time-frequency domain.

- The proposed method is evaluated for different types of noise like white Gaussian Noise, muscle artifacts, electrode motion and baseline wander at three different SNR levels i.e., 0 dB, 1.25 dB and 5 dB. The ECG signals which are available in MIT-BIH Arrhythmia database are used to conduct the experiments.

- The results show that the proposed method obtains a superior performance with better SNR and lower RMSE compared to WT with soft threshold [126] and WT with subband dependent threshold [70] based techniques which are usually used as an ECG signal enhancement technique.

- To quantify the significant difference of proposed method among all methods, the performances of different ECG enhancement techniques at 1.25 dB input SNR level are also compared using ANOVA based statistical evaluation procedure and it is noticed that the proposed method provides better performance compared to other methods.

- R-peak detection test is also conducted on enhanced ECG signal to evaluate the quality of the biology-related structural information preserved in the enhanced ECG signal. The sensitivity and positive predictivity results of R-peak detection for denoised ECG signals based on proposed method show the better performance compared to WT-Soft, WT-Subband methods and thus, this also validates the superiority of the proposed enhancement method.

- To show the quality of the structural information preserved in the denoised ECG signal, these are tested on ECG beat detection experiment using wavelet based and ST based combined feature sets individually. The proposed technique shows better performance there also.

CHAPTER 6

Conclusions and Future Work

6.1 Summary of the Work

This dissertation embodies the results of our investigations on feature extraction, feature optimization, classification and enhancement of ECG signals. In particular, our investigations have been addressed towards improving the performance of an ECG beat classification system while parallel efforts are made to reduce the computational load.

- In Chapter 2, a combined feature set based on S-transform (ST) has been proposed. In this chapter, the ST is effectively employed to extract the significant morphological features from ECG signals. The interpretation of the important signal information in the ST is apparent which will be beneficial to extract the important features from the ECG signal. The extracted S-transform based morphological feature set is insufficient to classify the ECG heartbeats due to significant variation in ECG morphology among different patients. Therefore, ECG morphological information is coupled with the timing information, which is more consistent among patients, in order to achieve high classification performance for a larger dataset. Four types of timing or temporal features are extracted from ECG signals such as (i) pre-RR interval, (ii) post-RR interval, (iii) average RR interval and (iv) local RR interval. The morphological feature set coupled with four temporal features are used to form the combined feature set which is applied to the input of the classifier to classify the ECG beats. These features are very useful for the detection, classification and quantification of relevant parameters of ECG signals. The two types of feature set are applied separately to the MLP neural network. The proposed method is evaluated on five heartbeat classes specified in the MIT-BIH arrhythmia database that are normal (N), ventricular ectopic beat (V), supra ventricular ectopic beat (S), fusion (F) and unknown (Q) as recommended by the Association for the Advancement of Medical Instrumentation (AAMI). The performance the proposed method is evaluated over the MIT-BIH arrhythmia database using standard performance metrics and the results are compared with the wavelet based method. The performances of the proposed technique is compared with the

wavelet transform (WT) based feature extraction method. Experimental results demonstrate that the proposed feature extraction method provides better detection sensitivity compare to the wavelet based feature extraction technique.

- In sequel, a classifier is proposed to detect the ECG beats of each patient individually in Chapter 3. ST based combined feature set is applied to the proposed least mean square (LMS) based multi-class SVM classifier. The aims of this classifier is to construct a hyperplane as the decision surface in such a manner that the margin of separation between the two classes is maximized. This requires solving a quadratic programming problem and is implemented using Kernel functions. The performance of the SVM mostly depends on these kernel functions and adjustable weight vectors. It is seen from the definition of LMS algorithm that it adjusts the filter coefficients to minimize the cost function. To implement this idea, LMS algorithm is adopted to modify the Lagrange multiplier, which in turn modifies the weight vector to minimize the classification error and maximize the width of the separation region between the clusters. If the system is an adaptive linear combiner, and if the input vector and the desired response are available, the LMS algorithm is generally the best choice because of its simplicity and ease of computation. Also, it does not require off-line gradient estimations or repetitions of data. LMS algorithm also provides a stable and robust performance against different signal conditions. Here, the classification error is represented by the minimum distance of data points from the margin of the separation region for those data points that fall inside the region of separation or make misclassification. As the number of iterations of LMS algorithm increases, weight vector performs a random walk about the solution of optimal hyperplane having a maximal margin that minimizes the error in the training phase and these updated weights are used in the testing phase to classify ECG beats. The wavelet based feature set and S-transform based combined feature set are applied individually to the multi-class SVM classifier and LMS based multi-class SVM classifier. Experiments are conducted on the benchmark of MIT-BIH arrhythmia database based on AAMI

standards and recommendations. Experimental results show that the proposed LMS based multi-class SVM classifier achieves a better detection performance than the standard multi-class SVM classifier.

- In Chapter 4, an optimization technique called bacteria foraging optimization algorithm (BFO) is introduced to optimize the feature vector. The goal of feature optimization is to choose a subset of available features by eliminating the unnecessary features. The dimensionality reduction made by feature optimization can carry out several advantages for a classification system: (i) a reduction in the cost of acquisition of the data, (ii) improvement in comprehensibility of the final classification model, (iii) a faster induction of the final classification mode, (iv) an improvement in the classification performance. ST based morphological feature set is appended with temporal features to form a combined feature set which forms the input to the classifier. The length of the combined feature set is too high. Therefore, BFO algorithm is used to reduce the length of the feature vector by removing the redundant and irrelevant features. Compared to other optimization methods BFO converges quickly in order to reach the global minimum solution. The feature set of each record is optimized individually by the BFO algorithm. The resultant optimized feature subset of each record is applied to the input of the LMS based multi-class SVM classifier to classify the ECG beats. The experiments are conducted on the benchmark of MIT-BIH arrhythmia database based on AAMI standards and recommendations. The classification performances show that the BFO optimized feature set with LMS based classifier achieves better beat detection performance compared to the existing methods.

- In Chapter 5, an ECG signal enhancement method is proposed based on S-transform to remove the noise from the noisy ECG signal. During the acquisition and transmission, ECG signals are generally affected by different noises like channel noise, muscle artifacts, electrode motion and baseline wander. Muscle artifacts are due to the movement of muscle between skin and electrode. Motion artifacts

are transient baseline changes caused by changes in the electrode-skin impedance with electrode motion. Baseline drift may be caused in chest-lead ECG signals due to coughing and breathing and the resulting movement of the chest, and because of movement of arms/legs in case of limb-lead ECG acquisition. The proposed method is evaluated for four different types of noises at three different SNR levels i.e., 0 dB, 1.25 dB and 5 dB. S-transform is used in this work to represent the noisy ECG signal in time-frequency domain. After that the high frequency noise components are removed by applying frequency domain thresholding. Hence, a frequency domain threshold has been defined at 200 Hz such that the frequency components below 200 Hz are retained and frequency components above 200 Hz are removed. Next, masking and filtering technique is applied to remove the unwanted noise components from the time-frequency domain represented ECG signal. The objective of masking is to remove the noise components whose frequencies are between the QRS complexes of the time-frequency domain represented ST matrix whereas that of the filtering technique is used to smoothen the boundaries of the time-frequency domain represented masked output. The filtered time-frequency domain signal is converted to time domain using the inverse S-transform. The proposed technique does not require any prior information like R-peak position or reference signal like auxiliary signal. This method is evaluated on ECG signals which are available in the MIT-BIH Arrhythmia database. The performance of the proposed method is compared with methods involving wavelet transform with soft thresholding (WT-Soft) and wavelet transform with subband dependent threshold (WT-Subband) that are commonly used for ECG enhancement. The performance of this method is evaluated based on the signal to noise ratio (SNR) and root-mean-square error (RMSE). The experimental results demonstrate that the proposed method shows better SNR and lower RMSE compared to WT-Soft and WT-Subband based techniques. To quantify the significant difference among all methods, the performances of different ECG signal enhancement techniques are compared using analysis of variance (ANOVA) based statistical evaluation

technique and it is seen that the proposed method yields superior performance compared to other methods. R-peak detection test is also conducted on the enhanced ECG signal in addition to measurement of SNR and RMSE to evaluate the quality of biology related information preserved in the enhanced ECG signal. The performance of R-peak detection for denoised ECG signals, in terms of sensitivity and positive predictivity using the proposed enhancement method, is also better than WT-Soft, WT-Subband based methods, and validates the superiority of the proposed method. To evaluate the quality of the information contained in the enhanced ECG signal, an automatic beat detection test is also conducted on the denoised ECG signals. Experimental results show that the performance of the enhanced beat based on proposed S-transform based method is better than enhanced ECG signal based on existing WT based methods.

- Finally, all the results embodied throughout the thesis prove the superiority of our different propositions irrespective of the type and amount of data and the model. We believe that the proposed method would also maintain the consistency of the results if some other ECG data set is used.

6.2 Future Research Directions

In this section, a variety of research directions, future scope and possible extensions of this thesis work are discussed.

- Although the combined features of S-transform based morphological features with temporal features performs significantly well for ECG beat classification, it is noticed that these features are unable to properly classify few beats of supraventricular (S) and normal (N) class. The QRS complex associated with an atrial premature beat of the class S has normal QRS duration and the same morphology as that of the class N. Therefore, one could think of using a complementary feature set of used one for properly distinguishing atrial premature and normal beat.

- A suitable feature transformation technique can be applied to the extracted feature vectors in order to improve the classification performance. The transformed feature vector should be linearly classifiable, low dimension in order to reduce the computational load and should contain the decorrelated features.

- Considerable amount of variation of normal and abnormal ECG signals among different patients sometimes lead to misclassifications of cardiac disorder. A possible solution is the development of an unsupervised classifier for ECG beat classification. An unsupervised classifier neither require foreknowledge of the classes, nor involve any training dataset for the classification of ECG beats.

- Analysis of other biosignals like elctromyogram (EMG) and electroencephalogram (EEG) are also important to diagnose the possible illness of human beings along with ECG signal analysis. EMG helps to diagnose the abnormalities in muscle or nerve inside the muscle and EEG can be used to diagnose the neurological illness and disease like epilepsy, tumour, cerebrovascular lesions, ischemia and problem associated with trauma. Therefore, further investigation can be made for detecting the possible illness based on analysis of these biosignals.

- Extracting the fetal ECG signal from the composite maternal ECG signal is the open issue of research. The maternal ECG signal is stronger than the fetal ECG signal. The background noise of muscle activity and fetal motion makes the detection capability difficult for the fetal ECG signal. Analysis of the extracted fetal ECG signal for automatic detection of cardiac abnormality is also of research interest.

References

[1] S. Haykin, *Neural networks.* New Delhi: Pearson Education Asia, 2002.

[2] P. de Chazal, M. O'Dwyer, and R. B. Reilly, "Automatic classification of heartbeats using ECG morphology and heartbeat interval features," *IEEE Trans. Biomed. Eng*, vol. 51, no. 7, pp. 1196 –1206, Jul. 2004.

[3] T. Ince, S. Kiranyaz, and M. Gabbouj, "A Generic and Robust System for Automated Patient-Specific Classification of ECG Signals," *IEEE Trans. Biomed. Eng.*, vol. 56, no. 5, pp. 1415–1426, May 2009.

[4] R. M. Rangayyan, *Biomedical Signal Analysis: A Case-study Approach.* Wiley-Interscience, New York, pp. 18-28, 2001.

[5] U. R. Acharya, P. S. Bhat, S. S. Iyengar, A. Roo, and S. Dua, "Classification of heart rate data using artificial neural network and fuzzy equivalence relation," *Pattern Recognition*, vol. 36, no. 1, pp. 61–68, 2003.

[6] U. R. Acharya, J. S. Suri, J. A. E. Spaan, and S. M. Krishnan, *Advances in Cardiac Signal Processing.* Springer, 2007.

[7] M. G. Khan, *Rapid ECG interpretation*, Third edition, 2003.

[8] L. Cromwell, F. J. Weibell, and E. A. Pfeiffer, *Biomedical Instrumentation and Measurements.* PHI Learning Private Limited, New Delhi, 2009.

[9] A. J. Moss and S. Stern, *Noninvasive Electro cardiology*, C. A. of Holter, Ed. London, Philadelphia, W.B. Saunder, 1996.

[10] R. S. Khadpur, *Handbook of Biomedical Instrumentation.* Tata McGraw Hill, 2010.

[11] U. R. Acharya, J. S. Suri, J. A. E. Spaan, and S. M. Krishnan, *Advances in Cardiac Signal Processing.* Springer, 2007.

[12] A. Cohen, *Biomedical Signal Processing.* CRC Press, Boca Raton, FL, 1988.

[13] N. Maglaveras, T. Stamkopoulos, K. Diamantaras, C. Pappas, and M. Strintzis, "ECG pattern recognition and classification using non-linear transformations and neural networks: A review," *International Journal of Medical Informatics*, vol. 52, pp. 191–208, 1998.

[14] S. G. Artis, R. G. Mark, and G. B. Moody, "Detection of atrial fibrillation using artificial neural networks„" *Proc. Comput. Cardiology*, pp. 173–176, 1991.

[15] L. T. Sheffield, "Computer-Aided Electrocardiography," *J Am Coll Cardiol*, vol. 10, no. 2, pp. 448–455, 1987.

[16] Z. Dokur and T. Olmez, "ECG beat classification by a novel hybrid neural network," *Computer Methods and Programs in Biomedicine*, vol. 66, pp. 167–181, 2001.

[17] Z. Dokur, T. O. lmez, and E. Yazgan, "Comparison of discrete wavelet and Fourier transforms for ECG beat classification," *Electron. Lett.*, vol. 35, no. 18, pp. 1502–1504, 1999.

[18] Z. Dokur, T. Olmez, E. Yazgan, and O. Ersoy, "Detection of ECG waveforms by neural networks," *Med. Eng. Phys.*, vol. 19, no. 8, pp. 738–741, 1997.

[19] K. Minami, H. Nakajima, and T. Toyoshima, "Real-time discrimination of ventricular tachyarrhythmia with Fourier-transform neural network," *IEEE Trans. Biomed. Eng.*, vol. 46, no. 2, pp. 179–185, Feb. 1999.

[20] T. Olmez, Z. Dokur, and E. Yazgan, "Classification of ECG waveforms by using genetic algorithms," in *Proc. 19th Annual Int. Conf. IEEE-EMBS, Chicago, USA*, 1997, pp. 92-94.

[21] B. G. Celler and P. Chazal, "Low computational cost classifiers for ECG diagnosis using neural networks," in *Proc. 20th Annual Int. Conf. IEEE-EMBS*, 1998, pp. 1337-1340.

[22] I. Jouny, P. Hamilton, and M. Kanapathipillai, "Adaptive wavelet representation and classification of ECG signals," in *Proc. 16th Annual Int. Conf. IEEE-EMBS*, 1994, vol. 2, pp. 1310-1311.

[23] O. Inan, L. Giovangrandi, and G. Kovacs, "Robust neural network based classification of premature ventricular contractions using wavelet transform and timing interval features," *IEEE Trans. Biomed. Eng.*, vol. 53, no. 12, pp. 2507–2515, Dec. 2006.

[24] R. Haberl, G. Jilge, and G. Steinbeck, "Spectral mapping of the electrocardiogram with Fourier transform for identification of patients with sustained ventricular tachycardia and coronary artery disease," *J. Eur Heart*, vol. 10, no. 4, pp. 316–322, 1989.

[25] T. Olmez, "Classification of ECG waveforms by using RCE neural network and genetic algorithms," *Electronics Letters*, vol. 33, no. 18, 1997.

[26] V. X. Afonso and W. J. Tompkins, "Detecting ventricular fibrillation," *IEEE Eng. Med. and Biol.*, pp. 152–159, Mar. 1995.

[27] S. Barro, R. Ruiz, D. Cabello, and J. Mira, "Algorithmic sequential decision-making in the frequency domain for life threatening ventricular arrhythmias and imitative artefacts: a diagnostic system," *J. Biomed. Eng.*, vol. 11, pp. 320–328, 1989.

[28] C. Li, C. Zheng, and C. Tai, "Detection of ECG characteristic points using wavelet transforms," *IEEE Trans. Biomed. Eng.*, vol. 42, no. 1, pp. 21–28, Jan. 1995.

[29] L. Y. Shyu, Y. H. Wu, and W. C. Hu, "Using wavelet transform and fuzzy neural network for VPC detection from the holter ECG," *IEEE Trans. Biomed. Eng.*, vol. 51, no. 7, pp. 1269–1273, 2004.

[30] J. Pan and W. J. Tompkins, "A Real-Time QRS Detection Algorithm," *IEEE Trans. Biomed. Eng.*, vol. 32, no. 3, pp. 230–236, Mar. 1985.

[31] Y. H. Hu, S. Palreddy, and W. Tompkins, "A patient-adaptable ECG beat classifier using a mixture of experts approach," *IEEE Trans. Biomed. Eng.*, vol. 44, no. 9, pp. 891–900, Sept. 1997.

[32] Y. H. Hu, W. J. Tompkins, J. L. Urrusti, and V. X. Afonso, "Applications of artificial neural networks for ECG signal detection and classification," *Journal of Electrocardiology*, vol. 26, pp. 66–73, 1993.

[33] L. Senhadji, G. Carrault, J. Bellanger, and G. Passariello, "Comparing wavelet transforms for recognizing cardiac patterns," *IEEE Eng. Med. Biol. Mag.*, vol. 14, pp. 167–173, 1995.

[34] S. Osowski and T. H. Linh, "ECG beat recognition using fuzzy hybrid neural network," *IEEE Trans. Biomed. Eng.*, vol. 48, no. 11, pp. 1265–1271, Nov. 2001.

[35] M. Lagerholm, C. Peterson, G. Braccini, L. Edenbrandt, and L. Sornmo, "Clustering ECG complexes using Hermite functions and self-organizing maps," *IEEE Trans. Biomed. Eng.*, vol. 47, no. 7, pp. 838–848, Jul. 2000.

[36] X. H. Han, X. M. Chang, L. Quan, X. Y. Xiong, J. X. Li, Z. X. Zhang, and Y. Liu, "Feature subset selection of gravitational search algorithms optimization," *Information Sciences*, vol. 281, pp. 128–146, 2014.

[37] A. Ebrahimzadeh and A. Khazaee, "Detection of premature ventricular contractions using MLP neural networks: A comparative study," *Measurement*, vol. 43, pp. 103–112, 2010.

[38] R. Ceylan and Y. Ozbay, "Comparison of FCM, PCA and WT techniques for classification ECG arrhythmias using artificial neural network," *Expert Systems with Applications*, vol. 33, no. 2, pp. 286–295, 2007.

[39] A. E. Zadeh, A. Khazaee, and V. Ranaee, "Classification of the electrocardiogram signals using supervised classifiers and efficient features," *Computer Methods and Programs in Biomedicine*, vol. 99, pp. 179–194, 2010.

[40] Y. H. Chen and S. N. Yu, "Selection of effective features for ECG beat recognition based on nonlinear correlations," *Artificial Intelligence in Medicine*, vol. 54, pp. 43–52, 2012.

[41] M. Javadia, S. Ali, A. A. Aranib, A. Sajedina, and R. Ebrahimpourb, "Classification of ECG arrhythmia by a modular neural network based on Mixture of Experts and Negatively Correlated Learning," *Biomedical Signal Processing and Control*, vol. 8, pp. 289–296, 2013.

[42] E. D. Übeyli, "Statistics over features of ECG signals," *Expert Systems with Applications*, vol. 36, pp. 8758–8767, 2009.

[43] A. D. Gaetano, S. Panunzi, F. Rinaldi, A. Risi, and M. Sciandrone, "A patient adaptable ECG beat classifier based on neural networks," *Applied Mathematics and Computation*, vol. 213, pp. 243–249, 2009.

[44] I. Güler and E. D. Übeyli, "ECG beat classifier designed by combined neural network model," *Pattern Recognition*, vol. 38, no. 2, pp. 199–208, 2005.

[45] C. Wen, M. F. Yeh, and K. C. Chang, "ECG beat classification using GreyART network," *IET Signal Process.*, vol. 1, no. 1, pp. 19–28, 2007.

[46] H. M. Rai, A. Trivedi, and S. Shukla, "ECG signal processing for abnormalities detection using multi-resolution wavelet transform and Artificial Neural Network classifier," *Measurement*, vol. 46, pp. 3238–3246, 2013.

[47] M. Engin, "ECG beat classification using neuro-fuzzy network," *Pattern Recognition Letters*, vol. 25, pp. 1715–1722, 2004.

[48] M. Korurek and B. Dogan, "ECG beat classification using particle swarm optimization and radial basis function neural network," *Expert Systems with Applications*, vol. 37, pp. 7563–7569, 2010.

[49] R. Ceylan, Y. Özbay, and B. Karlik, "A novel approach for classification of ECG arrhythmias: Type-2 fuzzy clustering neural network," *Expert Systems with Applications*, vol. 36, pp. 6721–6726, 2009.

[50] I. Christov, G. G. Herrero, V. Krasteva, I. Jekova, A. Gotchev, and K. Egiazarian, "Comparative study of morphological and time-frequency ECG descriptors for heartbeat classification," *Medical Engineering and Physics*, vol. 28, no. 9, pp. 876–887, 2006.

[51] Y. Özbay and G. Tezel, "A new method for classification of ECG arrhythmias using neural network with adaptive activation function," *Digital Signal Processing*, vol. 20, pp. 1040–1049, 2010.

[52] J. S. Wang, W. C. Chiang, Y. L. Hsu, and Y. T.C.Yang, "ECG arrhythmia classification using a probabilistic neural network with a feature reduction method," *Neurocomputing*, vol. 116, pp. 38–45, 2013.

[53] S. N. Yu and K. T. Chou, "Selection of significant independent components for ECG beat classification," *Expert Systems with Applications*, vol. 36, pp. 2088–2096, 2009.

[54] M. R. Homaeinezhad, S. Atyabi, E. Tavakkoli, H. Toosi, A. Ghaffari, and R. Ebrahimpour, "ECG arrhythmia recognition via a neuro-SVM-KNN hybrid classifier with virtual QRS image based geometrical features," *Expert Systems with Applications*, vol. 39, pp. 2047–2058, 2012.

[55] A. Daamouche, L. Hamami, N. Alajlan, and F. Melgania, "A wavelet optimization approach for ECG signal classification," *Biomedical Signal Processing and Control*, vol. 7, no. 4, pp. 342–349, 2012.

[56] A. K. Mishra and S. Raghav, "Local fractal dimension based ECG arrhythmia classification," *Biomedical Signal Processing and Control*, vol. 5, no. 2, pp. 114–123, 2010.

[57] D. Cvetkovic, E. D. Übeyli, and I. Cosic, "Wavelet transform feature extraction from human PPG, ECG, and EEG signal responses to ELF PEMF exposures: A pilot study," *Digital Signal Processing*, vol. 18, no. 5, pp. 861–874, 2008.

[58] H. Khorrami and M. Moavenian, "A comparative study of DWT, CWT and DCT transformations in ECG arrhythmias classification," *Expert Systems with Applications*, vol. 37, no. 8, pp. 5751–5757, 2010.

[59] Y. Kutlu and D. Kuntalp, "Feature extraction for ECG heartbeats using higher order statistics of WPD coefficients," *Computer methods and programs in biomedicine*, vol. 105, pp. 257–267, 2012.

[60] M. Moavenian and H. Khorrami, "A qualitative comparison of Artificial Neural Networks and Support Vector Machines in ECG arrhythmia classification," *Experts Suystems with Applications*, vol. 37, pp. 3088–3093, 2010.

[61] S. N. Yu and Y. H. Chen, "Electrocardiogram beat classification based on wavelet transformation and probabilistic neural network," *Pattern Recognition Letters*, vol. 28, pp. 1142–1150, 2007.

[62] P. de Chazal and R. B. Reilly, "A Patient-Adapting Heartbeat Classifier Using ECG Morphology and Heartbeat Interval Features," *IEEE Trans. Biomed. Eng.*, vol. 53, no. 12, pp. 2535–2543, Dec. 2006.

[63] W. Jiang and G. S. Kong, "Block-Based Neural Networks for Personalized ECG Signal Classification," *IEEE Trans. Neural Netw.*, vol. 18, no. 6, pp. 1750–1761, Nov. 2007.

[64] V. X. Afonso, W. J. Tompkins, T. Q. Nguyen, K. Michler, and S. Luo, "Comparing stress ECG enhancement algorithms," *IEEE Eng. Med. Biol. Mag.*, vol. 15, no. 3, pp. 37–44, 1996.

[65] Y. Wu, R. Rangayyan, Y. Zhou, and S. Ng, "Filtering electrocardiographic signals using an unbiased and normalized adaptive noise reduction system„" *Med. Eng. Phys.*, vol. 31, pp. 17–26, 2009.

[66] M. S. T. Slonim and E. Ovsyscher, "The use of simple FIR filters for filtering of ECG signals and a new method for post-filter signal reconstruction," in *Proc. Comput. Cardiol.*, 1993, pp. 871-873.

[67] O. Sayadi and M. B. Shamsollahi, "Model-based fiducial points extraction for baseline wandered electrocardiograms," *IEEE Trans. Biomed. Eng.*, vol. 55, no. 1, pp. 347–351, 2008.

[68] M. B. Velasco, B. Weng, and K. E. Barner, "ECG signal denoising and baseline wander correction based on the empirical mode decomposition," *Computers in Biology and Medicine*, vol. 38, no. 1, pp. 1–13, 2008.

[69] H. Liang, Z. Lin, and F. Yin, "Removal of ECG contamination from diaphragmatic EMG by nonlinear analysis," *Nonlinear Analysis*, vol. 63, pp. 745–753, 2005.

[70] S. Poornachandra, "Wavelet-based denoising using subband dependent threshold for ECG signals," *Digital Signal Processing*, vol. 18, no. 1, pp. 49–55, 2008.

[71] M. Alfaouri and K. Daqrouq, "ECG signal denoising by wavelet transform thresholding," *Am. J. Appl. Sci.*, vol. 5, no. 3, pp. 276–281, 2008.

[72] O. Sayadi and M. Shamsollahi, "Multi adaptive bionic wavelet transform: application to ECG denoising and baseline wandering reduction," *EURASIP J. Adv. Signal Process*, 2007.

[73] L. Sharma, S. Dandapat, and A. Mahanta, "ECG signal denoising using higher order statistics in wavelet subbands," *Biomedical Signal Processing and Control*, vol. 5, pp. 214–222, 2010.

[74] R. Sameni, M. B. Shamsollahi, C. Jutten, and G. D. Clifford, "A nonlinear Bayesian filtering framework for ECG denoising," *IEEE Trans. Biomed. Eng.*, vol. 54, no. 12, pp. 2172–2185, 2007.

[75] Q. Zhang and A. Benveniste, "Wavelet networks," *IEEE Trans. Neural Netw.*, vol. 3, no. 6, pp. 889–898, 1992.

[76] S. Poungponsri and X. H. Yu, "Electrocardiogram (ECG) signal modeling and noise reduction using wavelet neural networks," in *Proc. Int. Conf. on Automation and Logistics*, 2009, pp. 394-398.

[77] G. B. Moody and R. G. Mark, "The impact of the MIT-BIH Arrhythmia Database," *IEEE Eng Med and Biol*, vol. 20, no. 3, pp. 45–50, 2001.

[78] *Recommended Practice for Testing and Reporting Performance Results of Ventricular Arrhythmia Detection Algorithms*, Assoc. Adv. Med. Instrum., Arlington, VA, 1987 Std.

[79] E. D. Übeyli, "ECG beats classification using multiclass support vector machines with error correcting output codes," *Digital Signal Processing*, vol. 17, pp. 675–684, 2007.

[80] N. E. Huang, Z. Shen, S. R. Long, M. C. Wu, H. H. Shih, Q. Zheng, N. C. Yen, C. C. Tung, and H. H. Liu, "The empirical mode decomposition and the Hilbert spectrum for nonlinear and non-stationary time series analysis," *Proceedings of the Royal Society of London A: Mathematical, Physical and Engineering Sciences*, vol. 454, no. 1971, pp. 903–995, 1998.

[81] M. K. Das and S. Ari, "Electrocardiogram beat classification using S-transform based feature set," *Journal of Mechanics in Medicine and Biology*, vol. 14, no. 5, p. 1450066 (18 pages), 2014.

[82] R. G. Stockwell, L. Mansinha, and R. P. Lowe, "Localization of the complex spectrum: the S transform," *IEEE Trans. Signal Process.*, vol. 44, no. 4, pp. 998–1001, Apr. 1996.

[83] S. Ari and G. Saha, "In search of an optimization technique for Artificial Neural Network to classify abnormal heart sounds," *Applied Soft Computing*, vol. 9, pp. 330–340, 2009.

[84] M. Vetterli and C. Herley, "Wavelets and Filter Banks: Theory and Design," *IEEE Trans. Signal Processing*, vol. 40, no. 9, pp. 2207–2232, Sept. 1992.

[85] H. Ocak, "Automatic detection of epileptic seizures in EEG using discrete wavelet transform and approximate entropy," *Expert Systems with Applications*, vol. 36, no. 2, Part 1, pp. 2027–2036, 2009.

[86] R. C. Gonzalez and R. E. Woods, *Digital Image Processing.* Pearson education, 2006.

[87] S. Assous, A. Humeau, M. Tartas, P. Abraham, and J. L. Huillier, "S-transform applied to laser doppler flowmetry reactive hyperemia signals," *IEEE Trans. Biomed. Eng.*, vol. 53, pp. 1032–1037, 2006.

[88] P. Rakovi, S. E., L. J. Stankovi, and J. Jiang, "Time-frequency signal processing approaches with applications to heart sound analysis," *Computers in Cardiology*, vol. 33, pp. 197–200, 2006.

[89] C. C. Huang, S. F. Liang, M. S. Young, and F. Z. Shaw, "A novel application of the S-transform in removing powerline interference from biomedical signals," *Physiological Measurement*, vol. 30, pp. 13–27, 2009.

[90] P. K. Dash, S. R. Samantaray, G. Panda, and B. K. Panigrahi, "Power transformer protection using S-transform with complex window and pattern recognition approach," *IET Gener. Transm. Distrib.*, vol. 1, pp. 278–286, 2007.

[91] P. K. Dash, B. K. Panigrahi, D. K. Sahoo, and G. Panda, "Power Quality Disturbance Data Compression, Detection, and Classification Using Integrated Spline Wavelet and S-Transform," *IEEE Trans. Power Deliv.*, vol. 18, pp. 595–600, 2003.

[92] M. Eramian, R. Schincariol, L. Mansinha, and R. Stockwell, "Generation of aquifer heterogeneity maps using two-dimensional spectral texture segmentation techniques," *Mathematical Geology*, vol. 31, pp. 327–348, 1999.

[93] R. G. Stockwell, "S-Transform Analysis of Gravity Wave Activity," Master's thesis, Dept. of Physics and Astronomy, The University of Western Ontario, London, Ontario, Canada, 1999.

[94] N. V. George, "S Transform : Time-Frequency Analysis and Filtering," Master's thesis, NIT, Rourkela, India, 2009.

[95] R. G. Stockwell, "Why use the S-transform?" *in Pseudo-Differentials Operatores: PDEs and Time frequency analysis, ser. Fields Institute Communications, Wong, Ed. AMS*, vol. 52, pp. 279–309, 2007.

[96] M. K. Das and S. Ari, "ECG Beats Classification Using Mixture of Features," *International Scholarly Research Notices, Hindawi publication*, 2014 (in press).

[97] Y. Ozbay, R. Ceylan, and B. Karlik, "A fuzzy clustering neural network architecture for classification of ECG arrhythmias," *Computers in Biology and Medicine*, vol. 36, pp. 376–388, 2006.

[98] V. Vapnik, *Statistical learning theory.* New York: John Wiley, 1998.

[99] S. Abe, *Support Vector Machines for Pattern Classification.* Springer-Verlag, London, 2005.

[100] E. Çomak, A. Arslan, and I. Türkoglu, "A decision support system based on support vector machines for diagnosis of the heart valve diseases," *Computers in Biology and Medicine*, vol. 37, pp. 21–27, 2007.

[101] E. Comak and A. Arslan, "A new training method for support vector machines: Clustering k-NN support vector machines," *Expert Systems with Applications*, vol. 35, no. 3, pp. 564–568, 2008.

[102] M. K. Das and S. Ari, "Patient-Specific ECG Beat Classification Technique," *IET Healthcare Technology Letters*, vol. 1, no. 3, pp. 98–103, 2014.

[103] S. Ari, K. Hembram, and G. Saha, "Detection of cardiac abnormality from PCG signal using LMS based least square SVM classifier," *Expert Systems with Applications*, vol. 37, no. 12, pp. 8019–8026, 2010.

[104] D. Lin, N. Cristianini, C. Sugne, T. Furey, M. Ares, M. Brown, W. Grundy, and D. Haussler, *Knowledge-base Analysis of Microarray Gene Expression Data by using Support Vector Machines*. Springer, London, UK, 2000, ch. 1, pp. 262–267.

[105] I. El Naqa, Y. Yang, M. Wernick, N. Galatsanos, and R. Nishikawa, "A support vector machine approach for detection of microcalcifications," *IEEE Trans. Med. Imag.*, vol. 21, no. 12, pp. 1552–563, Dec. 2002.

[106] T. Ebrahimi, G. N. Garcia, and J. M. Vesin, "Joint time-frequency-space classification of EEG in a brain-computer interface application," *J. Appl. Signal Process.*, vol. 1, no. 7, pp. 713–729, 2003.

[107] T. Joachims, C. Ndellec, and C. Rouveriol, "Text categorization with support vector machines: learning with many relevant features," in *Proc. European Conf. Machine Learning (ECML), Berlin*, 1998, pp. 137-142.

[108] A. Kampouraki, G. Manis, and C. Nikou, "Heartbeat Time Series Classification with Support Vector Machines," *IEEE Trans. Inform. Technol. Biomed*, vol. 13, no. 4, pp. 512–518, Jul. 2009.

[109] R. Rifkin and A. Klautau, "In Defense of One-vs-All Classification," *J. Machine Learning Research*, vol. 5, pp. 101–141, 2004.

[110] C. W. Hsu and C. J. Lin, "A Comparison of methods for Multiclass Support Vector Machines," *IEEE Trans. Neural Netw.*, vol. 13, no. 2, pp. 415–425, Mar. 2002.

[111] P. Mitra, C. A. Murthy, and S. K. Pal, "Unsupervised feature selection using feature similarity," *IEEE Trans. Pattern Anal. Mach. Intell.*, vol. 24, pp. 301–312, 2002.

[112] X. Han, X. Chang, L. Quan, X. Xiong, J. Li, Z. Zhang, and Y. Liu, "Feature subset selection by gravitational search algorithm optimization," *Information Sciences*, vol. 281, pp. 128–146, 2014.

[113] J. Derrac, C. Cornelis, S. García, and F. Herrera, "Enhancing evolutionary instance selection algorithms by means of fuzzy rough set based feature selection," *Information Sciences*, vol. 186, pp. 73–92, 2012.

[114] H. Liu and L. Yu, "Toward integrating features selection algorithms for classification and clustering," *IEEE Trans. Knowl. Data Eng.*, vol. 17, pp. 491–502, 2005.

[115] C. Liu and H. Wechsler, "Evolutionary pursuit and its application to face recognition," *IEEE Trans. Pattern Anal. Mach. Intell*, vol. 22, no. 6, pp. 570–582, Jun. 2000.

[116] K. Passino, "Biomimicry of bacterial foraging for distributed optimization and control," *IEEE Control Systems Magazine*, vol. 22, no. 3, pp. 52–67, 2002.

[117] J. Adler, "Chemotaxis in bacteria," *Science*, vol. 153, pp. 708–716, 1966.

[118] H. Chen, Y. Zhu, and K. Hu, "Co-operative Bacterial Foraging Optimization," *Discrete Dynamics in Nature and Society*, vol. 2009, p. 17, 2009.

[119] O. P. Verma, R. Sharma, and D. Kumar, "Binarization Based Image Edge Detection Using Bacterial Foraging Algorithm," *Procedia Technology*, vol. 6, pp. 315–323, 2012.

[120] M. A. Bakhshali and M. Shamsi, "Segmentation of color lip images by optimal thresholding usingbacterial foraging optimization (BFO)," *Journal of Computational Science*, vol. 5, no. 2, pp. 251–257, 2014.

[121] P. D. Sathya and R. Kayalvizhi, "Modified bacterial foraging algorithm based mul-tilevel thresholding for image segmentation," *Engineering Applications of Artificial Intelligence*, vol. 24, pp. 595–615, 2011.

[122] R. Jakhar, N. Kaur, and R. Singh, "Face Recognition Using Bacteria Foraging Optimization-Based Selected Features," *International Journal of Advanced Computer Science and Applications*, pp. 106–111, 2011.

[123] M. Z. U. Rahman, R. A. Shaik, and D. V. R. K. Reddy, "Efficient sign based normalized adaptive filtering techniques for cancellation of artifacts in ECG signals: Application to wireless biotelemetry," *Signal Processing*, vol. 91, no. 2, pp. 225–239, 2011.

[124] C. Y. F. Ho, B. W. K. Ling, T. P. L. Wong, A. Y. P. Chan, and P. K. S. Tam, "Fuzzy multi wavelet denoising on ECG signal," *Electronics Letters*, vol. 39, pp. 1163–1164, 2003.

[125] A. K. Barros, A. Mansour, and N. Ohnishi, "Removing artifacts from electrocardiographic signals using independent components analysis," *Neurocomputing*, vol. 22, no. 13, pp. 173–186, 1998.

[126] E. Ercelebi, "Electrocardiogram signals de-noising using lifting-based discrete wavelet transform," *Computers in Biology and Medicine*, vol. 34, no. 6, pp. 479–493, 2004.

[127] J. S. Paul, M. R. Reddy, and V. J. Kumar, "A transform domain SVD filter for suppression of muscle noise artifacts in exercise ECG," *IEEE Trans. Biomed. Eng*, vol. 47, no. 5, pp. 654–663, 2000.

[128] B. Acar and H. Koymen, "SVD-based on-line exercise ECG signal orthogonalization," *IEEE Trans. Biomed. Eng.*, vol. 46, no. 3, pp. 311–321, 1999.

[129] T. Y. Ji, Z. Lu, Q. H. Wu, and Z. Ji, "Baseline normalisation of ECG signals using empirical mode decomposition and mathematical morphology," *Electronics Letters*, vol. 44, no. 2, pp. 82–83, 2008.

[130] S. Ari, M. K. Das, and A. Chacko, "Enhancement of ECG Signals using S-Transform," *Computers in Biology and Medicine*, vol. 43, no. 6, pp. 649–660, 2013.

[131] G. M. Friesen, T. C. Jannett, M. A. Jadallah, S. L. Yates, S. R. Quint, and H. T. Nagle, "A comparison of the noise sensitivity of nine QRS detection algorithms," *IEEE Trans. Biomed. Eng.*, vol. 37, no. 1, pp. 85–98, 1990.

[132] B. Mozaffary and M. A. Tinati, "ECG Baseline Wander Elimination using Wavelet Packets," *World Academy of Science, Engineering and Technology*, vol. 3, pp. 14–16, 2005.

[133] L. Sornmo and P. Laguna, *Electrocardiogram (ECG) Signal Processing*, I. John Wiley & Sons, Ed. Wiley Encyclopedia of Biomedical Engineering, 2006, pp. 1-16.

[134] D. Donoho, "De-noising by soft-thresholding," *IEEE Trans. Inform Theory*, vol. 41, pp. 612–627, 1995.

[135] R. G. Stockwell, "A basic efficient representation of the S-transform," *Digital Signal processing*, vol. 17, pp. 371–393, 2007.

[136] M. K. Das and S. Ari, "Analysis of ECG signal denoising method based on S-transform," *Innovation and Research in Biomedical Engineering (IRBM)*, vol. 34, no. 6, pp. 362–370, 2013.

[137] N. Otsu, "A Threshold Selection Method from Gray-level Histograms," *IEEE Trans. Systems, Man and Cybernetics*, vol. 9, pp. 62–66, 1979.

[138] D. K. Ghosh and S. Ari, "A static hand gesture recognition algorithm using k-mean based radial basis function neural network," in *Proc. 8th Int. Conf. Information, Communications, and Signal Processing (ICICS)*, 2011, pp. 1-5.

[139] E. R. Dougherty, *An introduction to morphological image processing*, W. Bellingham, Ed. SPIE Optical Engineering Press, 1992.

[140] S. D. Suman and M. Dutta, "Optimized noise canceller for ECG signals," *IJCA Special Issue on Intelligent Systems and Data Processing*, pp. 10–17, 2011.

[141] M. Varanini, G. D. Paolis, M. Emdin, A. Macerata, S. Pola, M. Cipriani, and C. Marchesi, "Spectral analysis of cardiovascular time series by the S-transform," *Computers in Cardiology*, pp. 383–386, 1997.

[142] U. Ulusoy, "Application of ANOVA to image analysis results of talc particles produced by different milling," *Powder Technology*, vol. 188, pp. 133–138, 2008.

[143] R. J. Freund, W. J. Wilson, and D. L. Mohr, *Statistical Methods*. 3rd edition, Acamedic Press, Elsevier, 2010.

[144] M. K. J. Oster, O. Pietquin and J. Felblinger, "Nonlinear Bayesian Filtering for Denoising of Electrocardiograms Acquired in a Magnetic Resonance Environment," *IEEE Trans. Biomed. Eng.*, vol. 57, no. 7, pp. 1628–1638, 2010.

[145] J. P. Martinez, R. Almeida, S. Olmos, A. P. Rocha, and P. Laguna, "A wavelet-based ECG delineator: evaluation on standard databases," *IEEE Trans. Biomed. Eng.*, vol. 51, no. 4, pp. 570–581, 2004.

[146] N. V. Thakor and Y. S. Zhu, "Applications of Adaptive Filtering to ECG Analysis : Noise Cancellation and Arrhythmia Detection," *IEEE Trans. Biomed. Eng.*, vol. 18, no. 8, pp. 785–794, 1991.

Publications

Journals

- **M. K. Das** and S. Ari, "Analysis of ECG signal denoising method based on S-transform," *Innovation and Research in Biomedical Engineering (IRBM), Elsevier*, vol 34, no. 6, pp. 362-370, 2013.
- **M. K. Das** and S. Ari, "Patient-Specific ECG Beat Classification Technique," *IET Healthcare Technology Letters*, vol. 1, no. 3, pp. 98-103, 2014.
- **M. K. Das** and S. Ari, "Electrocardiogram beat classification with S-transform based feature set," *Journal of Mechanics in Medicine and Biology*, Vol. 14, No. 5, pp. 1450066, 2014.
- S. Ari, **M. K. Das**, and A. Chacko, "Enhancement of ECG Signals using S-Transform", *Computers in Biology and Medicine, Elsevier*, vol. 43, no. 6, pp. 649-660, 2013.
- M. Thomas, **M. K. Das,** and S. Ari, "ECG Arrhythmia Classification using Dual Tree Complex Wavelet based features,T̃ *International Journal of Electronics and Communications (AEUE) , Elsevier,* vol. 69, no. 4, pp. 715-721, 2015.
- **M. K. Das**, and S. Ari, "ECG Beats Classification Using Mixture of Features," *International Scholarly Research Notices*, (In press) doi:10.1155/2014/178436, 2014.
- J. P. Sahoo, **M. K. Das**, S. Ari, and S. Behera, "Autocorrelation and Hilbert transform based QRS Complex detection in ECG Signal," *International Journal of Signal and Imaging Systems Engineering*, vol. 7, no. 1, 2014.

Conferences

- **M. K. Das** and S. Ari, "ECG Arrhythmia Recognition using Artificial Neural Network with S-transform based Effective Features," *IEEE INDICON-2013*, 13th to 15th Dec, 2013, IIT Bombay.

- **M. K. Das**, S. Ari, and Swagatika Priyadarshini, "On an Algorithm for Detection of QRS Complexes in Noisy Electrocardiogram Signal," *IEEE INDICON-2011*, BITS Pilani, Hyderabad, December 16-18, 2011.
- **M. K. Das**, D. K. Ghosh, and S. Ari, "Electrocardiogram (ECG) Signal Classification using S-transform, Genetic Algorithm and Neural Network," *IEEE CATCON*, December 6-8, 2013, Kolkata.
- M. Thomas, **M. K. Das**, and S. Ari, "Classification of Cardiac Arrhythmias based on Dual Tree Complex Wavelet Transform," *IEEE International Conference on Communication and Signal Processing-ICCSP'14*, Melmaruvathur, Tamilnadu, 3rd -5th, April, 2014.

Author's Biography

Manab Kumar Das was born and brought up in Madhakhali, a small village belongs to Contai sub-division, West Bengal and did his initial schooling from nearby schools. After that he moved on to Banamalichatta high school and passed the Higher Secondary from there in 1996. After schooling he started his engineering career and obtained B.Tech in Electronics and communication Engineering from Murshidabad College of Engineering and Technology under the Kalyani University in the year 2002 and subsequently he joined at Blue Star Limited Kolkata as associate service engineer. After working for two years and seven months he moved on to Mallabhum Institute of Technology as a faculty member. After that he completed M. Tech from National Institute of Technology Rourkela and obtained the degree in 2008. Then he again joined as a Sr. lecturer at Mallabhum Institute of Technology. In 2010 he took admission for Ph.D at National Institute of Technology, Rourkela. His area of interest is biomedical signal processing. During his research, he presented papers in International Conferences. He is also a student Member of IEEE. He can be contacted at: manabster@gmail.com & manabkrdas@gmail.com.